

# NMSSM interpretations of the observed Higgs signal

Florian Domingo, Georg Weiglein

*Deutsches Elektronen Synchrotron (DESY),  
Notkestraße 85, D-22607 Hamburg, Germany*

## Abstract

While the properties of the signal that was discovered in the Higgs searches at the LHC are consistent so far with the Higgs boson of the Standard Model (SM), it is crucial to investigate to what extent other interpretations that may correspond to very different underlying physics are compatible with the current results. We use the Next-to-Minimal Supersymmetric Standard Model (NMSSM) as a well-motivated theoretical framework with a sufficiently rich Higgs phenomenology to address this question, making use of the public tools **HiggsBounds** and **HiggsSignals** in order to take into account comprehensive experimental information on both the observed signal and on the existing limits from Higgs searches at LEP, the TeVatron and the LHC. We find that besides the decoupling limit resulting in a single light state with SM-like properties, several other configurations involving states lighter or quasi-degenerate with the one at about 125 GeV turn out to give a competitive fit to the Higgs data and other existing constraints. We discuss the phenomenology and possible future experimental tests of those scenarios, and compare the features of specific scenarios chosen as examples with those arising from a more global fit.

## 1 Introduction

After the discovery of a signal with a mass of about 125 GeV in the Higgs searches at the LHC [1, 2], the prime goal is now to identify the underlying nature of the new state and to determine the mechanism of electroweak symmetry breaking. While the properties of the observed state are compatible with the ones predicted for the Higgs boson of the Standard Model (SM) at the current level of precision, also a wide range of alternative interpretations could be possible, corresponding to very different underlying physics. In particular, in models with an extended Higgs sector the observed state would be accompanied by several other Higgs bosons, in contrast to the minimal formulation of the SM where a single  $SU(2)_L$ -doublet is responsible for electroweak-symmetry breaking.

Supersymmetry (SUSY) [3] is commonly regarded as the most appealing extension of the SM, since it provides a solution for stabilising the huge hierarchy between the Planck scale and the weak scale [4] and offers further attractive features such as unification of the gauge couplings and a natural candidate for cold dark matter in the Universe. A crucial prediction of supersymmetric extensions of the SM are their extended Higgs sectors: the holomorphicity of the superpotential (as well as the cancellation of gauge anomalies) implies that at least two  $SU(2)_L$  doublets with opposite hypercharge have to be present, so as to generate mass terms for both up- and down-quarks (in a Type II 2-Higgs-Doublet-Model fashion). The minimal supersymmetric extension of the SM (MSSM) [5] is based on the minimal Higgs sector of this kind comprising two Higgs doublets, whereas the Higgs sector of the next-to-minimal supersymmetric extension of the SM (NMSSM) [6, 7] contains an additional (complex) gauge-singlet. It has long been recognised that the NMSSM provides an elegant solution [8] to the “ $\mu$ -problem” [9] of the MSSM. In the context of the relatively high mass value of about 125 GeV of the observed state, this model has received particular attention lately since the mass of the light doublet-like state receives an additional contribution at lowest order as compared to the MSSM, which dominates at low values of  $\tan\beta$  (the ratio of the vacuum expectation values, v.e.v.’s, of the two Higgs doublets). In this case significantly

smaller higher-order corrections are required to obtain a Higgs-boson mass in the appropriate range [10] as compared to the MSSM, where the lowest-order prediction for the mass of the light CP-even Higgs boson is bounded from above by the mass of the Z boson,  $M_Z$ . Furthermore, also the singlet-doublet mixing can give rise to an uplift of the mass of the doublet state, provided that the CP-even singlet state is lighter than the doublet state. It has been argued in this context that the relaxed requirement on the size of the higher-order corrections as compared to the MSSM makes it possible to obtain a Higgs-mass prediction of about 125 GeV in a “more natural” way [11].

In the following we will focus on the NMSSM as a theoretically well-motivated alternative to the SM with a potentially rich phenomenology in the Higgs sector. For simplicity, we will restrict to the CP-conserving case, for which the spectrum of physical Higgs states of the NMSSM consists of three CP-even, two CP-odd and a pair of charged Higgs states (while we do not explicitly consider CP-violating effects giving rise to a mixture between the five neutral states, it should be noted that cases where a CP-even and a CP-odd state are nearly mass-degenerate essentially mimic a scenario where a single state is an admixture of CP-even and CP-odd components). Furthermore, while several versions of the NMSSM can be formulated, depending on the form of the singlet and singlet-doublet interaction terms in the superpotential, we will focus on the  $\mathbb{Z}_3$ -conserving version only, where the solution to the “ $\mu$ -problem” is more immediate (on the other hand, this simple model could lead to a domain wall problem [12] but we will not address this question here). The Higgs sector of this version of the NMSSM is characterised by six parameters (at tree-level), in contrast to the two parameters of the MSSM. While we shall borrow most of our notations from [6], we recall the Higgs terms entering the superpotential of the model:

$$W_{\text{NMSSM}} \ni \lambda S H_u \cdot H_d + \frac{\kappa}{3} S^3 \quad (1)$$

where  $S$  denotes the singlet (super)field,  $H_u$  and  $H_d$  the doublets, while  $\cdot$  stands for the  $SU(2)$  product.

When confronting the predictions of an extended Higgs sector with the observed signal and the limits from the Higgs searches at LEP, the TeVatron and the LHC, the most obvious interpretation of the signal at about 125 GeV is to associate it with the lightest CP-even Higgs boson of the considered model. The case where all other Higgs (as well as all new physics) states of a supersymmetric extension of the SM (and the same is true for various other extended Higgs sectors) are significantly heavier corresponds to the “decoupling region” of the model under consideration, where the couplings of the light Higgs boson to gauge bosons and SM fermions are very close to the ones of the SM. Revealing deviations of those couplings from their SM counterparts in such a case will require high-precision measurements, where in many cases the expected deviations do not exceed the level of a few per cent. An additional source of possible deviations from the SM could be decays of the SM-like state into new-physics particles. Such a decay could in particular occur into a pair of dark matter particles, if the mass of the latter is less than half of the mass of the Higgs state, i.e. below about 60 GeV. This would give rise to an invisible decay mode of the observed state, providing a strong motivation for searches of decays of the observed signal into invisible final states.

Besides the interpretation of the observed state as the lightest CP-even Higgs boson of an extended Higgs sector, it is also possible, at least in principle, to identify the observed signal with the second-lightest state of an extended Higgs sector. This interpretation would have the immediate consequence that there should be an (or more generally at least one) additional Higgs state *below* the one observed at about 125 GeV. The phenomenology of such a scenario is very different from the case of the decoupling limit discussed above, because of the presence of at least one more light state in the spectrum. Within the MSSM this interpretation is in principle possible [13, 14], but gives rise to a rather exotic Higgs sector where in fact all additional Higgs bosons are light, i.e. in the vicinity of the state at about 125 GeV or below. It is remarkable that a global fit within the MSSM within this interpretation has resulted in an acceptable fit probability [14], but lately this interpretation, which implies in particular a light charged Higgs boson below the mass of the top quark (see in particular Ref. [15]), has come under increased pressure from the limits obtained in the charged Higgs searches by ATLAS [16] and, more recently, CMS [17].

The NMSSM provides a well-suited and theoretically well motivated framework for investigating to what extent interpretations that go beyond the obvious case of a single light state in the decoupling limit

are compatible with the latest experimental results both with respect to the properties of the observed state and to the limits obtained from Higgs searches (as well as other existing constraints). It is the purpose of the present paper to perform such an analysis. It is obvious that compatibility with the observed signal requires much more than just a Higgs state (or possibly more than one) in the spectrum with a mass of about 125 GeV. In order to properly take into account the latest experimental results from Higgs search limits and from measurements of the properties of the observed state, we make use of the public tools **HiggsBounds** [18] and **HiggsSignals** [19], which incorporate a comprehensive set of results from ATLAS [20], CMS [21] and the TeVatron [22]. We do not explicitly impose limits from the direct searches for SUSY particles at the LHC. While some of the scenarios discussed in this paper could be affected by constraints from SUSY particle searches, we have checked that the qualitative features of the Higgs phenomenology of those scenarios are maintained also for somewhat heavier SUSY particle spectra. Note however that most of the SUSY spectra that we employ (especially for coloured particles) are beyond the mass-range tested in the Run-I of the LHC.

As mentioned above, already since the very early hints of a signal at about 125 GeV the Higgs sector of the NMSSM has found a lot of attention in this context. Besides the mass prediction in comparison with the MSSM case [11], the possibility of modified rates has been discussed, particularly in the diphoton channel [23]. Furthermore, the case of universal (or semi-universal) SUSY-breaking conditions at the GUT scale [24], gauge-mediation [25] and other related scenarios [26] have been considered in this context. The CP-violating version of the NMSSM also received some attention [27]. [28] analysed the fine-tuning in a  $\mathbb{Z}_3$ -violating version of the NMSSM and variants. Other groups confronted the presence of a Higgs state at this mass with direct searches for SUSY particles at the LHC or Dark-Matter constraints [29]. Scenarios with a light singlet-like state around  $\sim 100$  GeV have found considerable interest [30]. Another possibility involves a singlet and a doublet that are almost mass-degenerate at about 125 GeV and may mix with each other, see Ref. [31] (and the last reference of [23]). Several studies also suggested to exploit pair production processes at the LHC in order to distinguish the SM from the NMSSM and/or to look for a light singlet in this fashion [32]. Scenarios with a very light CP-odd (or CP-even) Higgs boson were addressed with several search proposals in direct production, unconventional light charged-Higgs decays, or cascade decays from SM-like / light singlet states; large Higgs-to-Higgs decays were also considered from the point of view of the SM-compatible nature of the observed state [33]. Recent studies of the properties of a light pseudoscalar in the NMSSM [34] have emphasized the relevance of indirect production modes for the investigation of this scenario at the LHC. In a different direction, the authors of [35] focussed on NMSSM Higgs scenarios with a low-scale doublet sector. Furthermore, [36], and more recently [37], studied the discovery prospects of NMSSM Higgs states in the LHC run at 13 TeV. In our analysis we go beyond the previous work in several respects: while many of the afore-mentioned analyses discussed scenarios which are compatible with existing limits, our inclusion of a fitting tool allows us to highlight the quality of the various scenarios in view of the available data. Furthermore, we aim at a comprehensive discussion from the point of view of the NMSSM Higgs phenomenology, hence do not confine to a specific scenario (within our assumptions on the model, perturbativity constraints and choices of simplicity with regards to the SUSY spectrum). We also focus on Higgs physics and thus try, without spoiling the physical content, to avoid emphasis on questions of secondary importance with respect to this topic (e.g. the details of the supersymmetric spectrum). Finally, much experimental data has become available in the last few years, narrowing the possibilities in the Higgs sector, and most of the recent developments are included within the tools on which our discussion is based.

The paper is organised as follows: in Sect. 2 we describe the framework that we use for the analyses in this paper, in particular the statistical approach used in our fits, the treatment of external constraints and the tools that we apply. As a first step of our analysis, in Sect. 3 we briefly consider the SM case and the corresponding decoupling limits of the MSSM and the NMSSM. The SM result is used for comparison with  $\chi^2$  analyses in different NMSSM scenarios, which we perform in Sects. 4–8. In Sect. 9, we focus on specific points of the NMSSM parameter space and discuss in more details the Higgs phenomenology and the consequences for future searches, should the corresponding spectrum be realised in nature. In Sect. 10 a more global scan is carried out, and the features observed in the global scan are discussed in view of the results obtained for the specific NMSSM scenarios that we have considered before. Sect. 11 contains our conclusions.

## 2 Framework of the analysis: treatment of external constraints and applied tools

The NMSSM parameter space is explored with the help of the spectrum generator `NMSSMTools_4.4.0` [38], computing the Higgs masses up to leading two-loop double-log order (we will be using the default mode only), in an effective potential approach. This code considers a certain number of phenomenological limits, several among which are kept within our analysis. The first class of such tests are consistency requirements and are (necessarily) included as hard cuts:

- stability of the EWSB-vacuum: positivity of the scalar squared-masses, absence of deeper minimum;
- absence of Landau poles below the GUT scale: while this requirement is sometimes omitted in order to probe effects associated with large values of the parameter  $\lambda$  and under the assumption that new-physics or specific properties of the non-perturbative regime would smoothen the theoretical difficulty of the Landau poles, we choose to keep this theoretical limit;
- requirement for Higgs soft squared-masses at the TeV scale: the potential-minimization procedure in NMSSMTools trades these masses for the Higgs v.e.v.'s, so that the naturalness requirement that soft masses intervene at the TeV scale must be checked explicitly;
- requirement for a neutralino LSP (the impact of which, however, is of secondary importance in our discussion).

Another type of constraints are supersymmetric searches at LEP. Given that we are chiefly interested in the Higgs sector, we also keep these limits under the form of a hard cut:

- $Z \rightarrow \text{inv. decay}$  ( $< 1.71 \cdot 10^{-3}$ )
- mass lower limits on squarks ( $m_{\tilde{t}} > 93.2 \text{ GeV}$ ,  $m_{\tilde{q}_{1,2}} > 100 \text{ GeV}$ ), gluino ( $m_{\tilde{g}} > 180 \text{ GeV}$ ), sleptons ( $m_{\tilde{l}} > 99.9 \text{ GeV}$ ), charginos ( $m_{\tilde{\chi}^\pm} > 103.5 \text{ GeV}$ );
- limits on  $\tilde{t} \rightarrow b l \tilde{N}$ ,  $\tilde{t} \rightarrow c \chi^0$ ,  $\tilde{b} \rightarrow b \chi^0$ .

We remind the reader that LHC limits on SUSY searches are not considered in our analysis. However, the SUSY spectra that we employ are typically beyond the mass-range of the searches in the Run-I. In this context, the inclusion of LEP limits as mentioned above has only a minor impact.

NMSSMTools also computes several low-energy observables:

- limits from the bottomonium sector: non-observation of a signal in  $BR(\Upsilon \rightarrow \gamma A \rightarrow \gamma l^+ l^-)$ , excessive contribution to the  $\eta_b(1S) - A$  mixing [39]. Only light CP-odd Higgs below  $\sim 10 \text{ GeV}$  are concerned by these constraints and the limits are kept as a 95% C.L. cut<sup>1</sup>.
- limits from  $B$ -factories (under a strong Minimal Flavour Violation hypothesis, i.e. neglecting all possible tree-level flavour-changing neutral currents):  $BR(B \rightarrow X_s \gamma)$ ,  $BR(B^+ \rightarrow \tau \nu_\tau)$ ,  $BR(\bar{B}_s \rightarrow \mu^+ \mu^-)$ ,  $BR(B \rightarrow X_s \mu^+ \mu^-)$ ,  $\Delta M_{d,s}$  [40]. Instead of treating the limits as a hard cut, we combine them in a  $\chi^2$  function relying on the central value and error bars computed in NMSSMTools:

$$\chi^2 = \sum_i \frac{(O_i^{\text{NMSSM}} - O_i^{\text{exp.}})^2}{\sigma_i^2 \text{theo.} + \sigma_i^2 \text{exp.}} \quad (2)$$

the corresponding experimental central values  $O_i^{\text{exp.}}$  and standard deviation  $\sigma_i^{\text{exp.}}$  are summarized in Table 1. The theoretical error estimate is the result of an involved calculation: errors relative to SM-like contributions are taken from the corresponding SM estimate; the uncertainty on new-physics contributions is estimated to 30% (if only leading-order effects are included) / 10% (if next-to-leading  $\alpha_S$  corrections are present) of the total corresponding contributions and are added

---

<sup>1</sup>Note that the points excluded by such limits are stored while scanning, however.

$O_i$	$BR(B \rightarrow X_s \gamma)$	$BR(B^+ \rightarrow \tau \nu_\tau)$	$BR(\bar{B}_s \rightarrow \mu^+ \mu^-)$	$BR(B \rightarrow X_s l^+ l^-)$ $ 1 \text{ GeV}^2 < s_{l^+ l^-} < 6 \text{ GeV}^2$	...
$O_i^{\text{exp.}}$	$3.43 \cdot 10^{-4}$	$1.14 \cdot 10^{-4}$	$3.2 \cdot 10^{-9}$	$1.6 \cdot 10^{-6}$	...
$\sigma_i^{\text{exp.}}$	$0.22 \cdot 10^{-4}$	$0.22 \cdot 10^{-4}$	$0.7 \cdot 10^{-9}$	$0.5 \cdot 10^{-6}$	...
...	$BR(B \rightarrow X_s l^+ l^-)$	$\Delta M_d$	$\Delta M_s$	$\Delta a_\mu^{\text{exp-SM}}$	
...	$ 14.4 \text{ GeV}^2 < s_{l^+ l^-}$				
...	$4.4 \cdot 10^{-7}$	$0.507 \text{ ps}^{-1}$	$17.719 \text{ ps}^{-1}$	$27.4 \cdot 10^{-10}$	
...	$1.2 \cdot 10^{-7}$	$0.004 \text{ ps}^{-1}$	$0.043 \text{ ps}^{-1}$	$9.3 \cdot 10^{-10}$	

Table 1: Experimental central values and uncertainties for  $B$  physics observables and  $(g-2)_\mu$  as implemented in NMSSMTool.4.4.0.

linearly to the SM error; additional error sources are mostly CKM matrix elements (taken from tree-level measurements exclusively) and hadronic parameters (decay constants, taken from lattice calculations); to obtain the final theoretical uncertainty range, both higher-order and parametric uncertainties are varied within these previously-discussed limits.

- $(g-2)_\mu$  [41]: similarly to  $B$ -observables, we add a contribution to the  $\chi^2$  with experimental-SM input shown in Table 1, where the errors have been added in quadrature. The theoretical uncertainty associated to new-physics contributions and higher orders is calculated as the sum of a fixed error  $2.8 \cdot 10^{-10}$ , a 2% error estimate on 1-loop contributions (which do not involve coloured particles) and a 30% error estimate on 2-loop effects (involving coloured particles).

Additionally, given that a candidate for the interpretation of the signal observed at the LHC seems necessary, we require that the spectrum produces one CP-even Higgs state in the mass-range [120, 131] GeV.

Other limits are deliberately ignored, at least as implemented within NMSSMTools:

- dark matter searches: relic-density (via MicrOMEGAs), XENON 100 [42]. The reasons for not taking such limits into account come from the observation that they are strongly dependent on the SUSY spectrum, while we want to focus on the Higgs sector: confining to collider constraints allows us to handle simple supersymmetric spectra, which play a secondary part in our analysis, while these would likely have to be finely adjusted if one were to include, e.g., the relic-density bounds. We note also that the dark matter phenomenology may involve mechanisms (e.g. light gravitino LSP) which may alter the conclusions in the dark sector, while all such considerations are not the focus of our discussion.
- LEP Higgs searches:  $e^+e^- \rightarrow Zh$ ,  $h \rightarrow \text{inv.}, 2\text{jets}, 2\gamma, \{2A \rightarrow 4b, 4\tau, 2b + 2\tau, \text{light pairs}\}, e^+e^- \rightarrow hA \rightarrow 4b, 4\tau, 2b + 2\tau, 3A \rightarrow \{6b, 6\tau\}, Z \rightarrow hA$  ( $Z$  width);
- TeVatron limits on  $t \rightarrow bH^+, H^+ \rightarrow cs, \tau\nu_\tau, W^+\{A_1 \rightarrow 2\tau\}$ ;
- LHC Higgs limits:  $t \rightarrow bH^+, m_h \in [122, 129] \text{ GeV}$ , effective  $h\gamma\gamma, hbb, hZZ$  couplings excessive [43].

LEP, TeVatron and LHC limits on Higgs searches are checked through the code `HiggsBounds_4.2.0` [18], which we interfaced to NMSSMTools via a subroutine. `HiggsBounds` is used with the default settings, using hard cuts on the allowed regions and an individual test for all Higgs states (‘full’ method). Note that the more sophisticated implementation of limits on the Higgs sector within `HiggsBounds` leads to divergences with the channel-after-channel checks implemented within NMSSMTools, in particular in the LEP  $e^+e^- \rightarrow hA$  channels: as a consequence, lighter Higgs (doublet-like) states are accessible, while the corresponding points would be rejected by NMSSMTools. The version of `HiggsBounds` which we use includes all the released LHC limits till the end of 2014.

Another remark concerns the distinction between ‘hard-cut constraints’ and ‘observables to include in our fit’: it is bound to carry some arbitrariness. One could object, for instance, that implementing LEP limits as ‘hard cuts’, one loses the sensitivity to small deviations in the LEP data so that no benefit is

associated in the fit. On the other hand, those may prove to be only statistical fluctuations. In practice, we treat all search limits as hard cuts while observables kept in the fit have been actually measured.

**HiggsSignals\_1.3.1** [19] performs the comparison to the TeVatron+LHC-observed Higgs data, delivering a  $\chi^2$  fit to the Higgs-measurement observables. The version we employ collects all released experimental material till the end of 2014. Here follow a few remarks concerning the setting of the options that are offered.

- *Statistical test method* - Two statistical methods, ‘peak-centered’ (comparing theoretical and experimental signals at masses determined by the experimental signals) and ‘mass-centered’ (comparing theoretical and experimental signals at the masses that are defined by the theoretical input) are available in HiggsSignals. Only the ‘peak-centered’ test shall be performed. 81 channels are tested within the analysis.
- *Higgs pdf* - The probability density function assumed for the Higgs boson mass is modelled as a gaussian.
- *Theoretical mass uncertainties* - We allow for a  $\pm 3$  GeV uncertainty on the theoretical Higgs mass predictions delivered by NMSSMTools. This ensures that the phenomenology that we are discussing applies to the NMSSM and not to an arbitrary spectrum. Given also that our study is limited by the density of the scans that we perform, the mass uncertainty smoothens the impact of phenomenological limits. On the other hand, one could argue that, in view of the Higgs-like signals at LHC, the interesting part of the phenomenological study concerns the workings of a given spectrum, irrespectively to the model hiding behind. Moreover, considering that the NMSSM has a large number of parameters in the Higgs sector, it may be possible to absorb a substantial part of the higher-order corrections within a shift in parameter space. In such a context, one could be concerned that large mass uncertainties might blur the phenomenology and provide unlikely spectra with undue attention. Yet this feature does not happen and the scenarios that we propose would appear with qualitatively comparable fit values even though the mass uncertainty was set to be smaller.

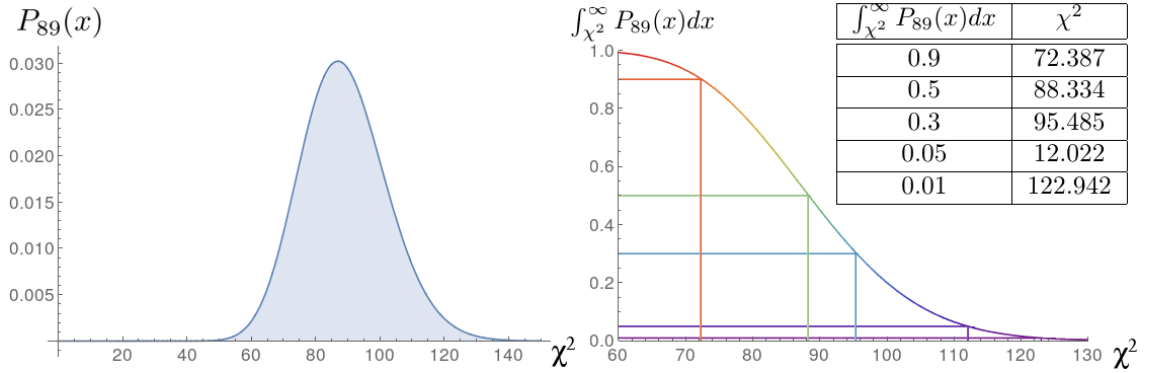


Figure 1:  $\chi^2$  distribution and a few values for the integral of its tail (P-values).

This  $\chi^2$  test to the Higgs-measurement data, delivered by HiggsSignals, is added to the corresponding tests from  $B$ -physics and  $(g-2)_\mu$ . The resulting quantity,  $\chi^2_{(total)}$ , will be at the center of our discussion in the following sections. Let us comment briefly on its interpretation. The  $\chi^2$  is the sum of squared deviations between experimental measurements and theoretical inputs, weighed by the corresponding uncertainties. Assuming the corresponding quantities are random and independent (gaussian) variables, the  $\chi^2$  would follow a probability law given by the  $\chi^2$ -distribution of  $N^{\text{th}}$  degree  $P_N$ , where  $N$  is the number of variables in the sum: in our case,  $N = 81 + 7 + 1 = 89$ , since there are 81 channels involved in the HiggsSignals test, 7  $B$ -observables and  $(g-2)_\mu$  finally. Correspondingly, one may define the compatibility of the  $\chi^2$  test (‘P-value’) as the probability to fall farther than the obtained  $\chi^2$  value (i.e.

the probability that the generated deviations be larger). With this definition, the compatibility of a  $\chi^2$  value with the test involving  $N$  degrees of freedom is obtained as:  $C(\chi^2) \equiv \int_{\chi^2}^{\infty} P_N(x) dx$ . In this context, for the  $\chi^2$  distribution of 89<sup>th</sup> degree, the compatibility of the spectrum with the data reaches 90% for  $\chi^2 \simeq 72$ , 50% for  $\chi^2 \simeq 88$ , 30% for  $\chi^2 \simeq 95$ , 5% for  $\chi^2 \simeq 112$  and 1% for  $\chi^2 \simeq 123$  (see Fig. 1). (Note that HiggsSignals directly provides an approximate P-value for the Higgs-fit.) This test would be the statistically relevant confrontation of one isolated point to the experimental data. This approach raises a few issues, however, as the corresponding statistics is then critically dependent on the list of tested channels and the precise definition of these. Moreover, we will not be considering isolated points but scan over various portions of the NMSSM parameter space, thus introducing degrees of freedom which would have to be subtracted from the statistical test. Absolute  $\chi^2$  values are thus difficult to interpret. Consequently, we will base our phenomenological discussion on relative  $\chi^2$ -differences with respect to a best-fit point, which prove to be a more robust interpretation in the given context.

### 3 SM and Decoupling limits

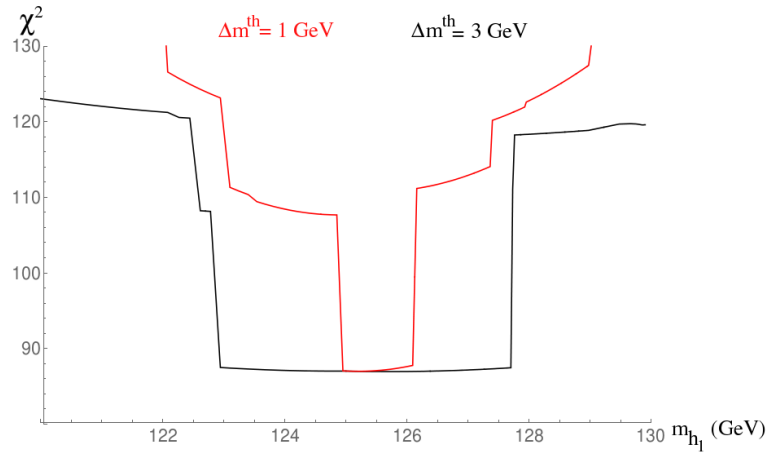


Figure 2:  $\chi^2$  in the SM-limit of the (N)MSSM, as a function of the SM-like mass:  $\tan\beta \in [1, 50]$ ,  $2M_1 = M_2 = \mu = 1$  TeV,  $M_3 = 3$  TeV,  $m_{\tilde{Q}} = 2$  TeV,  $m_{\tilde{L}} = 1$  TeV,  $A_t = -4$  TeV,  $A_{b,\tau} = -1.5$  TeV,  $M_A = 2$  TeV,  $A_\kappa = -1$  TeV,  $\lambda = \kappa = 1 \cdot 10^{-5}$ . While the uncertainty on the Higgs masses,  $\Delta m^{\text{th}}$ , is set to 3 GeV in the rest of the paper, we also include a plot for  $\Delta m^{\text{th}} = 1$  GeV here, in order to illustrate the impact of this quantity on the fit.

The Standard-Model limit of the NMSSM is obtained when decoupling the singlet sector – MSSM limit:  $\lambda \sim \kappa \rightarrow 0$ ; the singlet states then have vanishing couplings to their doublet counterparts, while an effective  $\mu$ -term,  $\mu \equiv \lambda \langle S \rangle$  is generated from the singlet v.e.v. – and pushing the masses of the MSSM non-standard states to very large values. The scale of the heavy doublet sector is controlled at tree-level by the parameter  $M_A$  – the doublet diagonal entry in the CP-odd Higgs mass matrix at tree-level – which can be used directly as an input (instead of  $A_\lambda$ ) within NMSSMTools: the decoupling condition reads  $M_A \gg M_Z$ . Similarly, the following scales enter the supersymmetric spectrum: the sfermion,  $m_{\tilde{f}}$ , gaugino,  $M_{1,2,3}$ , and higgsino,  $\mu$ , masses, which can be chosen far from  $M_Z$ . At low energy, one is then left with an effective SM, whose Higgs boson, the remaining light doublet Higgs state, has indeed SM-like couplings and a mass falling within the appropriate range ( $\sim 125$  GeV), provided soft stop terms  $A_t$  and moderate-to-large  $\tan\beta \gtrsim 10$  are chosen accordingly. New physics effects are then suppressed in accordance with the high scales that they involve or to the vanishing couplings of new states to the SM ones, so that this limit is virtually undiscernible (at low energy) from a genuine SM<sup>2</sup>. We consider this

<sup>2</sup>Note however that the higher the new-physics scales, the weaker becomes the case of supersymmetry as a solution to the hierarchy problem.

trivial scenario in order to ‘calibrate’ our fit – i.e. set a point of comparison with other NMSSM scenarios – and display our results in Fig. 2: the  $\chi^2$ -value is plotted as a function of the mass of the SM-like Higgs for a multi-TeV heavy supersymmetric and second-Higgs doublet spectrum. The best-fit points receive a  $\chi^2$  of about  $\sim 87$ , which statistically places the SM-limit within  $1\sigma$  compatibility with the considered observables. This fact is not surprising, since the measurements of the Higgs signal at the LHC are grossly consistent with a SM interpretation (within  $1\sigma$ ). Similarly, no tension develops in the  $B$ -sector, where the considered observables are also compatible with the SM. On the other hand, the SM-limit is difficult to reconcile with the anomalous magnetic moment of the muon, which generates a  $\chi^2$ -pull of  $\sim 8 - 9$  (depending on the chosen scale for the sleptons,  $m_{\tilde{l}}$ ): a limited departure from the strict SM limit – e.g. lowering sleptons and gaugino masses – would remedy this discrepancy. Finally, we wish to comment on the general aspect of the curves in Fig. 2: the minimum appears there as a broad step, extending from  $\sim 123$  GeV to  $\sim 128$  GeV. This appearance is driven by the treatment of the theoretical uncertainty on the Higgs masses,  $\Delta m^{\text{th}}$ , within HiggsSignals, as appears clearly when comparing both cases  $\Delta m^{\text{th}} = 1$  GeV and  $\Delta m^{\text{th}} = 3$  GeV.

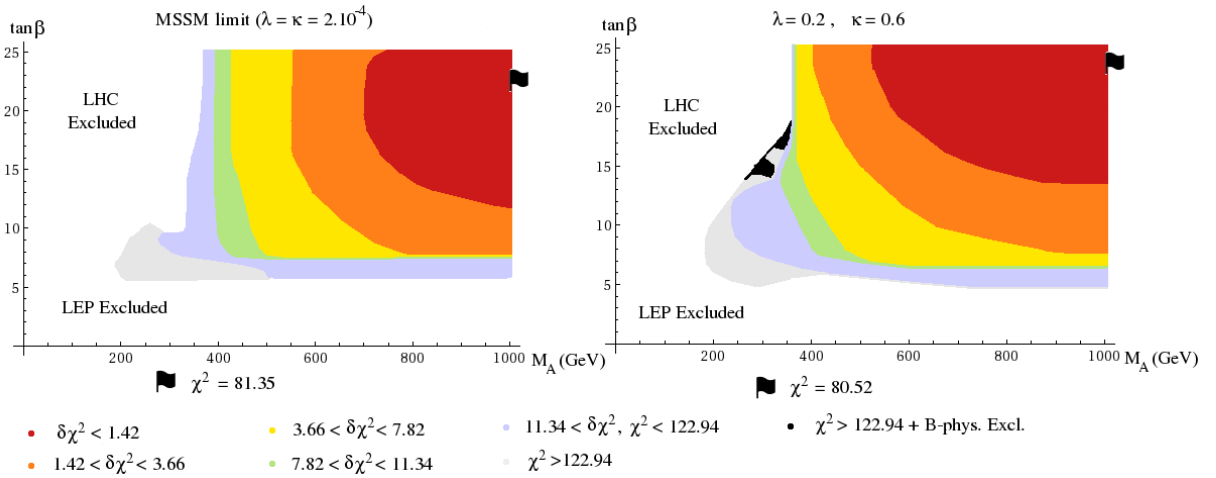


Figure 3: Scan in the  $\{M_A, \tan\beta\}$ -plane:  $\tan\beta \in [1, 25]$ ,  $M_A \in [50, 1000]$  GeV,  $A_\kappa \in [-1.5, 0]$  TeV,  $\mu = 200$  GeV,  $2M_1 = M_2 = 500$  GeV,  $M_3 = 1.5$  TeV,  $m_{\tilde{Q}_{1,2}} = 1.5$  TeV,  $m_{\tilde{Q}_3} = 1.1$  TeV,  $A_t = -2.3$  TeV,  $A_{b,\tau} = -1.5$  TeV.

Without turning to the full SM limit, the most frequent interpretation of the Higgs signal at  $\sim 125$  GeV within supersymmetric models consists in identifying it with the lightest Higgs state, this prejudice being motivated by the current absence of conclusive experimental signals for a Higgs boson at lower mass values. The corresponding configuration is most naturally achieved in the decoupling limit, that we define as  $M_A \gg M_Z$ , without necessarily requiring that the supersymmetric or the singlet spectra are much heavier: the light doublet state is then largely SM-like, at least at tree-level. The possible presence of new-physics particles at neighbouring scales might then affect the couplings of this light Higgs state at the radiative level, which would allow for tests in precision physics – unless the induced effect is negligible; note that the current LHC results allow for a relatively broad range of coupling strength in the vicinity of the SM values. The major concern in this configuration of the Higgs spectrum actually lies in generating a mass for the light doublet state in the appropriate range in order to identify it with the measured signals. In the MSSM limit ( $\lambda \sim \kappa \rightarrow 0$ ), this can be achieved by saturating the tree-level contribution to the mass  $\propto M_Z \cos 2\beta$  – therefore turning to  $\tan\beta \gtrsim 10$  – and relying on substantial loop corrections (heavy stops / large trilinear couplings). This solution can be extended to the NMSSM (i.e. departing from  $\lambda, \kappa \ll 1$ ), although specific NMSSM effects can also be employed, as we will show in the following sections. Here, we just illustrate the decoupling limit in Fig. 3, where we display the results of a scan in the plane  $\{M_A, \tan\beta\}$  both for the MSSM limit and a case with non-vanishing  $\lambda$  and  $\kappa$ . Both configurations lead to a fit result where the lowest  $\chi^2$  values are obtained in the range of large  $M_A$



( $O(\text{TeV})$ ) and significant  $\tan\beta$ , i.e. in the decoupling limit. The best-fit point is indicated in the plots by a flag. Note that the preference for  $\tan\beta \gtrsim 15$  is driven only partially by the requirement of a Higgs mass close to  $\sim 125$  GeV. The discrepancy of the SM with the anomalous magnetic moment of the muon can indeed be cured by supersymmetric contributions, which then favour sizable  $\tan\beta$ : this is the main pull in the  $\tan\beta$  direction, otherwise the  $\chi^2$  distribution is mostly flat as soon as  $\tan\beta \gtrsim 10$ . It should be noted that, while  $(g-2)_\mu$  in general favours large values of  $\tan\beta$  for a relatively heavy SUSY spectrum, the preferred range does of course depend on the details of the SUSY spectrum, and especially the masses of the sleptons and charginos / neutralinos. We also wish to comment that the main limiting factor at low  $\tan\beta$ , in Fig. 3, rests with the requirement of a Higgs state close to 125 GeV. As such this (LHC) constraint supersedes the LEP lower bound of  $\sim 114$  GeV for the mass of a SM-like state. Note also that the SUSY spectrum (and especially the masses and mixings in the stop sector) plays a crucial part in the resulting lowest value accessible for  $\tan\beta$  ( $\sim 5-6$  in Fig. 3), as it controls the magnitude of the radiative corrections to the mass of the light Higgs doublet.

## 4 Light CP-even singlet

A quite natural NMSSM scenario, already noted for its admissible application to a (speculative) enhancement of the  $h[\sim 125 \text{ GeV}] \rightarrow 2\gamma$  decay rate [23], is that of a light CP-even singlet state with mass under  $\sim 125$  GeV. This setup offers several interesting phenomenological features: the presence of a Higgs state around  $\sim 100$  GeV could account for a small excess observed in the  $h \rightarrow b\bar{b}$  LEP data [44]; furthermore, the mixing between singlet and doublet (for non-vanishing  $\lambda$ ) offers a lifting mechanism for the mass of the state identified with the LHC-observed signal; finally, the interplay with the singlet allows for an enhanced flexibility in the composition of the state at  $\sim 125$  GeV – the mixing matrix in the CP-even sector has now three mixing angles, instead of only one in the pure-doublet case – so that small deviations from SM-like couplings might be interpreted in this fashion. In contrast to the prejudice according to which light states should already have left tracks in experimental searches, the presence of a light CP-even singlet proves phenomenologically viable, as the large singlet component entails a suppressed production cross-section of this state – via a suppressed coupling to SM-particles, e.g. gauge bosons or fermions –, at colliders. Moreover, the singlet induces no major perturbation in the SM fermion and gauge-boson sectors. This scenario can be studied e.g. in the limit of a heavy decoupling  $SU(2)$  Higgs doublet.

In Fig. 4, we show such a region of the NMSSM parameter space, involving a heavy doublet sector ( $M_A = 1 \text{ TeV}$ ) and  $\tan\beta = 8$ : the points are distributed in the  $\{\kappa, \lambda\}$  plane. Points with  $\lambda^2 + \kappa^2 \gtrsim 0.7^2$  are discarded by the scan as they would lead to Landau Poles below the GUT scale. Moreover, the region with ‘large’  $\lambda$  and moderate  $\kappa$  tends to lead to unstable electroweak symmetry-breaking, as negative Higgs mass-squared are produced via the large singlet-doublet mixing (as soon as  $\tan\beta \gtrsim 5$ ). The best-fit points, with  $\chi^2$  down to  $\sim 75$ , involve a light singlet state: this fact is made evident when comparing the plots on both sides of Fig. 4, as the region including the best-fitting points (left-hand plot) largely coincides with that involving light singlets (right-hand plot). A determining factor for this correlation rests with the uplift of the mass of the light Higgs-doublet via the mixing effect (of only  $\sim 1-2$  GeV in the particular configuration of Fig. 4). Note that varying  $\tan\beta$  (or the squark spectrum) displaces the favoured region in the  $\{\kappa, \lambda\}$  plane: indeed the magnitude of the mass contribution, which originates from the mixing among Higgs-states and shifts the mass of the light doublet state to a value closer to the center of the LHC signals, changes accordingly. Another reason for the improved fit values in the presence of a light singlet is associated with small deviations (at the percent level) from the standard values in the couplings of the light doublet to SM particles: the mixing with the singlet results in an increased flexibility of the doublet-composition of the state, which in turn allows for a possibly improved match with the measured signals.

The composition of the two lightest CP-even states in the scan of Fig. 4 is displayed in the upper part of Fig. 5:  $S_{ij}$  denotes the orthogonal matrix rotating the CP-even Higgs sector from the gauge eigenstates – second index ‘ $j$ ’;  $j = 3$  stands for the singlet component – to the mass eigenbase – first index ‘ $i$ ’; the mass states are ordered with increasing mass. One observes that significant singlet-doublet mixing up to  $\sim 20\%$  can be reached in the vicinity of  $m_{h_1^0} \sim 100$  GeV, although best-fitting points show a mixing under  $\sim 5\%$ . This latter fact is related to the size of the mass-shift bringing the mass of the doublet-like

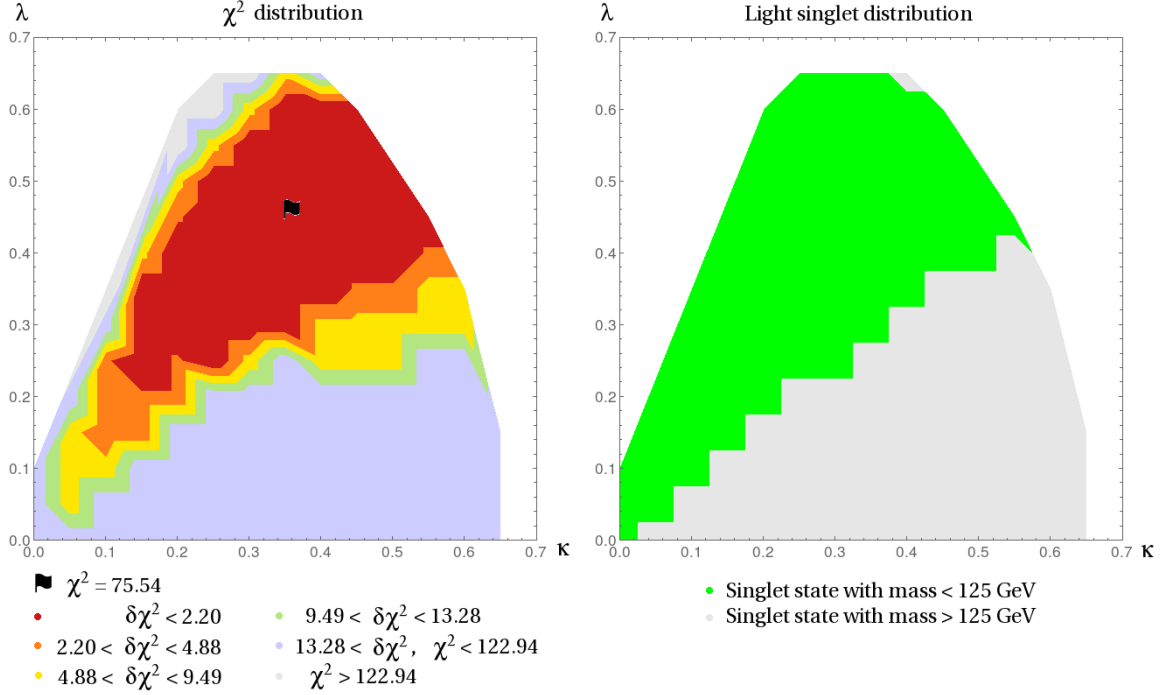


Figure 4: Scan in the  $\{\kappa, \lambda\}$ -plane for a heavy doublet sector:  $\tan\beta = 8$ ,  $M_A = 1$  TeV,  $A_\kappa \in [-2, 0]$  TeV,  $\mu \in [120, 2000]$  GeV,  $2M_1 = M_2 = 500$  GeV,  $M_3 = 1.5$  TeV,  $m_{\tilde{Q}_3} = 1$  TeV,  $m_{\tilde{Q}_{1,2}} = 1.5$  TeV,  $A_t = -2$  TeV,  $A_{b,\tau} = -1.5$  TeV. The plot on the left-hand side shows the  $\chi^2$  distribution in the plane while the one on the right identifies the region with light singlet states.

state  $m_{h_2^0}$  in agreement with the window of the LHC signal (larger mixing would lead to  $m_{h_2^0}$  beyond the desirable  $\sim 125$  GeV range in the present configuration).

This mass shift of the doublet state via its mixing with the light singlet,  $\Delta m_{h_2^0}$ , is defined in the following fashion: regarding the heavy doublet sector as essentially decoupled, the squared-mass matrix of the singlet and light-doublet CP-even Higgs states may be approximated as the decoupled block<sup>3</sup>:

$$\begin{pmatrix} m_{h_S^0}^2 & m_{h_S^0 h_D^0}^2 \\ m_{h_S^0 h_D^0}^2 & m_{h_D^0}^2 \end{pmatrix} = \begin{pmatrix} \cos\theta_S & -\sin\theta_S \\ \sin\theta_S & \cos\theta_S \end{pmatrix} \begin{pmatrix} m_{h_1^0}^2 & 0 \\ 0 & m_{h_2^0}^2 \end{pmatrix} \begin{pmatrix} \cos\theta_S & \sin\theta_S \\ -\sin\theta_S & \cos\theta_S \end{pmatrix} \quad (3)$$

Up to a sign, one can identify  $\cos\theta_S \simeq S_{13}$ , which determines the singlet-doublet mixing angle. In the presence of a lighter singlet-like state, the upward shift of the doublet state is defined as  $\Delta m_{h_2^0} \equiv m_{h_2^0} - \sqrt{m_{h_D^0}^2} \simeq m_{h_2^0} - \sqrt{m_{h_1^0}^2 + S_{13}^2(m_{h_2^0}^2 - m_{h_1^0}^2)}$ . This quantity, still for the scan of Fig. 4, is shown in the lower right-hand portion of Fig. 5: while the uplift in mass may reach up to  $\sim 8$  GeV, shifts of only 1 – 2 GeV are favoured by the fit in this particular scan. Note that the formula that we have just derived only makes sense if  $h_2^0$  is indeed the doublet-like state: for this reason, when displaying  $\Delta m_{h_2^0}$  as a function of  $m_{h_1^0}$ , we cut the plot at  $m_{h_1^0} < 120$  GeV, since, for  $m_{h_1^0} \gtrsim 120$  GeV, the doublet-like state is likely to become  $h_1^0$  in order to match the LHC signals at  $\sim 125$  GeV.

The plot on the lower left-hand side of Fig. 5 shows the squared-coupling of the singlet-like state  $h_1^0$  to  $Z$  bosons – controlling the production cross-section at LEP; it essentially coincides with  $1 - S_{13}^2$  here: at  $m_{h_1^0} \sim 100$  GeV, this quantity reaches  $\sim 5\%$  (for best fits) up to  $\sim 20\%$  of its SM value: for memory,

<sup>3</sup>Note that we derive here an approximate formula, under the assumption that the heavy doublet state has negligible effect. This approach is qualitatively justified, at least at the level of the mass shift, provided  $M_A \gg M_Z$ . A more exact expression, accounting for the heavy doublet state though losing somewhat in clarity, may be derived in a similar fashion however.

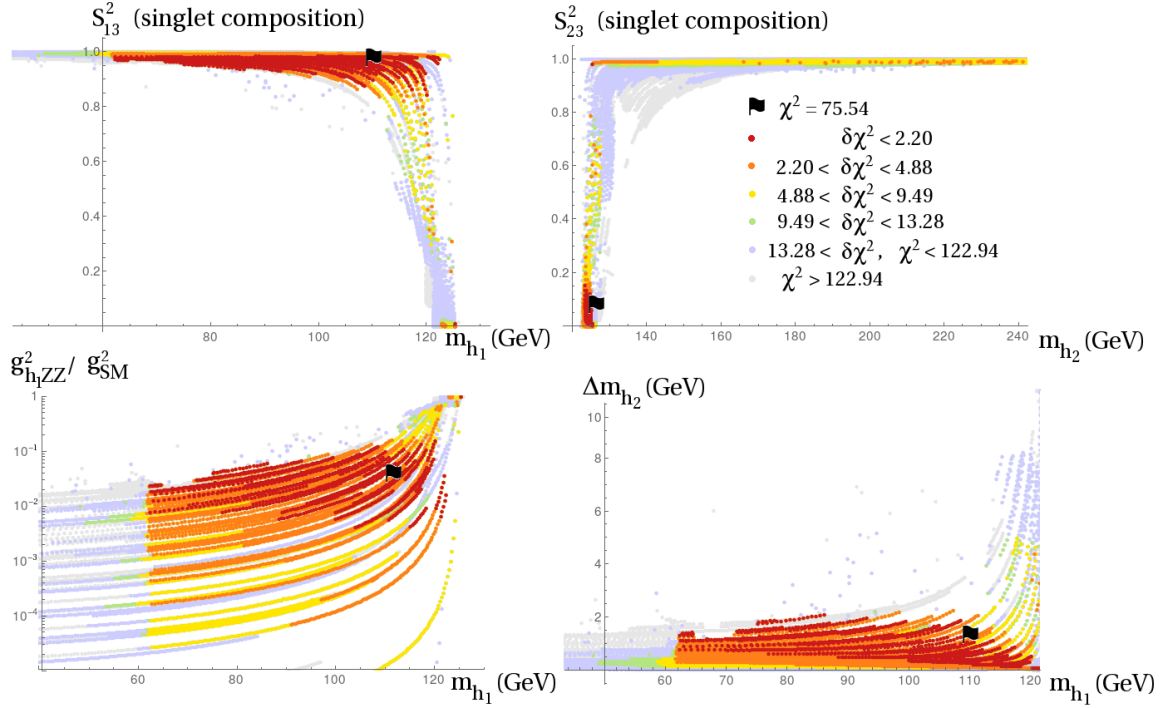


Figure 5: Same scan as in Fig. 4 but showing the characteristics of the CP-even states (mass, singlet-composition, relative squared coupling  $h_1 ZZ$ , mass-shift of the doublet-like  $h_2$ ).

the  $\sim 2.3\sigma$  LEP excess<sup>4</sup> in  $H \rightarrow b\bar{b}$  observed in this mass-range would be compatible with a Higgs-like state, the squared coupling strength of which is reduced to  $\sim 10\%$  of its SM value.

One can observe that (in this particular scan) the case where the lightest state is a doublet – represented by the limit  $S_{13}^2 \rightarrow 0$ ,  $m_{h_1^0} \rightarrow 125$  GeV – yields a slightly worse fit than the scenario with a lighter singlet: two factors are at work here. The first one is related to the value of the mass characterising the doublet (‘would-be-observed’) state in this limit: it typically reaches  $\sim 121 - 123$  GeV only – which lies on the margin of the uncertainty-allowed window. Note in particular that the mixing-effect tends to push the mass of the ‘visible’ state (now  $h_1^0$ ) into the ‘wrong direction’ (to lower it) when the singlet is heavier. Yet, for some of the points under consideration,  $m_{h_1^0}$  reaches  $\sim 125$  GeV, hence evades this first argument: in this case, the main penalty with respect to the points involving a lighter singlet originates from the details of the couplings of the ‘observed’ state to SM particles, hence of its production and decay rates at the LHC. While both configurations – with a lighter singlet or a lighter doublet – provide (doublet) couplings within a few percent of each other, and of those values that a SM Higgs boson at this mass would take, small deviations can provide a closer match to the LHC data. In our particular scan, for instance, the  $\gamma\gamma$  rate is slightly enhanced when the lighter state is dominantly singlet, resulting in an improved agreement with the ATLAS measurement.

More generally, the effects that the presence of a light singlet state may have on the couplings of the light doublet are related to the increased flexibility inherent in the  $3 \times 3$  Higgs-mixing matrix  $S_{ij}$  when compared to the case of a pure doublet  $2 \times 2$  matrix. While one degree of freedom controls the singlet-composition of the Higgs state at  $\sim 125$  GeV – i.e. its ‘invisible’, for phenomenological reasons subdominant, component –, the other two modulate the relative proportions amongst the two doublet components  $H_u$  and  $H_d$  – which are fixed in the case of pure doublets: in the limit  $M_A \gg M_Z$ , the corresponding  $H_d/H_u$  ratio would be  $\sim \tan^{-1} \beta$  –, therefore granting room for small deviations (or not, if the relative proportions are left unchanged) at the level of the couplings, with respect to the naive SM-like case. While this mechanism would offer an interpretation for slightly non-SM couplings, should

<sup>4</sup>Local significance without taking into account the ‘look-elsewhere’-effect.

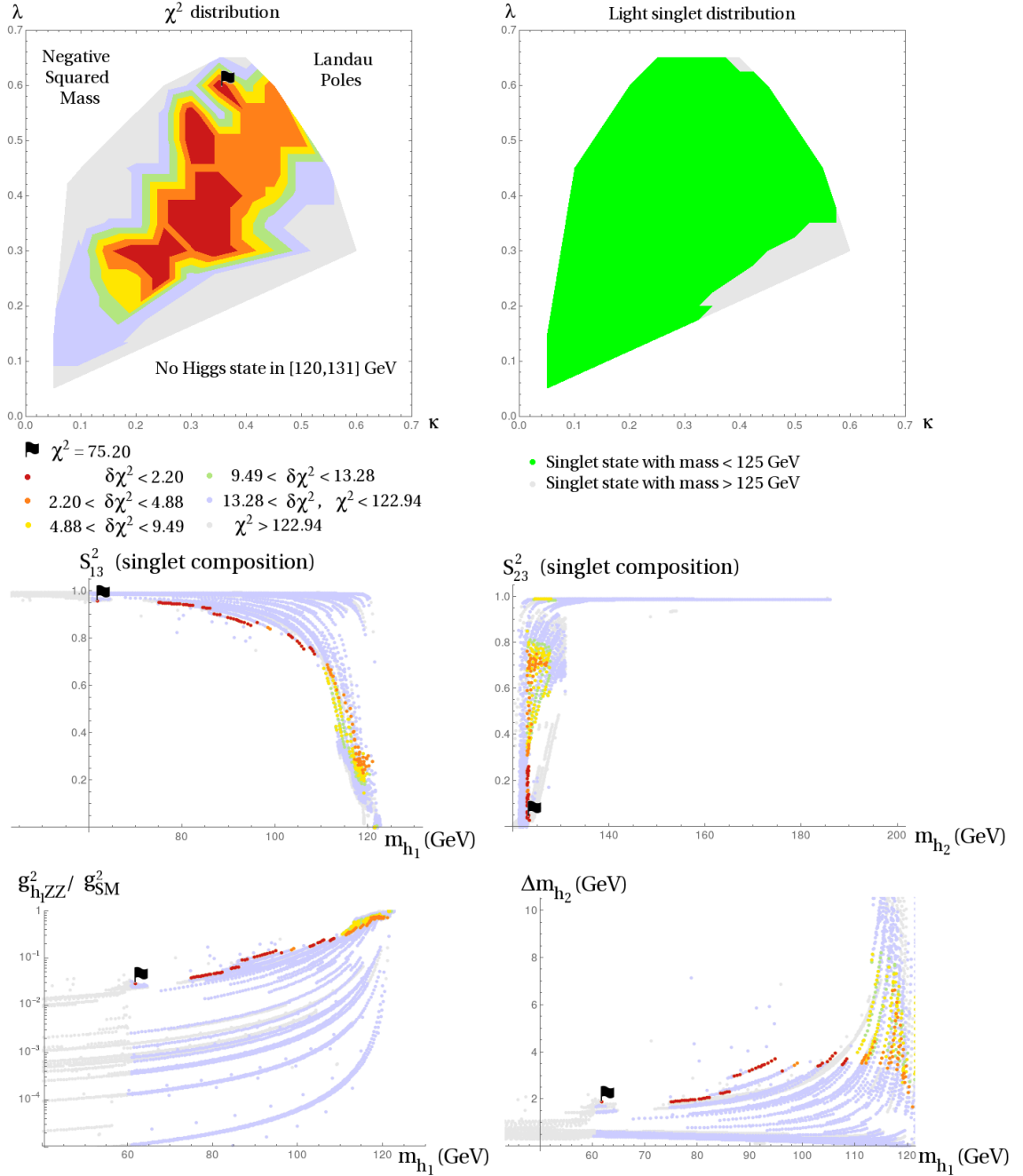


Figure 6: Scan in the  $\{\kappa, \lambda\}$ -plane for a heavy doublet:  $\tan\beta = 8$ ,  $M_A = 1$  TeV,  $A_\kappa \in [-2, 0]$  TeV,  $\mu \in [120, 2000]$  GeV,  $2M_1 = M_2 = 500$  GeV,  $M_3 = 1.5$  TeV,  $m_{\tilde{Q}_3} = 1$  TeV,  $m_{\tilde{Q}_{1,2}} = 1.5$  TeV,  $A_{t,b,\tau} = -1.5$  TeV.

this case be motivated by precision measurements of the Higgs properties, note that similar effects can also be obtained e.g. via loop-effects involving the supersymmetric spectrum. We shall come back to the question of non-standard couplings of the ‘observed’ state in the following section (5).

We complete this discussion with Fig. 6, whose scan differs from the previous one only by a lower value of the trilinear stop coupling  $|A_t|$  – which thus tends to decrease the magnitude of the corrections to the mass of the light doublet originating in radiative effects. The situation is essentially comparable to the

previous case, except for the fact that larger uplifts of the mass of the doublet-like  $h_2^0 - \Delta m_{h_2^0} \sim 2-4$  GeV – are now favoured. Larger singlet-doublet mixings, hence larger squared couplings of the light singlet to  $Z$  bosons,  $1 - S_{13}^2 \simeq 15 - 20\%$ , are correspondingly preferred, in the vicinity of  $m_{h_1^0} \sim 100$  GeV. With slightly heavier singlets  $m_{h_1^0} \simeq 110 - 115$  GeV, we observe that large mixings, up to  $\sim 25\%$  may appear. Note that the best-fit point lies in an isolated region with mass close to  $\sim 60$  GeV: this isolated position results both from the limited scan density and from the marginal situation with respect to the LEP limits.

Finally, we note that, in the plots of Fig. 5 and 6, the mass of the singlet may reach values as low as  $\sim 62$  GeV without spoiling the quality of the fit. The case of states under  $\sim 62$  GeV opens the possibility of  $h_2^0 \rightarrow 2h_1^0$  decays and will be treated in a separate section (6).

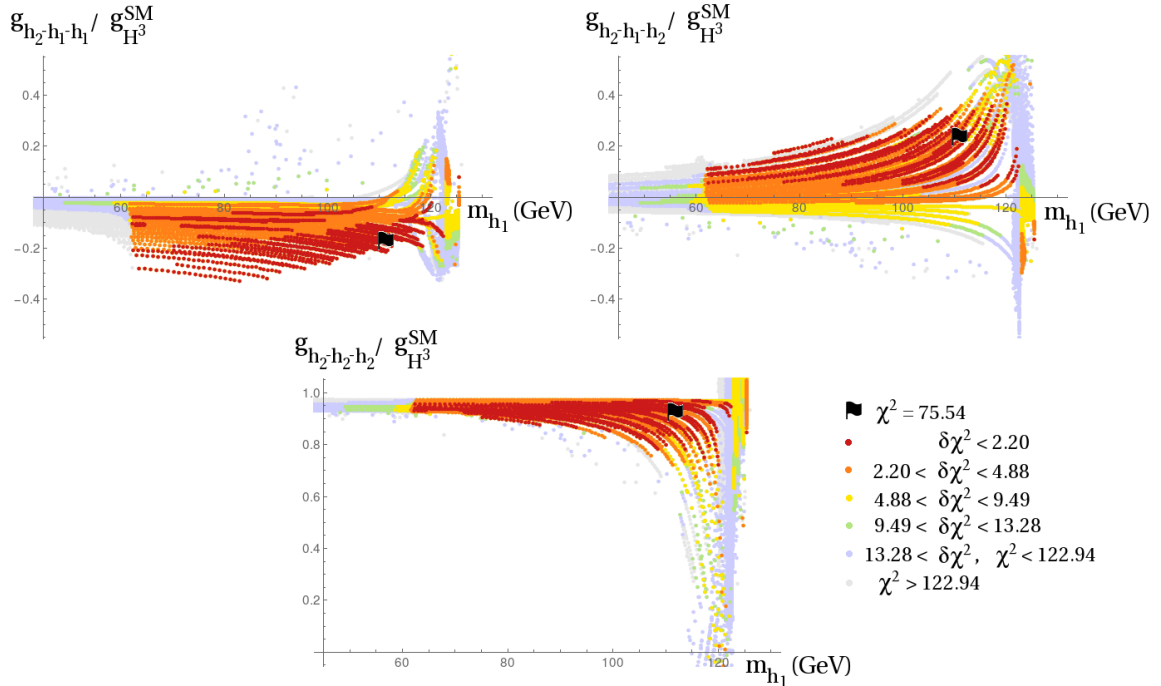


Figure 7: Same scan as in Fig. 4, now displaying the strength of the Higgs-to-Higgs couplings. The latter were normalized by the SM triple-Higgs coupling  $g_{H^3}^{SM} \simeq 192$  GeV (see text).

While precision tests at the level of the couplings of the Higgs state at  $\sim 125$  GeV could provide arguments in favour of this scenario involving a light singlet, as we already mentioned, the most convincing evidence would lie in the detection of the light singlet itself. The latter is likely to appear as a ‘miniature’ Higgs boson, i.e. with decay rates grossly comparable to those of a SM Higgs boson at the same mass but a reduced production cross-section (and a smaller width) – indeed the singlet component decouples from SM-particles and production is thus only achieved via a small doublet component. The observability of the singlet state thus critically rests with the magnitude of its doublet component. In the discussion above, we stressed that the doublet composition ( $1 - S_{13}^2$ ) of the light CP-even singlet may reach  $O(10\% - 20\%)$  and it is likely that the corresponding signal would be large enough to allow detection – at least in the form of a local excess, while discovery at the  $5\sigma$  level could remain challenging, provided the LHC searches are extrapolated to the low-mass region. Yet, apart from LHCb searches in the  $\tau\tau$  channel [45], which are still quite far from the necessary sensitivity in order to probe such a scenario, only the recent ATLAS results in the  $\gamma\gamma$  channel [46] consider masses below  $\sim 110$  GeV. (Note that, in the scans of Fig. 5 and 6, the typical cross-section at 8 TeV in the diphoton channel lies below 1 fb; see also the discussion of Fig. 11 below.) On the other hand, smaller singlet-doublet mixings, at the percent level or below, would also fit the picture adequately, allowing for a mass-uplift of the doublet and / or small variations in its couplings

to SM particles – such are actually the best-fit points of the scan in Fig. 4, which can be found in the appendix. The visibility of the light singlet in direct production should become increasingly difficult as its doublet component becomes small.

Alternative search strategies have been suggested, as the Higgs-to-Higgs couplings need not follow the same pattern as couplings to SM particles: singlet-doublet Higgs couplings could in principle allow for singlet production from e.g. the observed state, via Higgs-pair productions. It was stressed, however, that even such channels did not ensure the visibility of the light singlet, as the presence of this particle does not necessarily entail significantly larger inclusive rates than those of a single doublet state [32] (although an enhancement by a factor up to 2 – 3 has been reported for certain points). Let us highlight the fact that trilinear singlet-doublet couplings, while possibly as large as SM Higgs-to-Higgs couplings,  $g_{H^3}^{\text{SM}} \equiv \frac{3m_H^2}{\sqrt{2}v} \simeq 192 \text{ GeV}$ , where we took  $m_H^{\text{SM}} = 125.6 \text{ GeV}$ ,  $v \simeq 174 \text{ GeV}$ , may also remain much smaller without contradicting the light-singlet scenario. In Fig. 7, we display the strength of the triple Higgs couplings involving the light singlet and the light doublet in the scan of Fig. 4: while the trilinear coupling of the state  $h_2$  with mass  $\sim 125 \text{ GeV}$  remains SM-like, the couplings involving both singlet and doublet-like states reach only up to  $\sim 30\%$  of the SM-strength. Assuming that the cross section for pair production follows a similar pattern – which is only justified at high center of mass energy –, we see that a discovery in such channels would be challenging experimentally. On the other hand, pair production close to threshold is very sensitive to a small imbalance among triangle and box contributions so that the presence of a light singlet may affect this observable. An estimate of such effects goes beyond the scope of this paper, and we refer the reader to the discussions in [32]. As a summary, let us stress that, if Higgs-pair production is a viable search channel for light singlet states, should this state be present in nature, it does not automatically ensure the discovery of the singlet at the LHC. Production associated to Higgs-gauge couplings was also discussed in [36] but again depends critically on the magnitude of the doublet component of the light singlet-like state.

Other production modes would involve the supersymmetric spectrum or the heavy Higgs states. In particular, the decays  $h_3^0 \rightarrow h_1^0 h_1^0, h_1^0 h_2^0, h_2^0 h_2^0$  might be discovered for a resonant production of  $h_3^0$ . In this respect, NMSSM effects may intervene at several levels:

- The doublet-to-doublet Higgs couplings differ from their MSSM equivalent due to NMSSM-specific terms in the Higgs potential ( $\propto \lambda, \kappa$ ) so that the associated width may differ significantly.
- Singlet-doublet couplings induce a decay of the heavy Higgs into the singlet-like state.
- Kinematically accessible additional final states (e.g. singlinos) also affect the branching ratios of  $h_3^0$ . More generally, the branching ratios are strongly dependent on the details of the supersymmetric spectrum.
- The decay rates (into e.g.  $b\bar{b}, \gamma\gamma$ ) of the decay products  $h_1^0, h_2^0$  may vary with respect to the naive standard rates.

Unless the decay products  $h_1^0 h_1^0, h_1^0 h_2^0, h_2^0 h_2^0$  can be observed separately (using kinematical cuts), it would thus be difficult to infer the presence of a singlet from the inclusive rates, as several factors could explain a deviation from the predictions of a type II 2HDM.

Another remark on the decay rates of the light singlet is in order: as mentioned above, one may naively expect them to coincide (coarsely) with those of a SM Higgs boson at the same mass. Yet, it has also been stressed that these rates could show unconventional behaviours in specific cases, at low [47] or large  $\tan \beta$  [30]: couplings to down-type quarks could be suppressed indeed, which would lead to an apparent enhancement of decay channels such as  $c\bar{c}$  or  $\gamma\gamma$ . Extreme cases with an up-to-seven-times enhanced diphoton branching fraction of the singlet, allowing for cross-sections at the level of their SM equivalent – despite the reduced production cross-section –, have received much attention in view of their remarkable consequences on the possible discovery of such a singlet. We illustrate this possibility of non-conventional singlet rates with Fig. 8: with an intermediate value of  $\tan \beta = 12$ , we observe that the  $b\bar{b}$  branching fraction may be strongly suppressed, while the other rates (here  $c\bar{c}$  and  $\gamma\gamma$ ) are enhanced, together with acceptable fit values – note however that the best-fit points lie in a region of more SM-like behaviour.

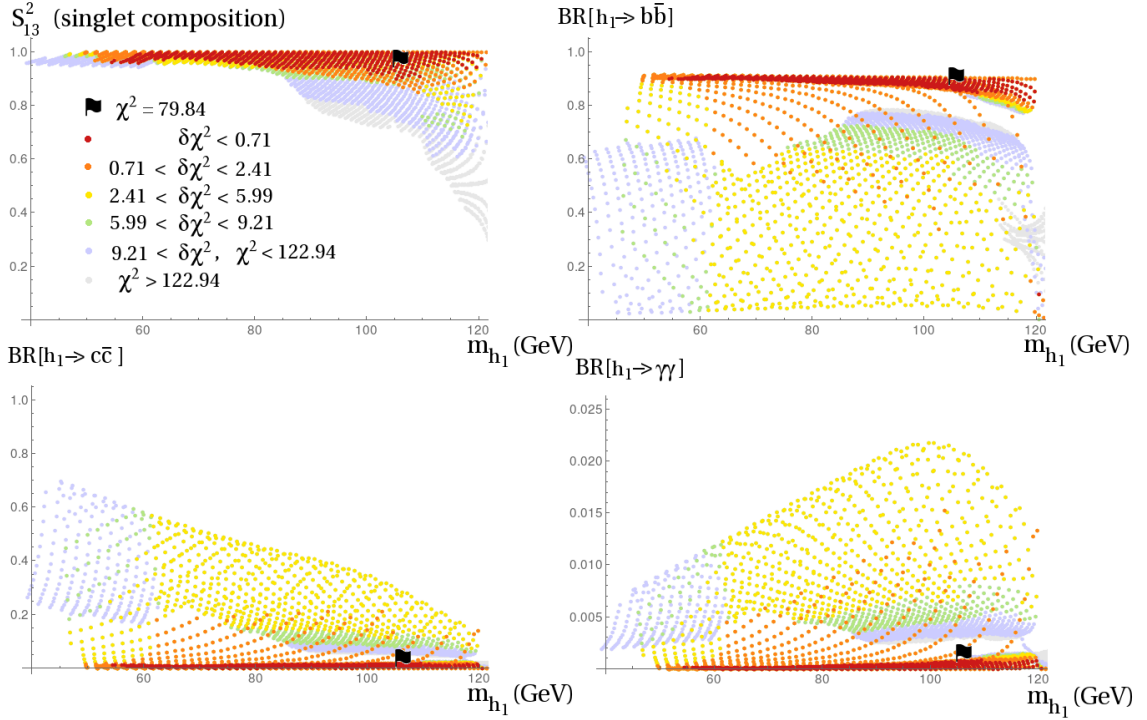


Figure 8: Modified rates of the light singlet:  $\lambda = 0.1$ ,  $\kappa = 0.05$ ,  $\tan\beta = 12$ ,  $M_A \in [0, 2]$  TeV,  $A_\kappa \in [-2, 0]$  TeV,  $\mu = 125$  GeV,  $2M_1 = M_2 = 500$  GeV,  $M_3 = 1.5$  TeV,  $m_{\tilde{Q}_3} = 1$  TeV,  $m_{\tilde{Q}_{1,2}} = 1.5$  TeV,  $A_t = -2$  TeV,  $A_{b,\tau} = -1.5$  TeV.

Note that points involving light singlets are quite common in the NMSSM parameter space. The only difficulty consists in stabilizing the low singlet mass and keeping the singlet-doublet mixing under control: too strong a mixing would push the squared mass of the lightest state towards negative values. The typical scale entering the singlet mass is  $\frac{\kappa}{\lambda}\mu$ , so that light singlets favour low ratios  $\kappa/\lambda$ . As  $\tan\beta$  increases, however, the balance among terms entering the mixing of the light doublet and singlet CP-even states is disturbed, such that the region with large  $\lambda$  and low  $\kappa$  becomes increasingly unstable. For larger values of  $\kappa/\lambda$ , one observes that  $\mu$  tends to be driven to low values  $\sim 100$  GeV – in order to keep the singlet mass at the electroweak scale without relying too much on accidental cancellations. This issue becomes even more severe when  $\lambda \sim \kappa$  becomes large: one then relies exclusively on the accidental cancellation in the singlet diagonal and the singlet-doublet mixing mass-matrix entries. It is therefore most natural to consider the scenario involving a light singlet in the low  $\tan\beta$  regime, allowing for small  $\kappa/\lambda$ : this is the focus of the next section.

## 5 Low $\tan\beta$ and large $\lambda$

The region with low  $\tan\beta$  ( $\sim 2$ ) and large  $\lambda$  ( $\sim 0.6 - 0.7$ ) is particularly interesting in the NMSSM parameter space: as we just mentioned, light CP-even singlets under  $\sim 125$  GeV appear most naturally there; furthermore, the squared mass of the light-doublet Higgs state receives an F-term contribution of the form  $\lambda^2 v^2 \sin^2 2\beta$  at tree-level (see e.g. Eq.(2.23) of [6]), which is maximized in this regime, so that significantly smaller radiative corrections than in the MSSM case are needed to reach the experimental value of the observed signal; finally, the region of low  $\tan\beta$  is ‘specific’ to the NMSSM, in the sense that current phenomenological requirements on the Higgs sector forbid it in the MSSM. One may typically consider this setup in the Peccei-Quinn (PQ) limit  $\kappa/\lambda \ll 1$  – note that, in view of the Landau Pole constraints, turning to relatively large values of  $\lambda$  automatically implies moderate values of  $\kappa$  anyway.



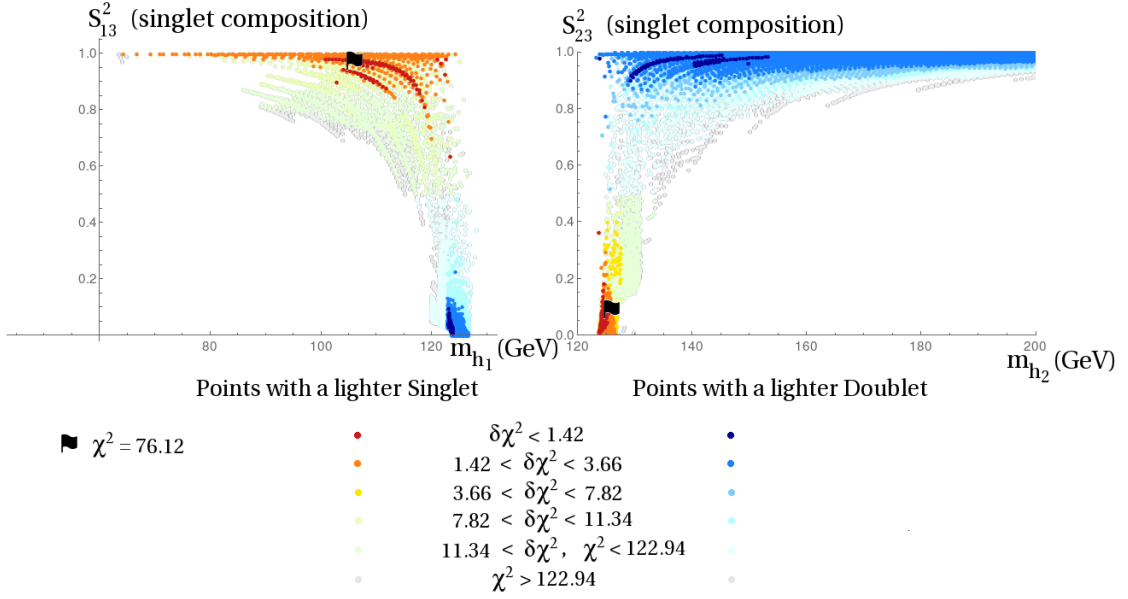


Figure 9:  $\chi^2$  in the PQ-limit of the NMSSM, with a very-light supersymmetric sector:  $\tan\beta = 2$ ,  $\lambda = 0.7$ ,  $\kappa = 0.1$ ,  $\mu \in [120, 2000]$  GeV,  $M_A \in [0, 3]$  TeV,  $A_\kappa \in [-500, 500]$  GeV,  $2M_1 = M_2 = 150$  GeV,  $M_3 = 1.5$  TeV,  $m_{\tilde{Q}_3} = 500$  GeV,  $m_{\tilde{Q}_{1,2}} = 1.5$  TeV,  $m_{\tilde{L}} = 110$  GeV,  $A_{t,b,\tau} = -100$  GeV.

Given that, in this context, one does not have to rely on large corrections from the stop sector to uplift the mass of the light doublet Higgs state into the mass range  $\sim 125$  GeV where it can be identified with the LHC-observed signal, we will consider moderate stop masses ( $\sim 0.5$  TeV) and trilinear couplings ( $\sim 0.1$  TeV). While we do not check the compatibility of this choice with LHC limits on supersymmetric searches, note that this is not a binding requirement but purely an illustration of the fact that radiative corrections to the Higgs mass are of lesser importance in this region of the parameter space: the specific tree-level contribution and / or the mixing with a light singlet are mechanisms enough to generate the mass of the light doublet Higgs state in the  $\sim 125$  GeV range. In fact, if in this regime the SUSY sector is such that it generates large radiative corrections to the mass of the light Higgs doublet state (e.g. via a sizable mixing in the stop sector), this would lead to predictions for the mass of the light doublet state in the region of low  $\tan\beta$  and large  $\lambda$  that tend to be higher than the mass value detected at the LHC – up to  $\sim 140$  GeV if it is the lightest CP-even state and beyond if it is the second lightest: see e.g. [10]. Yet, a Higgs mass that is compatible with the observed value can still be obtained even in the presence of large contributions from both the NMSSM tree-level and SUSY radiative corrections through the effect of the mixing between the doublet and the singlet. This mixing effect lowers the mass of the light CP-even doublet, provided the singlet is heavier. Note finally that  $B$ -physics is of almost no concern in this scenario since both charged-Higgs and supersymmetric effects remain small, due to a heavy  $H^\pm$  (decoupling limit) and low  $\tan\beta$  (absence of an enhancing-factor in radiative effects). On the other hand, low values of  $\tan\beta$  tend to suppress supersymmetric contributions to  $(g-2)_\mu$ , translating into a typical pull of a few units in  $\chi^2$ . The presence of light sleptons / charginos / neutralinos (with mass close to 100 GeV) could balance this effect, however, so that we will assume low masses for these states in the following.

Fig. 9 shows the  $\chi^2$  distribution in a scan where  $\tan\beta = 2$ ,  $\lambda = 0.7$ ,  $\kappa = 0.1$ , and the supersymmetric spectrum is relatively light (at least for the third generation of sfermions, with small trilinear couplings). The plots illustrate how the fit distributes in terms of the mass and singlet composition – i.e. singlet component squared  $S_{i3}^2$  – of the first and second lightest CP-even Higgs states. Points where the lightest Higgs state has a dominantly singlet nature ( $S_{13}^2 > 0.5$ ) are shown in yellow-red shades. Bluish tones



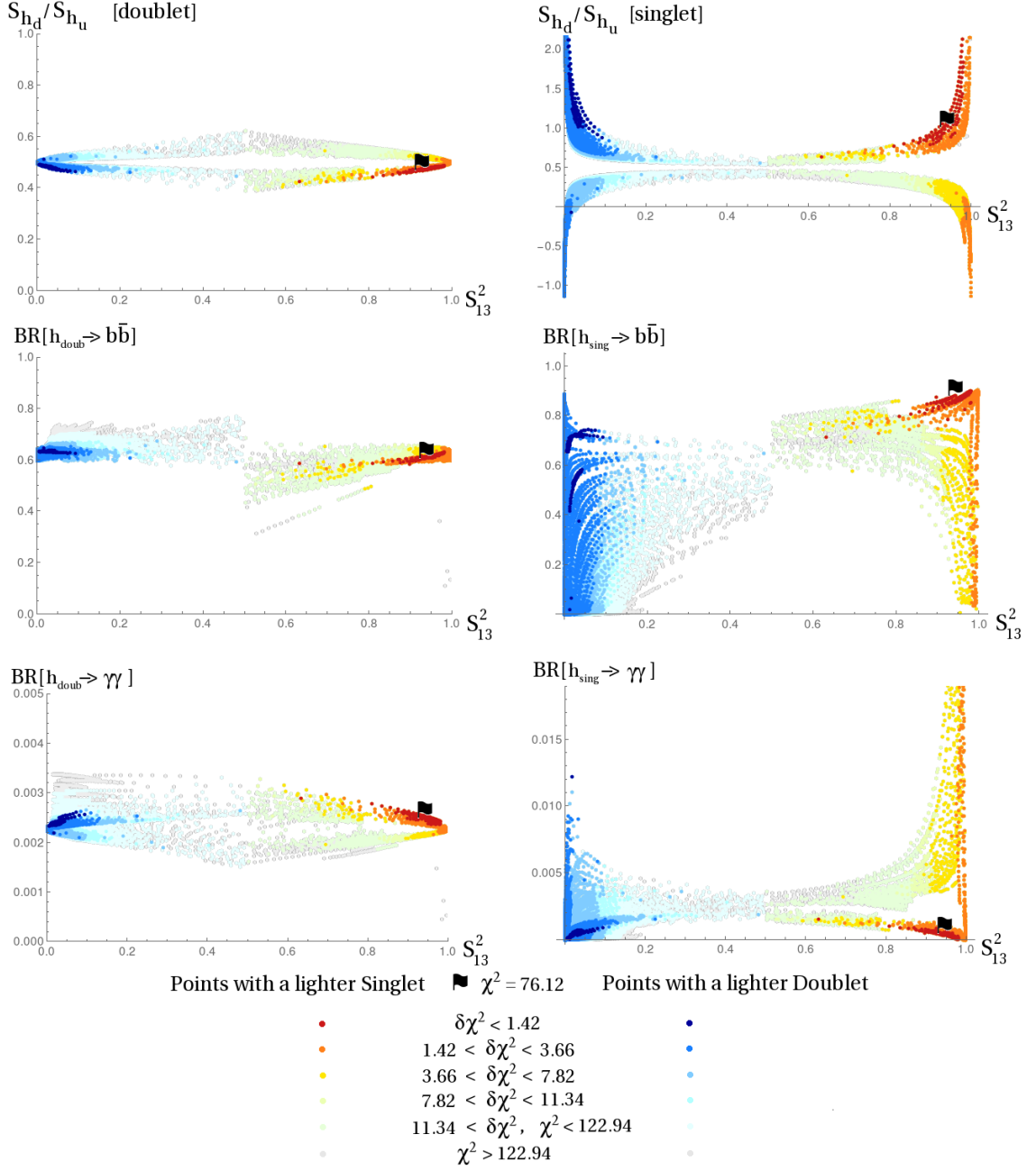


Figure 10: Same scan as in Fig. 9: consequences of the three-state mixing on the couplings of the light states are shown. The plots on the left concern the mostly-doublet state (identified with the observed signal at  $\sim 125$  GeV); those on the right give information concerning the lighter (yellow-red points) or heavier (bluish points) singlet. The first pair of plots displays the proportion of  $H_d/H_u$  components (in comparison to the value  $\tan^{-1}\beta = 0.5$  expected in the decoupling limit). The branching ratios into  $b\bar{b}$  and  $\gamma\gamma$  are provided in the lower part of the figure.

correspond to points where the lightest state is dominantly doublet ( $S_{13}^2 < 0.5$ ). Both configurations give an excellent agreement with the measurements reported by the LHC and the TeVatron, and their fit values improve somewhat on the SM limit. One observes that the best fit points (with  $\chi^2 \sim 76 - 79$ )

tend to cluster in the vicinity of  $S_{13}^2 = 0$  or 1, that is for moderate singlet-doublet mixing. This seems reasonable since one expects a ‘full’ doublet state at  $\sim 125$  GeV: the corresponding experimental signals would have been suppressed in proportion to the singlet composition otherwise. Still, fairly large values of the mixing ( $S_{13}^2 \sim 0.5$ ) turn out to be a possible scenario, giving acceptable  $\chi^2 \sim 77-80$ : this situation occurs only when both states are almost degenerate and within a few GeV of  $\sim 125$  GeV. This last configuration will be studied in more detail in section 7.

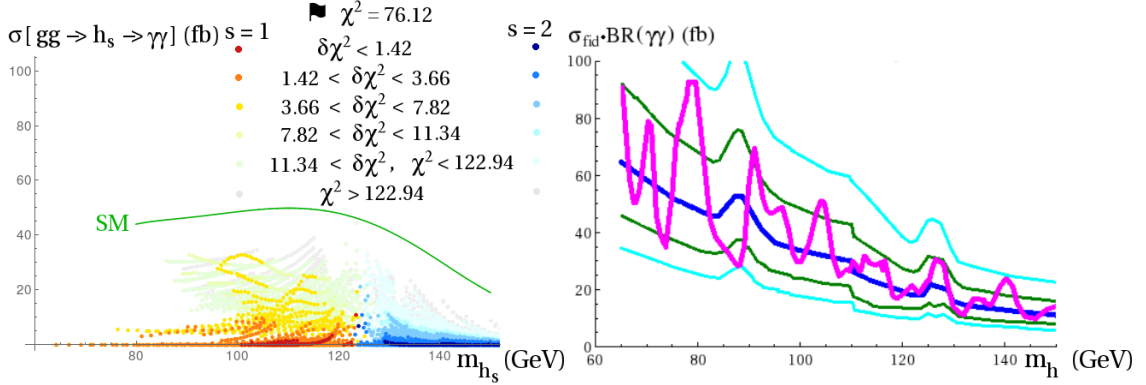


Figure 11: On the left: gluon-gluon-fusion cross-section for the mostly-singlet state, then decaying into a pair of photons, for a center of mass energy of 8 TeV, resulting from the scan of Fig. 9; the corresponding value for a SM Higgs boson is given by the green curve. On the right, a reproduction of the ATLAS limit on the fiducial cross-section for a light Higgs state (in the presence of the  $\sim 125$  GeV one) decaying into photons.

In Fig. 10, we display some information concerning the coupling properties of the light states to SM particles obtained with the scan of Fig. 9: the plots on the left-hand side illustrate the possible effects that the three-state mixing could have on the couplings of the doublet-like state – the one which is identified with the LHC-observed signal. The plot on the upper part shows the proportion of  $H_d/H_u$  components in this state as a function of the mixing: deviations of up to  $\sim 25\%$  appear relative to the naive ratio  $0.5 = \tan^{-1} \beta$  (expected in the decoupling limit), and the maximal effects are obtained for maximal mixing  $S_{13}^2 \sim 0.5$ . Deviations at the level of the branching ratios reach  $\sim 25\%$  for  $b\bar{b}$  and  $\sim 50\%$  for  $\gamma\gamma$ . Note that best fit regions favour more moderate variations however. Note also that, even for large mixings, the deviations in doublet proportions or in branching ratio may remain negligible.

The plots on the right-hand side of Fig. 10 provide similar information but concerning the singlet-like state. We observe that the corresponding coupling properties may depart very significantly from the naive behaviour when the state is almost purely singlet – that is, in the vicinity of  $S_{13}^2 \sim 0$  and  $\sim 1$  – and that the corresponding points offer excellent fit to the Higgs data. The  $b\bar{b}$  channel may then become subdominant while the diphoton channel is enhanced by a factor of up to  $\sim 7$ . In such a spectacular case, the light singlet could be more easily observed in direct production at the LHC. On the other hand, the fit tends to associate the large diphoton branching fraction tightly with the limit of a pure singlet state, that is with vanishing production cross-sections. Note also that the naive scenario of a singlet-like state with dominant decays towards down-type fermions is also represented and actually provides the best-fit points of the scan. Unconventional decay rates also appear as a possibility when the singlets are beyond  $\sim 125$  GeV (blue points), even though the maximal diphoton rates remain below  $\sim 1\%$ .

In Fig. 11, we study how the Higgs production cross-section at 8 TeV compares to the ATLAS limits on the fiducial cross-section for the diphoton decay channel [46]. We estimated the cross-section for the light Higgs states of the scan of Fig. 9 in the following way: we multiplied the SM gluon-gluon-fusion cross-section delivered by SUSHI [48] by the squared effective coupling of  $h_1^0$  to gluons, relative to its SM value at the same mass, and the diphoton branching ratio of  $h_1^0$ . We observe that the cross-section may almost reach the order of magnitude probed experimentally, both when the singlet is heavier or lighter than 125 GeV (note that in the immediate vicinity of 125 GeV, comparing the cross-section of the

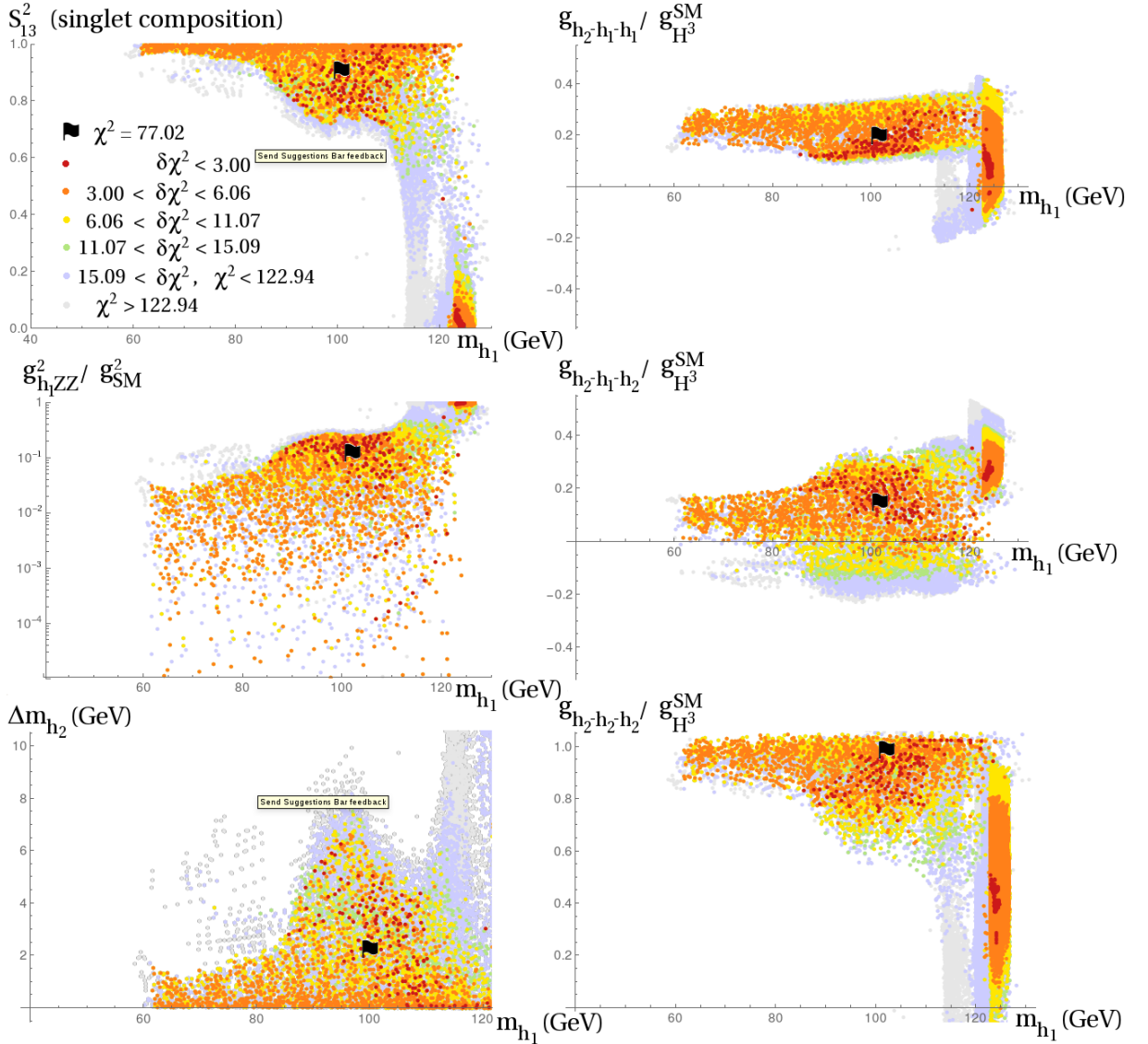


Figure 12: Similar to Fig. 9, but with an additional scan on  $\tan \beta \in [1, 4]$  and  $\lambda \in [0.6, 0.7]$  in order to probe possible singlet-doublet mixing. On the left-hand side, from top to bottom: singlet composition of the light CP-even Higgs state, squared coupling of the light Higgs state to  $Z$ -bosons relative to the SM, size of the mass-uplift for the doublet state (as defined in the previous section). On the right-hand side: magnitude of the triple Higgs couplings (relative to  $g_{H^3}^{SM}$ ).

mostly-singlet state with the ATLAS limit has limited sense, due to the possibly large mixing between singlet and doublet states), although the best-fitting points tend to cluster around much smaller values – at or below the 1 fb range. Further searches in the low-mass region, in the diphoton but also in the fermionic channels, would be an interesting probe and place limits on the light-singlet scenario.

In Fig. 12, we vary  $\tan \beta$  and  $\lambda$  somewhat so as to modulate the strength of the F-term contribution to the tree-level doublet Higgs mass. As a result, larger singlet-doublet mixings are favoured: the two-state mixing uplift can indeed compensate the decreased tree-level contribution and thus help maintain the mass of the light doublet state in the vicinity of  $\sim 125$  GeV. In agreement with our discussion in section 4, we observe that large singlet-doublet mixing, up to  $\sim 25\%$ , may be achieved for a singlet mass in the range  $[90 - 100]$  GeV, with excellent fit-values to the Higgs measurement data. Therefore, this low

$\tan\beta$  regime also motivates the search for a light singlet state, possibly responsible for the  $\sim 2.3\sigma$  (local) excess in the LEP  $e^+e^- \rightarrow Zh \rightarrow b\bar{b}$  channel. The magnitude of the mass uplift for the doublet state in this region may again reach up to 6 – 8 GeV, as we observe on the plot on the bottom left-hand side of Fig. 12.

Concerning the prospects of discovery of the light state in pair production, the Higgs-to-Higgs couplings in the scan of Fig. 12 are displayed on the right-hand side of this figure. The typical magnitude is about 10 – 40% of  $g_{H^3}^{\text{SM}}$  for  $h_2 - h_1 - h_1$ , 0 – 30%, for  $h_2 - h_2 - h_1$ , and 85 – 100%, for  $h_2 - h_2 - h_2$  (in the region where the lightest state is a singlet). The impact of the singlet-doublet couplings on the apparent Higgs pair production cannot be simply estimated as the latter depends on several interfering diagrams. We see however that the typical couplings reach  $\sim 30\%$  of the pure-doublet value.

Although all these observations are essentially similar to our discussion in section 4, the crucial point rests upon the fact that such a Higgs phenomenology is also achievable in this low  $\tan\beta$  / large  $\lambda$  regime, *without* relying on large radiative corrections to the Higgs masses. This provides a motivation for relatively-light supersymmetric spectra (at least, as far as the third generation is concerned). In the case where the search for stops at the LHC would provide experimental support for such a configuration, deviations of the Higgs couplings from the SM expectations could be generated at the loop level and be addressed in precision tests.

## 6 Light CP-odd (even) Higgs states under $m_{h[125]}/2$

A durably-considered NMSSM scenario (see for instance [49]) is that involving light neutral states, e.g. a light CP-even singlet or a light CP-odd state, allowing for unconventional Higgs decays ( $h \rightarrow 2A_1/2h_1$ ). As the width of a SM-like Higgs is quite narrow –  $\sim 4$  MeV at  $\sim 125$  GeV –, Higgs-to-Higgs decays can easily dominate the width of a Higgs state as soon as they are kinematically allowed. This configuration could have explained the invisibility of a doublet Higgs state  $h$  at LEP – provided  $m_h \gtrsim 85$  GeV (i.e. above the limit from the decay-mode independent search [50]) and  $A_1 \rightarrow \tau^+\tau^-$  would represent the dominant decay channel of the pseudoscalar. Furthermore, this mechanism suggested an interpretation of the  $2.3\sigma$  (local) excess in  $e^+e^- \rightarrow Zh \rightarrow b\bar{b}$  originating from suppressed branching ratios into SM particles of a CP-even state at  $\sim 100$  GeV, instead of a suppressed production as in the case of a light singlet, and would have led to a reduced visibility of the conventional channels at the LHC – even if the light CP-even doublet had been heavier than 100 GeV. Considering the success of these conventional searches and the approximately SM-like behaviour of the LHC-observed state, Higgs-to-Higgs decays of the SM-like state no longer appear as a favoured option, unless one would correspondingly enhance the SM-like modes, which is not easily achieved in the context of the NMSSM. Yet, we already noted in the previous sections that the existence of light states – under the kinematic threshold at  $\sim 62$  GeV – was still possible (see e.g. Fig. 5); we will discuss here under what conditions. In brief, if the invisible decay channel is not kinematically closed, compatibility with the measured rates of the observed signal demands the decoupling of the light state – suggesting a singlet-like nature with reduced Higgs-to-Higgs couplings [33].

Fig. 13 shows how the fit distributes in the presence of light CP-odd Higgs states. Note that the SUSY sector, in particular the mixing in the stop sector, is set to provide radiative corrections to the mass of the light doublet Higgs of the appropriate magnitude in view of the signal at  $\sim 125$  GeV, as already discussed in section 3. While  $\tan\beta$  is left free, larger values  $\gtrsim 10$  are accordingly favoured by the requirement of a SM-like Higgs state at  $\sim 125$  GeV, but also by  $(g-2)_\mu$  (for which the exact preferred range is determined by our choice of spectrum in the slepton, neutralino and chargino sectors). One observes in the plot on the top left-hand quadrant that, when the CP-odd Higgs is lighter than half of the mass of the ‘observed’ Higgs, its doublet composition<sup>5</sup> must fall under  $\sim 1\%$  to provide an acceptable fit to the data, while fairly larger singlet-doublet mixings are allowed beyond this mass. This condition can be interpreted as follows: if the channel  $h[\sim 125 \text{ GeV}] \rightarrow 2A_1$  is not kinematically forbidden and  $A_1$  has a significant doublet component, doublet Higgs couplings lead to a large (dominant) decay of the

<sup>5</sup>Similarly to the CP-even case, we denote the mixing matrix in the CP-odd sector as  $P_{ij}$ , with  $i$  the mass-state index and  $j$  the flavour index;  $j = 3$  stands for the singlet component.

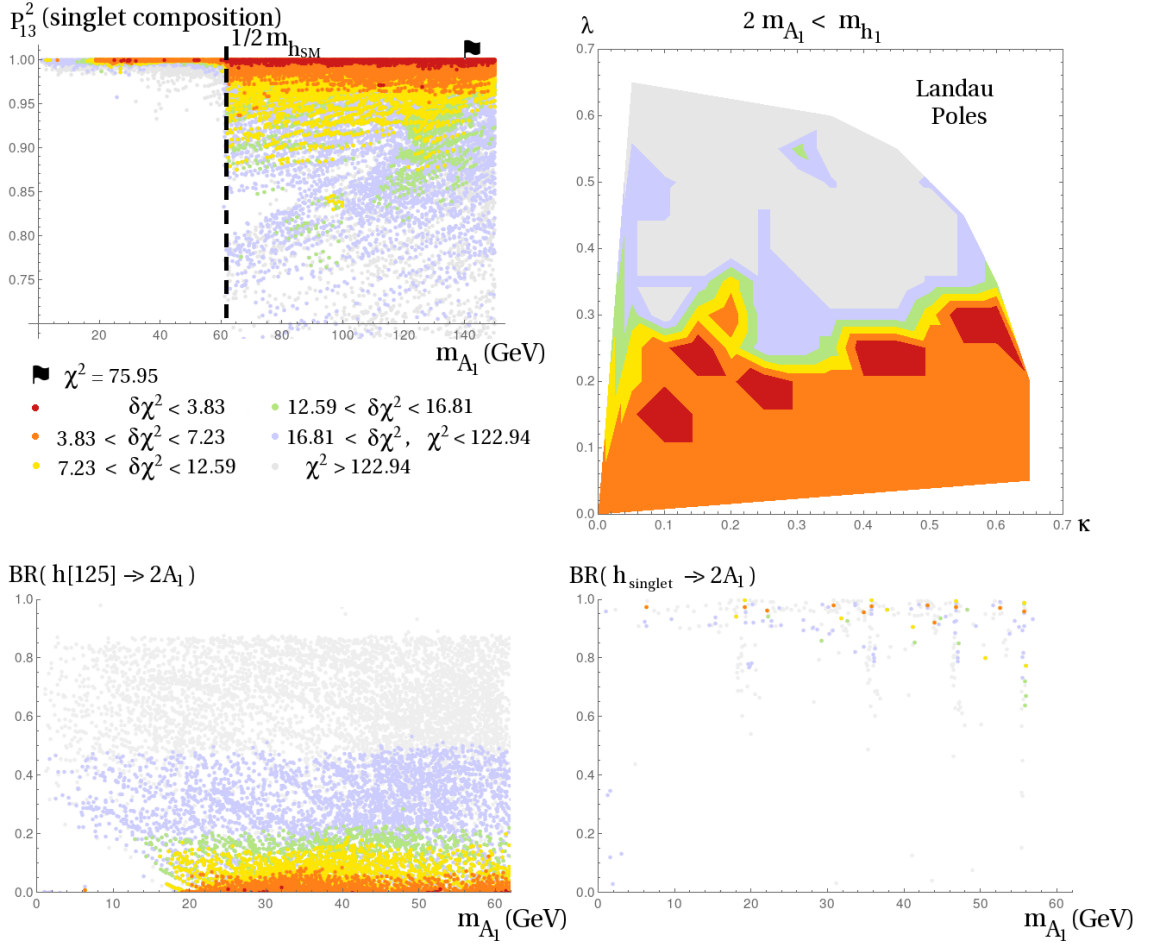


Figure 13:  $\chi^2$  in the presence of a light CP-odd Higgs:  $\tan\beta \in [2, 22]$ ,  $M_A \in [200, 1200]$  GeV,  $\mu \in [120, 1600]$  GeV,  $A_\kappa \in [-400, 400]$  GeV,  $\lambda \in [2 \cdot 10^{-4}, 0.65]$ ,  $\kappa \in [2 \cdot 10^{-4}, 0.65]$ ,  $2M_1 = M_2 = 500$  GeV,  $M_3 = 1.5$  TeV,  $m_{\tilde{Q}_{1,2}} = 1.5$  TeV,  $m_{\tilde{Q}_3} = 1.2$  TeV,  $A_t = -2.5$  TeV,  $A_{b,\tau} = -1.5$  TeV. The top-left plot shows the distribution of  $\chi^2$  as a function of the light CP-odd mass and the singlet composition of this state ( $P_{13}^2$ ); on the right, distribution of the points with  $m_{A_1} < 62$  GeV in the  $\{\kappa, \lambda\}$  plane. The figures at the bottom give the branching ratios  $h[\sim 125 \text{ GeV}] \rightarrow 2A_1$  on the left and  $h_{\text{singlet}} \rightarrow 2A_1$  (in the presence of a singlet as the lightest CP-even state) on the right.

state  $h[\sim 125 \text{ GeV}]$  – which is identified with the LHC Higgs discovery – into a pair of pseudoscalars; yet, this is in contradiction with the roughly standard behaviour of the signal observed at the LHC, hence a disfavoured possibility; it thus follows that the light pseudoscalar with mass under the threshold must be essentially singlet in nature, for its presence not to spoil the fit to LHC Higgs data. Note, on the other hand, that for masses beyond 62 GeV, the doublet composition of the light CP-odd state can reach up to  $\sim 100\%$ , as we will discuss in the light-doublet section (8). However, apart from this rather isolated possibility, LHC limits – in particular searches in the  $\tau\tau$  channel – do not leave much room for heavy Higgs doublets under  $\sim 400$  GeV (see e.g. Fig. 3): as a result, the doublet composition of the light CP-odd state (beyond 62 GeV), though possibly larger than for masses below the threshold, does not take large intermediate values (or only for disfavoured fits).

Coming back to CP-odd states under the kinematic threshold of  $h[\sim 125 \text{ GeV}] \rightarrow 2A_1$ , one would naively expect favoured values of the parameter  $\lambda$  to remain moderate, in order to suppress singlet-doublet couplings which may still allow for a significant decay width of the SM-like state into singlet

pseudoscalars. Yet, when one considers the distribution of the points with  $m_{A_1}$  under 62 GeV in the  $\{\kappa, \lambda\}$  plane (right-hand side of Fig. 13), it turns out that values of  $\lambda$  up to 0.3 still give an excellent fit to the LHC / TeVatron data. Two factors should be considered in order to understand this fact. The first one is related to the observation that the decay  $h[\sim 125 \text{ GeV}] \rightarrow 2A_1$  receives a kinematic suppression in the immediate vicinity of the kinematic threshold: this effect leaves some manoeuvring space for moderate  $h[\sim 125 \text{ GeV}] - A_1 - A_1$  couplings. However, the second, and main, reason for the compatibility of rather large values of  $\lambda$  with the Higgs measurement data in the presence of a light  $A_1$  originates from accidental cancellations within the  $h[\sim 125 \text{ GeV}] - A_1 - A_1$  coupling. The latter indeed involves several terms (which are pondered by mixing angles and numerical coefficients):

1. doublet-doublet interactions  $\propto g^2 v$ : their effect on the  $h[\sim 125 \text{ GeV}] - A_1 - A_1$  coupling is suppressed when the pseudoscalars have a mostly singlet nature, as we mentioned before;
2. singlet-singlet interactions  $\propto \kappa A_\kappa$  and  $\kappa^2 s$ : the state at  $\sim 125 \text{ GeV}$  being essentially doublet (to ensure a SM-like behaviour), such terms would also contribute little to the  $h[\sim 125 \text{ GeV}] - A_1 - A_1$  coupling; some effect can develop in proportion to the singlet component of the CP-even doublet, however;
3. singlet-doublet interactions  $\propto \lambda^2 v$ ,  $\propto \lambda \mu$ ,  $\propto \lambda M_A^2 / \mu$ ,  $\propto \lambda \kappa v$  and  $\propto \kappa \mu$ : they naively dominate the couplings of the light CP-even doublet and the singlet pseudoscalar.

The interplay of these various terms can thus give rise to very small  $h[\sim 125 \text{ GeV}] - A_1 - A_1$  couplings for certain points in the NMSSM parameter space. Note however that radiative corrections are likely to spoil the cancellation at tree-level – leading corrections to the Higgs couplings are included within NMSSMTools as well –, but their main effect simply consists in shifting in the parameter space the regions with accidentally vanishing  $h[\sim 125 \text{ GeV}] - A_1 - A_1$  coupling: the corresponding case is of course a peculiar region of parameter space where different contributions conspire, albeit possible. We observe, in Fig. 14, that best-fitting points in the scan of Fig. 13 indeed involve negligible values of the coupling  $h[\sim 125 \text{ GeV}] - A_1 - A_1$ .

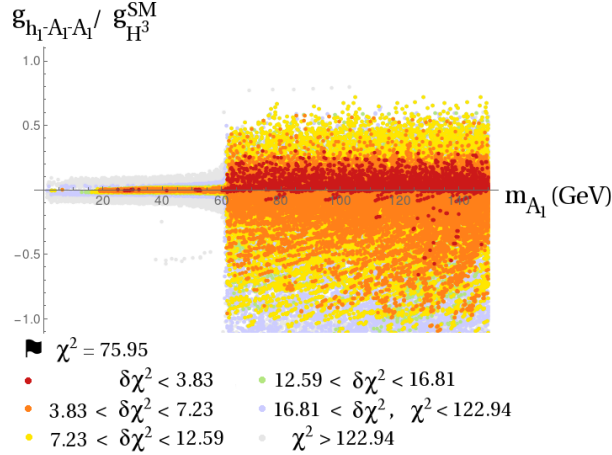


Figure 14: Triple Higgs coupling  $h_1 - A_1 - A_1$  in the scan of Fig. 13, relative to the SM value  $g_H^{\text{SM}}$ .

In view of the early LHC results, the maximal branching ratio into lighter Higgs states of the state at  $\sim 125 \text{ GeV}$  which remains compatible with the observed signals had been estimated at  $\sim 20\%$  [33, 51]. In the bottom left-hand quadrant of Fig. 13, the unconventional branching ratio  $BR(h[\sim 125 \text{ GeV}] \rightarrow 2A_1)$  is displayed as a function of the Higgs mass. Best-fit (yellow-to-red) points cluster within  $BR(h[\sim 125 \text{ GeV}] \rightarrow 2A_1) < 20\%$  indeed. Interestingly, a light CP-odd Higgs may coexist with a light CP-even singlet-like state at reduced  $\kappa/\lambda$ : the CP-even singlet may then decay dominantly into  $2A_1$ , as shown in the plot at the bottom right-hand corner of Fig. 13. In this configuration, the observability of such



a CP-even singlet state is hindered both by its reduced production cross-section and its unconventional decay. However, this setup typically requires that  $BR(h[\sim 125 \text{ GeV}] \rightarrow 2A_1)$  be suppressed through an accidental cancellation of the  $h[\sim 125 \text{ GeV}] - A_1 - A_1$  coupling.

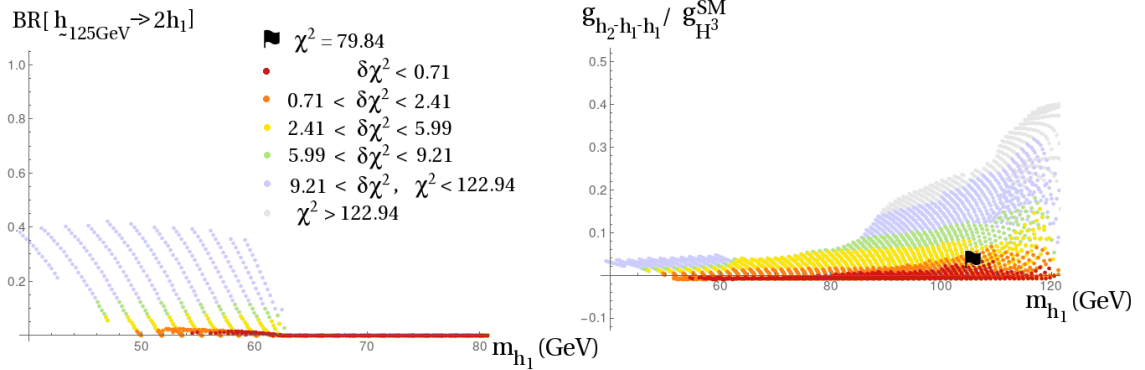


Figure 15: Scan of Fig. 8. Decay rate of the state at  $\sim 125 \text{ GeV}$  into the light state and magnitude of the  $h_2 - h_1 - h_1$  coupling (relative to  $g_{H^3}^{\text{SM}}$ ).

The case of light CP-even states with mass under the decay threshold of the observed state essentially follows the same principles: from Figs. 5, 6, 9 and 12, we observe that light CP-even singlets under  $\sim 62 \text{ GeV}$  do not seem to offer particularly good fits to the Higgs-measurement data, as points with acceptable fit values drastically disappear from the low-mass tail under  $\sim 62 \text{ GeV}$ . Note that in the corresponding plots,  $\lambda$  tended to be large, so that the decay  $h_2 \rightarrow 2h_1$  would typically retain a significant branching fraction (which is disfavoured by the fit), even though  $h_1$  is purely singlet: this explains why no red points persist at  $S_{13}^2 \simeq 1$  below  $62 \text{ GeV}$  in these plots, contrarily to the case of  $P_{13}^2 \simeq 1$  in Fig. 13. An example for this scenario can be found in Table 4 (Point 9). In Fig. 8, on the contrary, we observe points with mass down to  $40 \text{ GeV}$ , some of them having an excellent fit value. The fact that these points are dominantly singlet was already a requirement from LEP limits. However, in Fig. 15, we display the magnitude of the branching fraction  $BR(h_2^0 \rightarrow 2h_1^0)$  and the  $h_2^0 - h_1^0 - h_1^0$  coupling: reduced values are evidently preferred below the threshold.

From this discussion, it follows that the success of the conventional Higgs searches prohibits<sup>6</sup> possible light Higgs states below  $\sim 62 \text{ GeV}$  to play a significant part in the phenomenology of the state which was discovered by the LHC, but also to intervene in connection to other standard particles: we have observed indeed that a condition for suppressed Higgs-to-Higgs decays laid in an almost-pure singlet nature of the light Higgs state. Therefore, the latter does not possess relevant couplings to SM-fermions or gauge bosons – these develop only in proportion to the doublet components. As a consequence, direct production of the light state, e.g. via its coupling to a quark line (in associated production with tops or  $b$ 's), proves even less promising than searches in Higgs-to-Higgs processes: the corresponding cross-sections would indeed receive suppression factors of the form  $\sim (1 - S_{13}^2) / (1 - P_{13}^2)$  for a CP-even / CP-odd state<sup>7</sup>. On the other hand, the existence of such avoidant states remains a phenomenological possibility. The most straightforward search channel remains a possible decay (with branching ratio of a few percent) of the state observed at  $\sim 125 \text{ GeV}$  towards the light (pseudo)scalars, which may result in pairs of  $b\bar{b}$ 's,  $\tau\bar{\tau}$ 's or  $\gamma\gamma$ 's in the final state. Note that these remarks are consistent with the results of the recent analysis [34]. Other search channels would involve new Higgs or supersymmetric particles, depending critically on the characteristics of these states.

<sup>6</sup>Note that this conclusion holds for the NMSSM only. Although this is likely to prove a common trend in most models where such light (pseudo)scalars are directly associated with the Higgs sector, there also exist theoretical frameworks where the light state has naturally suppressed couplings to the SM-like Higgs boson, without necessarily decoupling from SM-particles.

<sup>7</sup>Extreme values of  $\tan\beta$  may partially compensate this suppression in the couplings to down-type quarks and leptons, however.

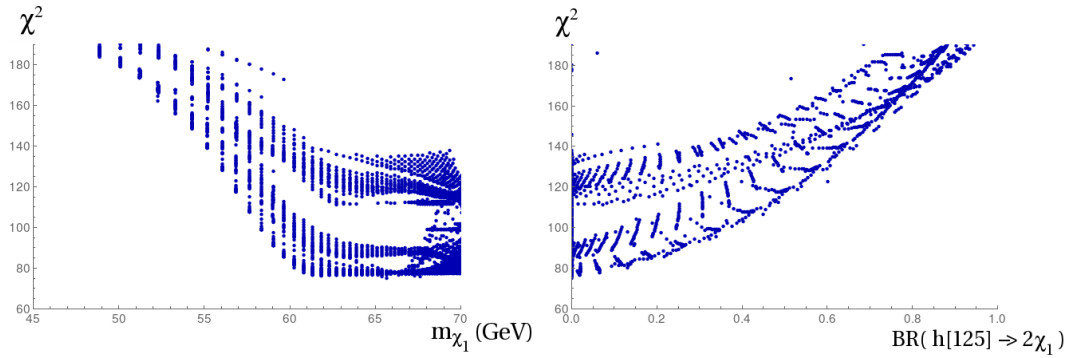


Figure 16:  $\chi^2$  in the presence of a light singlino: the input corresponds to the scan of Fig. 9. The mass of the light Higgs doublet was constrained to fall within  $[124, 127]$  GeV.

As a side-remark, let us mention that another type of unconventional Higgs decays would involve light supersymmetric particles, e.g. a light singlino. This scenario has raised interest in dark matter studies [42]. While our framework is not suited to discuss dark matter phenomenology, we may still comment on the tentative presence of a light neutralino with mass under  $\sim 62$  GeV from the point of view of Higgs physics. Decays of the Higgs state which is identified with the signal observed at the LHC into a pair of light neutralinos (invisible decay) would indeed lead to a suppression of the rates in the conventional search channels, which contradicts the LHC / TeVatron results (unless this effect would be compensated by an enhanced production mode). In the case of a light singlino, the corresponding width is related to  $\lambda^2$ , so that large values of  $\lambda$  are again disfavoured as long as this decay channel is kinematically open. Fig. 16 in the low  $\tan\beta$  / large  $\lambda$  regime illustrates this comment: the region below the threshold for  $h[125 \text{ GeV}] \rightarrow 2\chi_1^0$  gives rise to rather large  $\chi^2$  values. A comparable limit would apply in the presence of light binos: the couplings to a light doublet Higgs would then be of electroweak magnitude, which could lead to a disfavoured decay of the Higgs state towards neutralinos. However, contrarily to the case of light scalar states, the constraints on light new fermions are typically milder since such decays are of a similar type to the standard channels, hence less likely to dominate the branching ratio as soon as the kinematical threshold opens.

## 7 Two states in the vicinity of $\sim 125$ GeV

In [31] the possible presence of two CP-even Higgs states in the vicinity of  $\sim 125$  GeV was highlighted, the rates of both states adding while the experimental resolution remained too broad to distinguish between them. Note that, while individual channels – e.g. searches in the diphoton final state – provide an excellent precision on the mass where the Higgs signals are centered, it will be challenging for ATLAS and CMS, because of the limited detector resolution, to resolve two Higgs signals separated by less than  $2-3$  GeV. On the theoretical side, a typical separation scale is the SM Higgs width of 4 MeV. The aim in [31] originally consisted in exploiting the presence of two states in the signal region, so as to enhance the diphoton and  $ZZ$  rates in the context of a NUHM version of the NMSSM – thence explaining tentative deviations of the apparent Higgs rates from the standard values via this approximate degeneracy of Higgs states. In this section, we shall discuss such configurations in more detail.

While the CP-even singlet and the light doublet may be close in mass, requiring them to lie within a few 100 MeV / 1 GeV demands that the mixing entry in the mass matrix approximately vanishes. This is a tuning requirement, in general, unless one moves to the MSSM limit of the NMSSM (and it is then still necessary to adjust the diagonal entries of the mass matrix so that they are approximately equal). As a consequence of the small size of this off-diagonal mass entry, both states can be quasi degenerate while their composition, hence their coupling properties to SM particles, may vary from that of pure singlet / doublet to strong admixtures. Note that the typical widths involved ( $\lesssim 4$  MeV) are



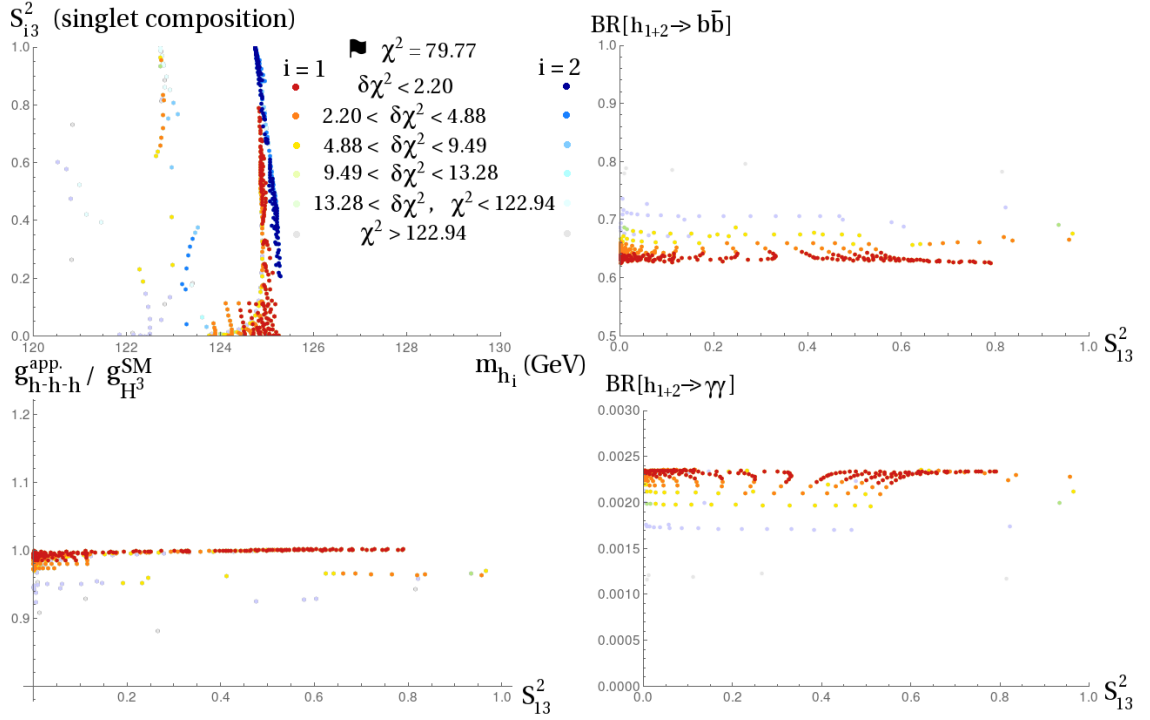


Figure 17: Quasi-degenerate CP-even states in the MSSM limit:  $\lambda = \kappa = 1 \cdot 10^{-3}$ ,  $\tan \beta \in [3, 22]$ ,  $M_A \in [100, 2000]$  GeV,  $A_\kappa \in [-2, 0]$  TeV,  $\mu \in [120, 2000]$  GeV,  $2M_1 = M_2 = 500$  GeV,  $M_3 = 1.5$  TeV,  $m_{\tilde{Q}_{1,2}} = 1.5$  TeV,  $m_{\tilde{L}} = 300$  GeV,  $m_{\tilde{Q}_3} = 1.2$  TeV,  $A_t = -2.5$  TeV,  $A_{b,\tau} = -1.5$  TeV.  $BR(h_{1+2} \rightarrow \dots)$  denote the apparent ‘global’ decay rates related to the two light, almost degenerate, CP-even Higgs states.  $g_{h-h-h}^{app}$  represents the apparent trilinear Higgs coupling accounting for both states. Only points with  $m_{h_2^0} - m_{h_1^0} < 1$  GeV have been retained in the scan.

still very small compared to the mass differences which we are considering, so that interference effects such as those discussed in [52] should remain small. Therefore, as long as the two single states are not resolved, the overall behaviour in interactions with SM particles would naively coincide with that of the doublet-like state taken alone. Only the apparent Higgs-to-Higgs couplings may show deviations – to which even a HL-LHC is unlikely to be sensitive to, due to the limited experimental precision, and which would still have to be disentangled from other sources of non-standard Higgs-to-Higgs couplings for the state at  $\sim 125$  GeV. On the other hand, the composition of the apparent light doublet may differ slightly from that of a pure doublet state due to the three-state mixing effects (similarly to what we discussed in sections 4 and 5): here again, this effect could account for small deviations from the standard rates. On the side of the singlet, the simplest case consists in having all particles to which it directly couples (CP-odd singlet, higgsinos) heavier than half its mass: then, the only possible decay products are SM particles, the corresponding widths depending exclusively on the doublet component. In this context, the singlet does not contribute to the total width. If, on the contrary, significant decays of the singlet towards other new-physics states are allowed, then we are back to a case similar to what we discussed in section 6: indeed, the singlet-doublet mixing would then dilute the branching ratios into standard particles, and could hence contradict the signals observed at LHC – large singlet-doublet mixings would then be disfavoured. This second configuration will not emerge from the scans.

We have already come across points involving quasi-degenerate CP-even Higgs states, e.g. in section 5: some examples have been recorded in Table 5 below. As a first illustration of this scenario, we consider the MSSM limit in Fig. 17: the off-diagonal mass term between singlet and light doublet state is then naturally suppressed. One observes, however, that significant singlet-doublet mixing, up to 50% can develop for favourable fit values, provided the two states are almost degenerate. On the other hand, no

effect at the level of the rates is expected in the MSSM limit (because of the decoupling of the singlet). We display the apparent branching ratio into  $b\bar{b}$  and  $\gamma\gamma$  as a function of the singlet-doublet mixing on the right-hand side of Fig. 17, for points where  $m_{h_2^0} - m_{h_1^0} < 1$  GeV: while some variations are present, these are entirely independent of the mixing or the presence of the singlet, and their origin can actually be traced back to the scale of the heavy doublet sector ( $M_A$ ) and the value of  $\tan\beta$ , hence appears as a pure doublet effect. Similarly, consequences on Higgs pair production are minimal since the singlet-doublet interactions are suppressed in this limit. While singlet-singlet interactions formally enter the relevant Higgs-to-Higgs couplings, the associated effects are projected onto the doublet component – due to the coupling to SM particles in the process of the Higgs production – and vanish when summed over both degenerate states. In the lower left-hand quadrant of Fig. 17 one observes indeed that the apparent trilinear Higgs coupling accounting for both states in the vicinity of  $\sim 125$  GeV remains SM-like. Therefore, in this scenario, only the presence of two separate peaks in the Higgs searches – as the result of a large mixing between the singlet and the doublet state –, with widths adding to  $\sim 4$  MeV, would be observable and document the quasi-degeneracy of the singlet with the light doublet. On the other hand, the singlet could also be almost degenerate but remain (almost) unmixed, in which case, its ‘peak’ would remain invisible.

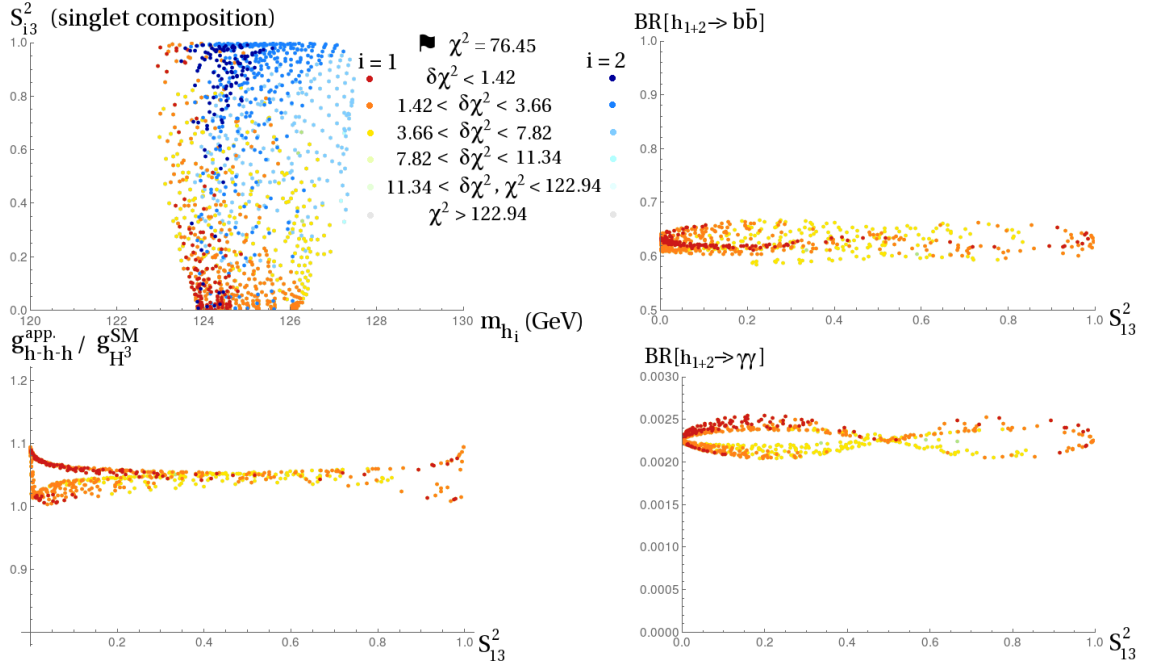


Figure 18: Quasi-degenerate CP-even states in the low  $\tan\beta$  / large  $\lambda$  regime:  $\tan\beta = 2$ ,  $\lambda = 0.7$ ,  $\kappa = 0.1$ ,  $\mu \in [120, 1200]$  GeV,  $M_A \in [0.8, 3]$  TeV,  $A_\kappa \in [-300, 0]$  GeV,  $2M_1 = M_2 = 150$  GeV,  $M_3 = 1.5$  TeV,  $m_{\tilde{Q}_3} = 500$  GeV,  $m_{\tilde{Q}_{1,2}} = 1.5$  TeV,  $m_{\tilde{L}} = 110$  GeV,  $A_{t,b,\tau} = -100$  GeV. Only points with  $m_{h_2^0} - m_{h_1^0} < 1$  GeV were retained in the scan.

The same configuration is considered in Fig. 18, but in a different regime: we turn to the low  $\tan\beta$  / large  $\lambda$  region again. Only points where the two lightest CP-even states have masses within 1 GeV of each other are kept in this scan. Deviations at the percent level can be observed in the apparent rates into SM-particles. The corresponding effect is obviously associated with the three-state mixing – this is most visible in the case of the  $\gamma\gamma$  channel – in contrast to the case of the MSSM limit. Note that pure doublet effects are negligible here as  $M_A \gg M_Z$  and  $\tan\beta$  is fixed. Large singlet-doublet couplings affecting the apparent triple-Higgs coupling at  $\sim 125$  GeV may develop as well, leading to a  $\sim 10\%$  increase (at most) of the apparent trilinear Higgs coupling (see the lower left-hand quadrant).

Note that while this kind of scenario may occur in different parameter regimes, the existence of a doublet state at  $\sim 125$  GeV always relies on the mechanisms described in the previous sections, i.e.

substantial radiative corrections driven by the SUSY spectrum and larger  $\tan\beta$  or the specific tree-level contribution associated with large  $\lambda$  and low  $\tan\beta$ . On the other hand, singlet-doublet mixing does not provide a mass uplift for the doublet in the scenario under consideration.

Another possibility would consist in the presence of a CP-odd state in mass-proximity to the SM-like state. Such a scenario might even be considered as a CP-conserving approximation of the CP-violating case, where the observed state would appear as a superposition of CP-even and CP-odd components. Considering LHC limits associated with Higgs searches in the  $\tau\tau$  channel as well as (indirectly) with top decays to a charged Higgs, it proves difficult to admit a (pure) CP-odd doublet state in the desired mass range. The possibility of a CP-odd Higgs close to  $\sim 125$  GeV thus rests with singlet-like states, which may however carry a significant doublet component. In Fig. 13, one observes that a doublet composition of 5 – 10% still receives an acceptable fit to the data in the vicinity of  $\sim 125$  GeV. The fermion rates at  $\sim 125$  GeV would be the observables that are most significantly affected in this setup, with an apparent increase of a few percent, while also the diphoton channel may receive a small subsidiary contribution.

Note that in the CP-even as in the CP-odd case, the additional state may well be purely singlet so that it would remain undetected in direct production due to vanishing couplings to SM particles. Only at the level of pair productions, making use of Higgs-to-Higgs couplings, would there be a deviation from the naive one-particle case – which would be extremely challenging to detect with sufficient precision experimentally. Note also that, e.g. in the MSSM limit, a singlet that is mass degenerate with the state at  $\sim 125$  GeV could even have no impact at all on the rates or on multi-Higgs production.

## 8 Two-light-doublet scenario

Identifying the LHC signal with a heavy doublet state – which suggests that a lighter Higgs doublet state has eluded searches so far – is a scenario which was originally considered in the MSSM [13, 14]. It was recently put under further pressure by the publication of charged Higgs searches in top decays [16] – see the newest reference in [18] for a discussion in the context of the MSSM – and [17], however. In this section, we will discuss the situation in the context of the NMSSM.

The presence of a light CP-even Higgs – with mass below 125 GeV – in the spectrum does not entail major phenomenological difficulties by itself. Indeed we have already outlined two possible strategies which allow such a scenario to evade LEP limits:

- the production cross-section at LEP could be suppressed by a small coupling of the light Higgs state to electroweak gauge bosons – we have discussed above how a singlet Higgs naturally fulfills this requirement;
- the decays in the standard search channels could be blurred by large non-conventional decays – in this case, the difficulty lies in explaining why these unconventional decays do not affect the observed state at  $\sim 125$  GeV.

While the success of the LHC Higgs searches makes the second approach difficult to implement in a realistic model, the first strategy remains viable, even in the case of a doublet state – even though the cancellation of the couplings of the light Higgs to electroweak gauge bosons is then largely accidental. Turning to direct limits from the LHC, it is to be noted that searches in the  $\tau\tau$  channel for an additional Higgs boson essentially disfavour neutral states with mass above  $\sim 110$  GeV, while the light doublet can be well below 100 GeV. In practice, we could indeed find NMSSM parameter points where a light doublet Higgs with vanishing couplings to electroweak gauge bosons – typically in the 70 GeV mass range – escapes all direct limits.

Yet, if all the CP-even doublet states are at or below 125 GeV, the correlations of the masses in the doublet sector will force the other doublet masses – those of the CP-odd and charged states – to be close.

Indeed, as a good approximation, we have:

$$\begin{aligned}
m_{H^\pm}^2 &\simeq M_{A,\text{eff}}^2 + M_W^2 - \lambda^2 v^2 \\
m_{A,\text{doub}}^2 &\simeq M_{A,\text{eff}}^2 \\
m_{h_{1,\text{doub}}}^2 &\simeq \frac{1}{2} \left[ M_{A,\text{eff}}^2 + M_Z^2 - \sqrt{(M_{A,\text{eff}}^2 - M_Z^2)^2 \cos^2 2\beta + (M_{A,\text{eff}}^2 + M_Z^2 - 2\lambda^2 v^2)^2 \sin^2 2\beta} \right] \\
m_{h_{2,\text{doub}}}^2 &\simeq \frac{1}{2} \left[ M_{A,\text{eff}}^2 + M_Z^2 + \sqrt{(M_{A,\text{eff}}^2 - M_Z^2)^2 \cos^2 2\beta + (M_{A,\text{eff}}^2 + M_Z^2 - 2\lambda^2 v^2)^2 \sin^2 2\beta} \right] + \delta_{\text{rad}}
\end{aligned} \tag{4}$$

In this list of (approximate) masses for the doublet states,  $M_{A,\text{eff}}$  does not exactly correspond to the NMSSMTools input  $M_A$ , but represents a corrected value absorbing radiative corrections. There are, of course, additional deviations at the loop level, and  $\delta_{\text{rad}}$  only denotes the bulk of the large shift due to top/stop effects – hence associated to the  $H_u$  flavour.

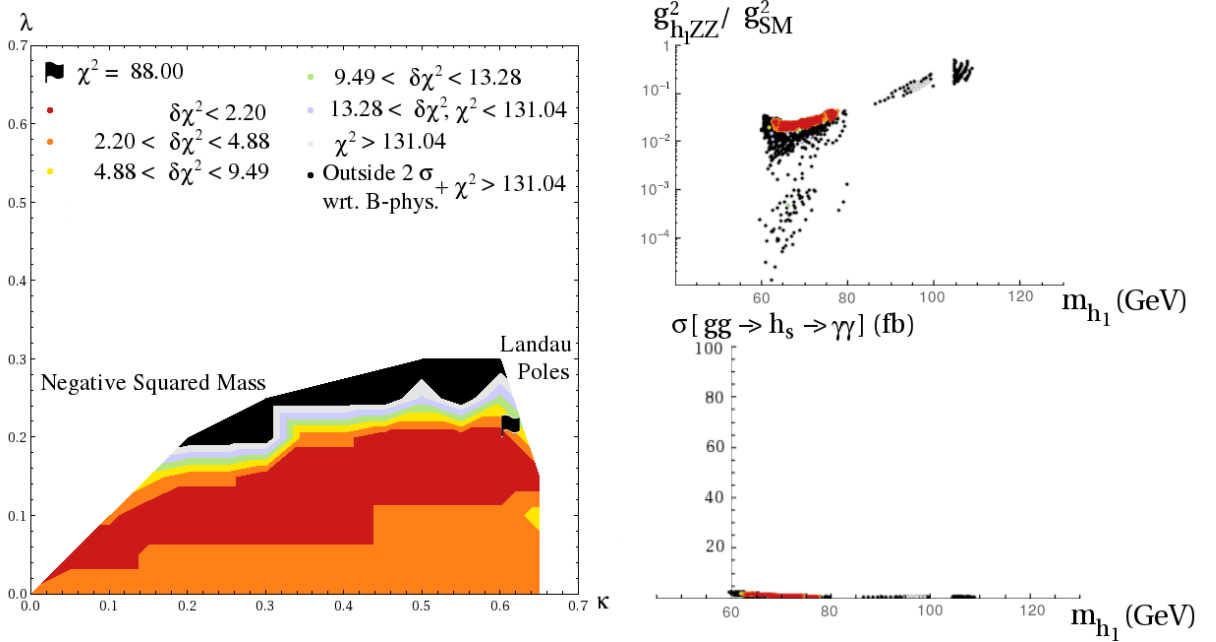


Figure 19: Left plot: Scan in the  $\{\kappa, \lambda\}$ -plane:  $\lambda \in [2 \cdot 10^{-4}, 0.65]$ ,  $\kappa \in [2 \cdot 10^{-4}, 0.65]$ ,  $\tan \beta \in [3, 20]$ ,  $M_A = 130$  GeV,  $\mu \in [100, 300]$  GeV,  $A_\kappa \in [-1.5, 0]$  TeV,  $2M_1 = M_2 = 500$  GeV,  $M_3 = 1.5$  TeV,  $m_{\tilde{Q}_{1,2}} = 1.5$  TeV,  $m_{\tilde{Q}_3} = 1.1$  TeV,  $A_t = -2.3$  TeV,  $A_{b,\tau} = -1.5$  TeV. On the right: coupling properties of the light CP-even doublet to  $Z$ -bosons (upper part) and the typical cross-section for the production of this state in the 8 TeV run of the LHC in gluon-gluon fusion, with a diphoton decay (lower plot). The colour coding remains the same as in the plot on the left.

The CP-odd doublet Higgs causes limited concern as its mass typically falls under 100 GeV and its presence was tested at LEP only via pair production processes (since a CP-odd Higgs has vanishing couplings to gauge bosons). Only when its mass falls below the threshold  $\sim 125/2$  GeV does it entail indirect limits from the LHC measurement – in accordance with our discussion in section 6.

On the other hand, the existence of a light charged Higgs is problematic in view of the existing limits. This possibility is already severely constrained in view of the tensions that it produces in the  $B$ -sector – e.g. in the channels  $B \rightarrow X_s \gamma$ ,  $B^+ \rightarrow \tau \nu_\tau$  or  $B_s \rightarrow \mu^+ \mu^-$ . Yet, to the price of a  $\chi^2$  pull of at least  $\sim 4$ , these flavour limits could be satisfied. On the other hand, a light charged Higgs opens the possibility of top decays: these channels have been investigated by ATLAS [16] and CMS [17], e.g. in the  $b\bar{\tau}\nu_\tau$  final state, and the current constraints exclude all the points that were preferred by the fit performed in Fig.19.

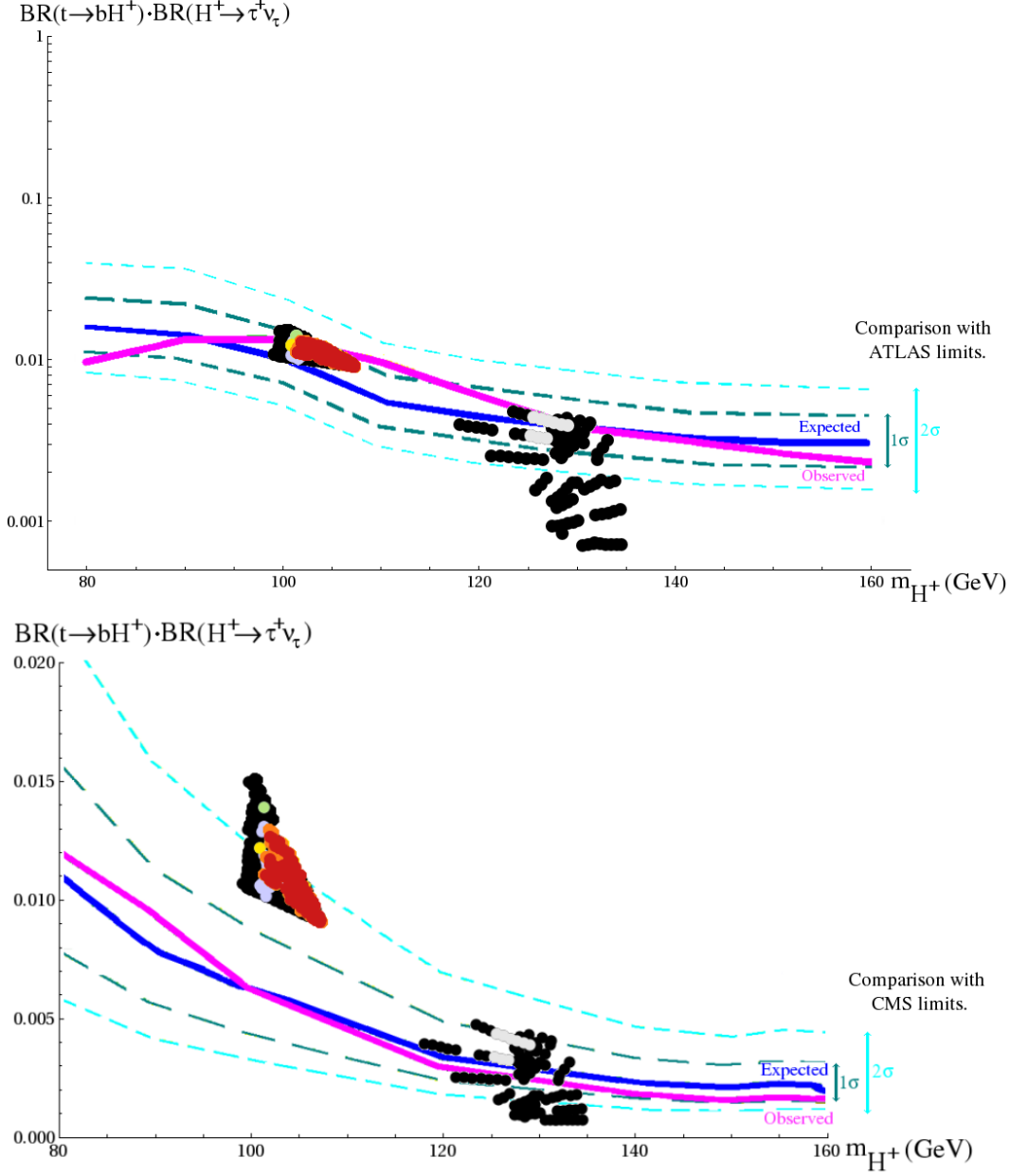


Figure 20:  $BR(t \rightarrow H^+ b) \cdot BR(H^+ \rightarrow \tau^+ \nu_\tau)$  in the scan of Fig. 19; the limits from ATLAS [16] (upper plot) and CMS [17] (lower plot) on this branching ratio  $BR(t \rightarrow H^+ b)$  – assuming a 100% decay  $H^+ \rightarrow \tau^+ \nu_\tau$  – are reproduced for comparison.

In order to illustrate the workings of the recent LHC constraints on  $t \rightarrow bH^+$ , we turn to older versions of HiggsBounds – 4.1.3 – and HiggsSignals – 1.2.0 – where LHC results of the summer 2014 had not yet been included. To set a reference, the best-fit point in the SM-limit then receives a  $\chi^2$  of<sup>8</sup>  $\sim 94$ . We then consider the region in the NMSSM parameter space where  $M_A = 130$  GeV is set as a fixed input. The results are shown in the  $\{\kappa, \lambda\}$  plane in Fig. 19. The best-fitting points are obtained for  $\lambda \sim 0.2$ . They have a somewhat better  $\chi^2$  than the SM limit –  $\chi^2 \sim 88.0$  – and provide the following

<sup>8</sup>The higher  $\chi^2$  value in this previous version is related to a revision of the tests in the diphoton channel (both in the presentation of the experimental data and its implementation within HiggsSignals).

spectrum:  $m_{h_2} \simeq 125.0$  GeV,  $m_{H^\pm} \simeq 107$  GeV and light  $H_d$ -like doublet states (CP-even and odd) around  $70 - 75$  GeV (i.e.  $M_{A,\text{eff}} \sim 70$  GeV); the singlet states are much heavier (beyond 1 TeV) and play no role in the electroweak Higgs phenomenology. The  $h_2$ -rates are essentially SM-like, which explains the quality of the fit. On the right part of Fig. 19, one observes that the squared coupling of the light CP-even doublet state to  $Z$ -bosons is reduced (of the order  $10^{-2}$ ), while its typical production cross-section in the 8 TeV run of the LHC, accompanied by a diphoton decay, would amount to about a few fb's only.

Version 4.1.3 of HiggsBounds included the ATLAS limits on top decays [16], and we show on the upper part of Fig. 20 how the points of the scan in Fig. 19 compare with these constraints – note that the corresponding experimental bounds have been obtained under the assumption of a 100%  $H^+ \rightarrow \tau^+ \nu_\tau$  decay, so that we rescale our points by a factor  $BR(H^+ \rightarrow \tau^+ \nu_\tau)$ : while sitting on the edge of the exclusion limit, the light doublet scenario appears compatible with these constraints. On the other hand, the more recent CMS limits on  $t \rightarrow H^+ b$  [17] had not been included within HiggsBounds, and we display them in the lower part of Fig. 20. All the best-fitting region is excluded while the few remaining points at  $m_{H^\pm} \simeq 130$  GeV – disconnected from the best-fit region due to the interplay of constraints – do not offer interesting fit qualities. Therefore, while the light doublet scenario might still be realized in regions with reduced  $BR(t \rightarrow H^+ b)$ , the current limits discard most of the associated parameter space.

## 9 Highlight of specific points

In this section, we focus on specific points in the parameter space, found in the vicinity of the best-fit points of the various plots presented thus far (see Table 5, in the appendix), and aim at discussing the associated Higgs phenomenology in more detail. Note again that, although the supersymmetric spectra have some impact on the phenomenology – Higgs mass,  $(g - 2)_\mu$ ,  $B$ -physics, etc., they are not strictly tied to the respective scenarios – i.e. analogous Higgs properties should be accessible with different, e.g. heavier SUSY spectra: the corresponding characteristics are thus purely illustrative and we shall not discuss the prospects of discovering such states at the LHC. Table 2 provides the NMSSMTools inputs and the Higgs spectra of the considered points, while Table 3 gives the Higgs couplings to SM particles. While most of the qualitative features that we discussed in the previous sections enter the characteristics of the few points presented below, we would like to caution the reader against reducing the discussed phenomenology to those specific points.

The first point is characteristic of the decoupling limit: the heavy-doublet states are at  $\sim 1$  TeV, so as to decouple from the SM-like Higgs, while  $\tan \beta \gg 1$  to maximize the tree-level contribution to the mass of this light state (we stress that the rather large value  $\tan \beta = 22.5$  is actually driven by the anomalous magnetic moment of the muon). While  $\lambda$  and  $\kappa$  do not vanish, which means that one is far from the MSSM limit, the impact of the singlet states on the light doublet Higgs is negligible, and the CP-even singlet is actually quite heavy ( $\sim 1200$  GeV). Correspondingly the light doublet state, at 125.0 GeV, is SM-like, with couplings to SM-particles within a few percent of their values at the same mass for a genuine SM Higgs boson: the corresponding rates at the LHC are thus comparable (still within a few percent). Distinguishing this point from the SM via the properties of the ‘observed Higgs’ would thus require a high precision on the couplings, achievable most likely at a Linear Collider only – note also that one may get even closer to a SM Higgs scenario via further decoupling of the heavy states. The heavy doublet states are essentially  $H_d$  in nature, hence give very large couplings (enhanced by the large value of  $\tan \beta$ ) to bottoms and taus (for the neutral states). All other couplings to SM particles are suppressed (which is characteristic of the large  $\tan \beta$  regime), so that decays into bottoms and taus dominate the branching ratio of the heavy neutral states. Typical production modes would be gluon-gluon fusion or production in association with  $b$ 's. Note that, even though LHC searches at 13/14 TeV could likely probe such heavy states, e.g. in the  $\tau^+ \tau^-$  channel, even larger masses of the heavy doublet states would be easily possible in this scenario. Moreover, should the heavy doublet states be discovered, the question of distinguishing such a point, in the Higgs sector, from a MSSM scenario remains open: the heavy CP-even singlet, lightly coupled to SM-particles, is likely to evade detection. As an additional feature for this point – additional but not binding: light CP-odd singlets are not a generic feature of this decoupling scenario – however, one observes that the CP-odd singlet is quite light,  $\sim 110$  GeV. Although its large singlet component of  $\sim 99.7\%$  leads to a significant suppression of the couplings of this state

NMSSMTools Parameters	Point 1 Decoupling limit	Point 2 Light singlet	Point 3 Low $\tan\beta$ + light s.	Point 4 2 CP-even $\sim 125$ GeV	Point 5 Light $A$ $H \rightarrow 2A$	Point 6 Light doublet
$\lambda$	0.2	0.55	0.699	0.7	0.05	0.1
$\kappa$	0.6	0.45	0.1	0.1	0.05	0.25
$\tan\beta$	22.5	8	2	2	19	12.25
$\mu_{\text{eff}}$ (GeV)	200	125	330	714	125	187.9
$M_A$ (GeV)	1000	1000	801	1694	1200	130
$A_\kappa$ (GeV)	-8.5	-288	-122	-176.9	-5	-1100
$M_1$ (GeV)	250	250	75	75	250	250
$M_2$ (GeV)	500	500	150	150	500	500
$M_3$ (TeV)	1.5	1.5	1.5	1.5	1.5	1.5
$m_{\tilde{Q}_{1,2}}$ (TeV)	1.5	1.5	1.5	1.5	1.5	1.5
$m_{\tilde{Q}_3}$ (TeV; if $\neq m_{\tilde{Q}_{1,2}}$ )	1.1	1	0.5	0.5	1.2	1.1
$m_{\tilde{L}}$ (GeV)	300	200	110	110	300	250
$A_t$ (TeV)	-2.5	-2	-0.1	-0.1	-2.5	-2.3
$A_{b,\tau}$ (TeV; if $\neq A_t$ )	-1.5	-1.5	/	/	-1.5	-1.5
Higgs Spectrum						
$m_{h_1}$ (GeV)	125.0 D	105.6 S	102.1 S	125.1 D/S	125.1 D	62.8 D
$m_{h_2}$ (GeV)	973 D	125.0 D	125.3 D	125.2 S/D	249 S	125.6 D
$m_{h_3}$ (GeV)	1192 S	986 D	796 D	1693 D	1174 D	605 S
$m_{A_1}$ (GeV)	109.7 S	307 S	165.4 S	280 S	43.7 S	63.3 D
$m_{A_2}$ (GeV)	976 D	983 D	800 D	1695 D	1174 D	1245 S
$m_{H^\pm}$ (GeV)	976	980	790	1690	1177	101.5
$S_{13}^2$	$\sim 0\%$	97%	91%	48.4%	0.1%	$\sim 0\%$
$S_{23}^2$	0.3%	1.6%	8%	51.4%	99.9%	$\sim 0\%$
$S_{33}^2$	99.7%	1.0%	0.9%	0.2%	$\sim 0\%$	$\sim 100\%$
$P_{13}^2$	99.7%	99.5%	98%	99.7%	$\sim 100\%$	$\sim 0\%$
$P_{23}^2$	0.3%	0.5%	1.6%	0.3%	$\sim 0\%$	$\sim 100\%$
$M_W$ [err] (GeV)	80.372[17]	80.373[17]	80.410[20]	80.393[21]	80.371[17]	80.397[17]
$\chi^2$ (/89 obs.)	81.2	76.1	76.0	80.5	80.2	81.4 (excl.)

Table 2: Highlighted points: NMSSMTools input and Higgs spectra.

to SM particles (hence of its production cross-section), the couplings to down-type fermions are again enhanced by the large value of  $\tan\beta$ , so that one may look for a signal in the  $\tau^+\tau^-$  and  $b\bar{b}$  channels – in associated production with  $b$ 's. The signal in the  $\gamma\gamma$  channel would be strongly suppressed so that the current ATLAS limits [46] have no impact for this point. Remember also from Fig. 13 that CP-odd singlets between 63 and  $\sim 150$  GeV with slightly larger doublet components are also possible, which would improve their observability, although this feature would typically be associated with a lowered mass for the heavy Higgs-doublet states. Another possibility lies in exploiting triple-Higgs couplings for a production of  $A_1$  in pairs. Furthermore, the associated production of  $A_1$  with a  $Z$ -boson only proceeds via the tiny doublet component of  $A_1$ , hence is also suppressed.

The second point is representative of the light-singlet scenario of the NMSSM. Much that has been said in connection with the previous point, especially concerning the heavy doublet states, remains valid – note however that the lower value of  $\tan\beta$  decreases the importance of the branching ratios of the heavy doublet states into down-type fermions in favour of cascade decays, via light Higgs or SUSY states, which hence affects the search strategy. The light CP-even doublet again shows SM-like couplings (within a few percent), except for the couplings to down-type fermions, which are slightly reduced: this results from the perturbation among  $H_u$  and  $H_d$  components, which is itself related to the triple-state mixing in the presence of a singlet component. As a consequence, LHC rates into gauge bosons are slightly enhanced

Couplings <sup>2</sup> /SM	Point 1	Point 2	Point 3	Point 4	Point 5	Point 6
$h_1 WW$	1.0	0.017	0.082	0.515	0.999	0.027
$h_1 ZZ$	1.0	0.017	0.082	0.515	0.999	0.027
$h_1 gg$	0.968	0.015	0.058	0.517	0.980	13.0
$h_1 \gamma\gamma$	1.002	0.001	0.048	0.469	1.002	0.357
$h_1 t\bar{t}$	1.0	0.014	0.059	0.494	0.999	0.007
$h_1 b\bar{b}$	1.035	0.853	0.215	0.600	1.027	149
$h_1 \tau\bar{\tau}$	1.035	0.855	0.218	0.604	1.027	150
$h_2 WW$	$1 \cdot 10^{-7}$	0.983	0.918	0.485	0.001	0.973
$h_2 ZZ$	$1 \cdot 10^{-7}$	0.983	0.918	0.485	0.001	0.973
$h_2 gg$	0.008	0.973	1.079	0.563	0.001	1.232
$h_2 \gamma\gamma$	0.003	1.023	0.955	0.493	0.001	0.894
$h_2 t\bar{t}$	0.002	0.986	0.945	0.507	0.001	1.000
$h_2 b\bar{b}$	502	0.800	0.813	0.405	0.014	1.043
$h_2 \tau\bar{\tau}$	505	0.800	0.810	0.401	0.014	1.054
$h_3 WW$	$6 \cdot 10^{-5}$	$6 \cdot 10^{-6}$	$3 \cdot 10^{-5}$	$3 \cdot 10^{-7}$	$8 \cdot 10^{-7}$	$2 \cdot 10^{-6}$
$h_3 ZZ$	$6 \cdot 10^{-5}$	$6 \cdot 10^{-6}$	$3 \cdot 10^{-5}$	$3 \cdot 10^{-7}$	$8 \cdot 10^{-7}$	$2 \cdot 10^{-6}$
$h_3 gg$	$8 \cdot 10^{-5}$	0.013	0.437	0.276	0.005	$3 \cdot 10^{-6}$
$h_3 \gamma\gamma$	0.002	0.089	3.06	0.059	0.011	0.002
$h_3 t\bar{t}$	$1 \cdot 10^{-4}$	0.016	0.246	0.249	0.003	$3 \cdot 10^{-6}$
$h_3 b\bar{b}$	1.634	63.2	3.80	3.60	360	$7 \cdot 10^{-4}$
$h_3 \tau\bar{\tau}$	1.641	63.3	3.97	3.99	361	$7 \cdot 10^{-4}$
$A_1 WW$	0	0	0	0	0	0
$A_1 ZZ$	0	0	0	0	0	0
$A_1 gg$	0.028	$1 \cdot 10^{-4}$	0.008	0.002	$2 \cdot 10^{-4}$	14.4
$A_1 \gamma\gamma$	0.032	1.455	0.106	0.014	0.008	2.45
$A_1 t\bar{t}$	$6 \cdot 10^{-6}$	$8 \cdot 10^{-4}$	0.004	$8 \cdot 10^{-3}$	$6 \cdot 10^{-9}$	0.007
$A_1 b\bar{b}$	1.589	0.325	0.060	0.012	$8 \cdot 10^{-4}$	149
$A_1 \tau\bar{\tau}$	1.596	0.326	0.062	0.013	$8 \cdot 10^{-4}$	150
$A_2 WW$	0	0	0	0	0	0
$A_2 ZZ$	0	0	0	0	0	0
$A_2 gg$	0.019	0.028	0.343	0.299	0.016	$4 \cdot 10^{-8}$
$A_2 \gamma\gamma$	0.054	0.098	0.546	0.380	0.038	$6 \cdot 10^{-5}$
$A_2 t\bar{t}$	0.002	0.016	0.246	0.249	0.003	$2 \cdot 10^{-8}$
$A_2 b\bar{b}$	502	63.5	3.80	3.67	360	$4 \cdot 10^{-4}$
$A_2 \tau\bar{\tau}$	505	63.7	3.94	3.99	361	$4 \cdot 10^{-4}$

Table 3: Highlighted points: Higgs squared couplings to SM particles.

(while the  $b\bar{b}$  and  $\tau^+\tau^-$  channels are slightly suppressed): increased precision on the Higgs decays would thus prove interesting in such a configuration. The central test of this scenario however rests with the observability of the light CP-even singlet at  $\sim 106$  GeV: its reduced doublet component  $\leq 3\%$  indeed entails suppressed rates (due to the reduced production cross-section), at the percent level of those of a SM Higgs boson at the same mass. The corresponding cross-section at 8 TeV for the diphoton final state is at the level of  $10^{-3}$  fb. Direct searches thus carry little chance of success on short timescales. Again, one could then search the light state in Higgs pair production.

The third point is also an example of a light singlet Higgs, although it differs from the previous one in two respects: it involves very low  $\tan\beta = 2$ , and the light singlet has a significant doublet component  $\sim 9\%$ . The first feature, low  $\tan\beta$ , plays a key role, together with  $\lambda \sim 0.7$ , in increasing the mass of the ‘observed’ state in the presence of a light squark spectrum. We remind the reader that this effect is not bound to the presence of a light CP-even singlet (see section 5). The second aspect,  $S_{13}^2 \sim 9\%$ ,



has consequences on the – however still challenging – observability of the light singlet at  $\sim 102$  GeV, as apparent LHC rates into  $b\bar{b}$  and  $\tau^+\tau^-$  would now reach a somewhat larger fraction ( $\sim 6 - 8\%$ ) of the corresponding values for a SM Higgs boson at this mass – remember from sections 4, 5 that the doublet components of the light singlet may take phenomenologically viable values as large as  $\sim 20\%$ . The corresponding signal would also fit the LEP excess in the  $b\bar{b}$  channel adequately enough. Note, though, that the  $h_1 \rightarrow \gamma\gamma$  rate is not particularly large ( $\sim 25\%$  of its SM value at this mass), and the corresponding cross-section at 8 TeV is under 1 fb for this particular example. On the other hand, as for the previous point, the rates of the SM-like state would give rise to slight excesses in the vector channels / a slight suppression in the down-type fermion channels.

Several (a priori separable) features are present for the fourth point. First, as for the previous point, the low  $\tan\beta = 2$  and large  $\lambda = 0.7$  ensure that the mass of the light doublet state is generated in the correct range  $\sim 125$  GeV, despite a light sfermion spectrum and negligible trilinear couplings. Furthermore, the heavy doublet sector is essentially decoupled again. The most remarkable aspect of this point however rests with the fact that the light CP-even doublet and singlet states are almost mass-degenerate (within  $\sim 0.1$  GeV). Moreover, both quasi-degenerate states are mixed at almost  $\sim 50\%$ , which means that they carry ‘half a SM-like Higgs boson’ each (in their contribution to the LHC rates). Ideally, one should try and resolve experimentally the two states (their width is about 2 MeV). Another strategy consists in looking for deviations in the Higgs pair production rate, as singlet-doublet contributions would modify the apparent trilinear Higgs couplings at  $\sim 125$  GeV. The various couplings read (in units of  $g_{H^3}^{\text{SM}}$ ):  $\sim 0.83$  for  $h_1 - h_1 - h_1$ ,  $\sim -0.16$  for  $h_1 - h_1 - h_2$ ,  $\sim 0.35$  for  $h_1 - h_2 - h_2$  and  $-0.53$  for  $h_2 - h_2 - h_2$ . The apparent triple-Higgs coupling accounting for both states (in connection to external SM particles) gives  $\sim 205$  GeV, which represents a  $\sim 7\%$  increase with respect to the SM value (very difficult to resolve).

The fifth point is another example of the decoupling limit. Its aspect that we wish to discuss, however, is the presence of a CP-odd state at  $\sim 44$  GeV, that is below the  $h_1 \rightarrow 2A_1$  threshold. Yet, the corresponding width is strongly suppressed, in accordance with the LHC data, resulting in a branching ratio of only  $BR(h_1 \rightarrow 2A_1) \sim 10^{-4}$ . The couplings of the CP-even state at  $\sim 125.1$  GeV and its rates at the LHC are thus essentially SM-like. On the other hand, the light CP-odd Higgs is almost a pure singlet so that it will evade detection in direct production. Production of  $A_1$  from a heavier state is also problematic, as only the CP-even singlet  $h_2$  has a sizable decay into this state. Therefore, the most serious hope for the observation of such a  $A_1$  would still lie in increased precision in the characteristics of  $h_1$  at future colliders. This point illustrates the extreme possibility of a light CP-odd state devoid of any phenomenological impact on the standard sector. As we stressed in section 6, however, it still makes sense to test a  $BR(h_1 \rightarrow 2A_1)$  in the few percent range.

In the case of the sixth point, the whole doublet sector lies below  $\sim 125$  GeV, with very light neutral states at  $\sim 63$  GeV while the charged Higgs has a mass of 101.5 GeV. Expectedly, the couplings of  $h_1$  to SM gauge bosons are suppressed, which accounts for its invisibility at LEP. Its diphoton cross-section at 8 TeV is at the level of 1 fb, as that of the light  $A_1$  state. The couplings of the heavy doublet state, at  $\sim 125.6$  GeV, are reasonably close to their SM value, resulting in SM-like cross-sections for the corresponding state (within a few percent): it thus offers an acceptable interpretation of the observed signals as the competitive  $\chi^2$  proves. Yet this point is discarded by Higgsbounds: indeed,  $BR(t \rightarrow H^+b) \sim 1.12 \cdot 10^{-2}$  (together with  $BR(H^- \rightarrow \tau\nu_\tau) \simeq 0.97$ ) is beyond the recent limits established by CMS. Much tension is also present in  $B$ -physics observables where  $BR(B \rightarrow \tau\nu_\tau)$  and  $BR(\bar{B}_s \rightarrow \mu^+\mu^-)$  lie beyond 2 standard deviations.

While electroweak precision observables were not included within our fit, predictions for  $M_W$  are displayed in Table 2, using the tools presented in [53]; the values given in brackets (in MeV) are estimates of the theoretical uncertainty. Comparing these values with the current experimental measurement ( $M_W^{\text{exp.}} = 80.385 \pm 0.015$  GeV), we observe that all points remain within  $1\sigma$  deviation of the experimental average, with possible tensions at low  $\tan\beta$  or in the presence of light doublet states.

## 10 Attempt at a ‘global’ scan

Performing a global scan over the NMSSM parameter space proves to be both a challenging and potentially even misleading task. The NMSSM Higgs sector involves 6 degrees of freedom ( $\lambda, \kappa, \tan\beta, M_A, \mu, A_\kappa$ )

at lowest order, to which one should also add the stop masses and trilinear coupling ( $A_t$ ), which have an important impact via loop corrections. The rest of the supersymmetric spectrum cannot be altogether left out from a scan if one keeps e.g.  $(g-2)_\mu$  and the requirement for a neutralino LSP in the process. Moreover, some scenarii that we described in the previous sections and which provide a reasonable or even an excellent fit to LHC/TeVatron data involve specific parameter configurations (so that one obtains the appropriate spectrum/couplings), hence disappear or become uncompetitive if the scanning density is too loose. On the other hand, keeping a tight scanning density over so many variables would require both long scan durations and huge storage capacities.

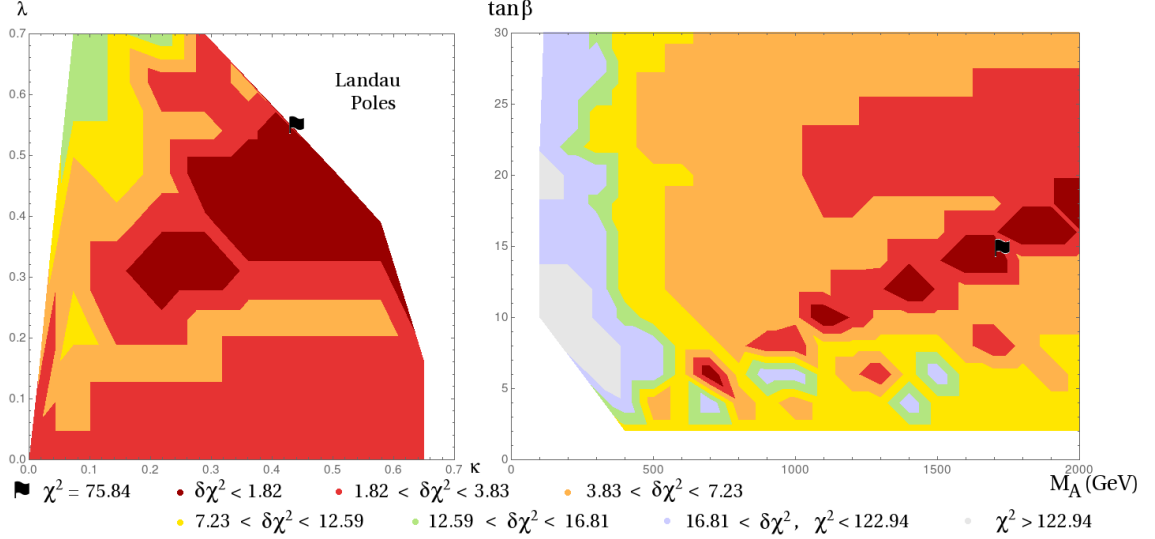


Figure 21: Parameter space in the ‘global’ scan:  $\tan\beta \in [2, 30]$ ,  $\mu \in [120, 2000]$  GeV,  $M_A \in [100, 2000]$  GeV,  $A_\kappa \in [-2000, 200]$  GeV,  $\lambda \in [2 \cdot 10^{-4}, 0.7]$ ,  $\kappa \in [2 \cdot 10^{-4}, 0.65]$ ,  $2M_1 = M_2 = 500$  GeV,  $M_3 = 1.5$  TeV,  $m_{\tilde{Q}_3} = 1$  TeV,  $m_{\tilde{Q}_{1,2}} = 1.5$  TeV,  $A_t = -2.5$  TeV,  $A_{b,\tau} = -1.5$  TeV,  $m_{\tilde{L}} = 250$  GeV. The distribution of the  $\chi^2$  fit, relative to the best-fit point is shown in crimson ( $\delta\chi^2 < 2.20$ ), red ( $\delta\chi^2 < 3.83$ ), orange ( $\delta\chi^2 < 7.23$ ), yellow ( $\delta\chi^2 < 12.59$ ), green ( $\delta\chi^2 < 16.81$ ) and blue ( $\chi^2 < 122.94$ ); grey dots represent points with  $\chi^2 > 122.94$ , black dots give  $B$ -physics or  $(g-2)_\mu$  outside  $2\sigma$  (and  $\chi^2 > 122.94$ ).

Under these conditions, we settled for the following procedure. Since new NMSSM effects, with respect to the MSSM, essentially involve the tree-level parameters, we decided to freeze the supersymmetric input to a ‘good’ MSSM value (large  $A_t$  and relatively massive squarks, along with light sleptons) and scanned over the 6 tree-level Higgs input quantities:  $\lambda \in [2 \cdot 10^{-4}, 0.7]$  –10 values,  $\kappa \in [2 \cdot 10^{-4}, 0.65]$  –10 values,  $\tan\beta \in [2, 30]$  –15 values,  $M_A \in [100, 2000]$  GeV –20 values,  $\mu \in [120, 2000]$  GeV –20 values,  $A_\kappa \in [-2000, 200]$  GeV –20 values, for a total of about  $12 \cdot 10^6$  points (with about 15% of them not being excluded and representing a data storage of about 0.6 Gbytes). Note that, under these conditions, a large one-loop contribution to the SM-like CP-even Higgs mass is generically present, allowing for a good-fit in the decoupling limit; the benefit of large  $\lambda$ ’s (although not maximal) at low  $\tan\beta$  is not spoiled, however (the MSSM tree-level mass would still be too small to provide a phenomenologically viable Higgs boson at low  $\tan\beta$ ).

We show the outcome of this scan in the  $\{\kappa, \lambda\}$  and the  $\{M_A, \tan\beta\}$  planes in Fig. 21: one observes that the best-fitting points ( $\chi^2 \lesssim 77.5$ ) lay in the  $\lambda \sim \kappa \sim 0.3 - 0.5$  region and draw a band from ( $M_A \sim 500$  GeV,  $\tan\beta \sim 5$ ) to ( $M_A \sim 2000$  GeV,  $\tan\beta \sim 15$ ): they involve a light CP-even singlet. Next follow points fitting very well ( $\chi^2 \sim 77.5 - 79$ ) in the decoupling limit with large  $\tan\beta$  ( $M_A \gtrsim 1$  TeV,  $\tan\beta \gtrsim 20 - 25$ ). Points in the low  $\tan\beta$  limit do not give competitive fits as they suffer from a large pull from  $(g-2)_\mu$  (they still receive  $\chi^2 \sim 85$ , improving on the SM-limit). Fig. 22 shows the singlet composition of the lightest Higgs state. In addition to the best-fitting scenarios that we just discussed – and which are easily recognizable here: light singlets at  $S_{13}^2 \sim 1$  and mass in the range  $[63, 120]$  GeV, decoupling limit

for  $S_{13}^2 \sim 0$  and  $m_{h_1^0} \rightarrow 125$  GeV –, one observes that light singlet states under  $\sim 62$  GeV may come with acceptable fit values, although their doublet components have to be strongly suppressed. Points involving a large singlet-doublet mixing are also found in the vicinity of  $m_{h_1^0} = 125$  GeV. Furthermore, one observes a few points close to the x-axis for  $m_{h_1} \lesssim 100$  GeV: they correspond to the light doublet scenario. While they result in a poor fit to the observed Higgs data  $\chi^2 \gtrsim 135$ , they escape exclusion from the unobserved top decay to a charged Higgs (with mass  $\sim 110$  GeV here) due to a suppressed branching ratio at large values of  $\tan\beta$  ( $\gtrsim 20$ ). Finally, note that the light CP-odd Higgs scenario is only represented by light CP-odd doublets (hence offers a poor fit to the Higgs data due to suppressed conventional channels for the state at  $\sim 125$  GeV) in our scan: light CP-odd singlets are barely represented as the scan density allows for very few points with low  $|A_\kappa|$ .

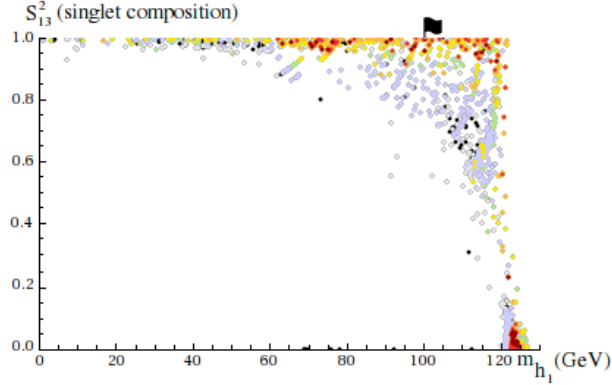


Figure 22: Singlet composition of the light Higgs state in the global scan. (Colour code as in Fig. 21.)

Fig. 23 shows the properties of the heavier Higgs states. The plot on the top left-hand corner shows that the points which give the best fit tend to come with a light second-lightest Higgs state: this can be either the SM-like doublet state at  $\sim 125$  GeV or a slightly heavier singlet. We also find a good fit in a region with mass values of  $\gtrsim 1$  TeV: there, the second-lightest Higgs can be either singlet or heavy-doublet in nature. Interestingly, sizable mixings of the singlet with the heavy doublet state lead to fit values of secondary quality (orange vertical lines, where the ‘line’ shape is an artefact of the scan using discrete values of  $M_A$ ). In the top right-hand corner, the plot shows the composition of the heaviest CP-even state. Unsurprisingly, this state is the heavy doublet state for the best fit points – which involve light singlet states, as follows from our discussion above. However, a good fit is also obtained for the case where the singlet is very heavy, as indicated by the red points forming a horizontal line at  $S_{23}^2 = 1$  (note that the apparent interruption in red points at 2.9 TeV is an artefact of the scan and that the corresponding ‘red line’ actually continues for heavier masses, not displayed in the figure). The plot in the lower row shows the  $\chi^2$  distribution on the plane defined by the masses of the two heaviest CP-even Higgs states. Two favoured regions appear: one, for  $m_{h_2} \sim 125$  GeV and  $m_{h_3} \gtrsim 0.7$  TeV, corresponds to the scenario with a light singlet state; on the contrary, in the other preferred region both  $m_{h_2}$  and  $m_{h_3}$  are heavier than 1 TeV, corresponding to the scenario where one doublet state is light while both the singlet state and the other doublet state are very heavy. Note that both these preferred regions share the common feature to involve a heavy doublet state with a mass close to or above 1 TeV: this is characteristic of the decoupling limit and gives rise to the fact that the light doublet state has SM-like properties.

Let us now investigate the outcome of this global scan in terms of the various scenarii that we considered. Representatives of all the types of spectra that we discussed are found: their best-fit points are summarized in Table 4.

- Point A is the best-fit point of the whole scan. It exhibits a light CP-even singlet at  $\sim 101$  GeV. As for the doublet sector, it is characteristic of the decoupling limit. That this best-fitting point involves a light CP-even singlet demonstrates clearly that this scenario is currently the most interesting and motivated one arising in the context of the NMSSM. The doublet component of the light state is

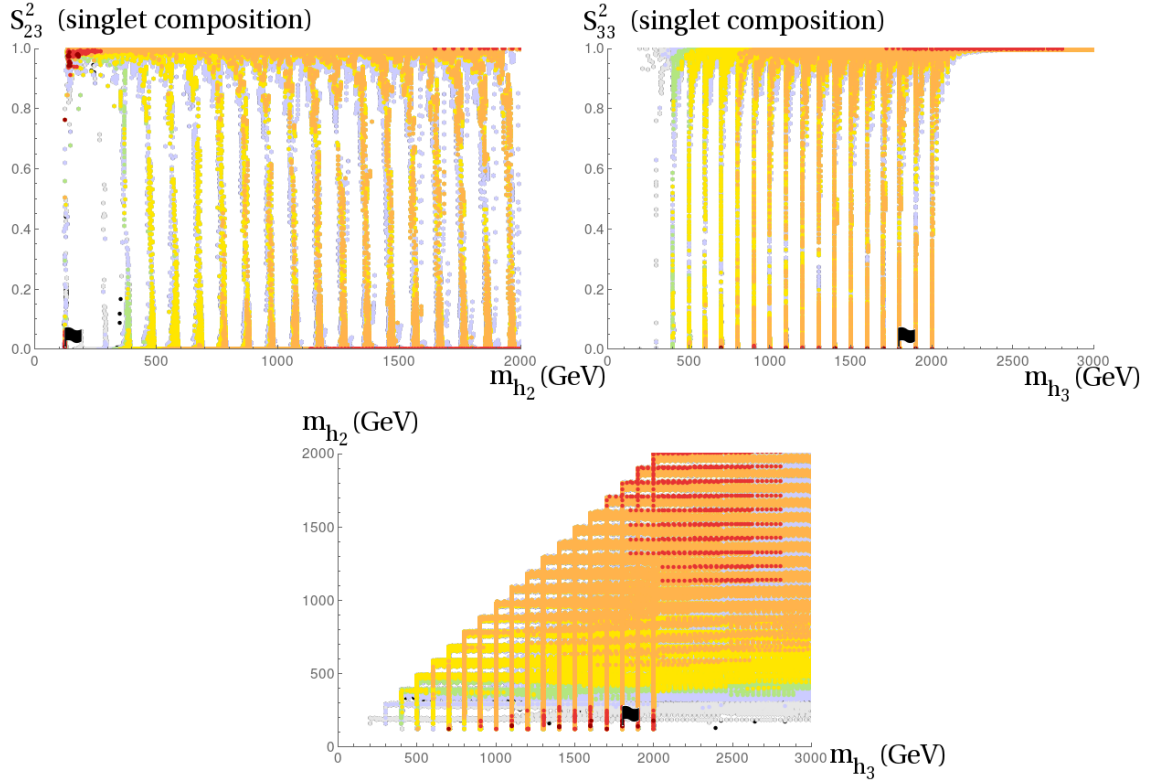


Figure 23: Characteristics of the heavier CP-even Higgs states in the global scan. (Colour code as in Fig. 21.) In the first row, we show the singlet composition of the second (left) and third (right) CP-even Higgs state as a function of their masses. The plot below shows the distribution of the fit in the plane defined by the masses of the two heavier Higgs states. Note that the ‘ladder’ and ‘grid’ structures in this plot are artefacts of the scan.

of the order of 2%, so that the associated signals in direct production should be expected at the percent level of those of a SM Higgs boson.

- Point B involves a light CP-even doublet state below 100 GeV. The associated  $\chi^2$  is quite high, illustrating the limited pertinence of this interpretation of the LHC data.
- Points C and D are two representatives of the NMSSM at low  $\tan \beta$  and large  $\lambda$ : in the first case, the CP-even singlet state is lighter than the doublet at  $\sim 125$  GeV, while it is heavier in the second case. Note that  $(g - 2)_\mu$  is a major pull in the present case, due to both low  $\tan \beta$  and moderately light sleptons/neutralinos/charginos. In both cases, the mostly-singlet state has a doublet component at the percent level only, leading to suppressed production rates.
- Point E is a representative of the decoupling limit at ‘large’  $\tan \beta$ , although not in the MSSM limit. The large value of  $\tan \beta \sim 18$  is essentially driven by  $(g - 2)_\mu$ . The heavy doublet states have large masses ( $\sim 2$  TeV), while a CP-even singlet with a  $\sim 2\%$  doublet component appears at  $\sim 200$  GeV.
- Point F gives the best fit value for the MSSM limit: this is again a ‘Decoupling Limit’-like point with large  $\tan \beta$ , heavy  $H^\pm$ ,  $H^0$ ,  $A^0$  doublet states and even heavier singlets. The presence of relatively light sleptons and a bino at  $\sim 250$  GeV together with large  $\tan \beta$  allow for a satisfactory fit to  $(g - 2)_\mu$ , while, for all other aspects, this point could be regarded as belonging to the SM limit.
- Two CP-even states, mixing singlet and light doublet almost at the level of 25%, intervene close to

Parameters	Point A (light sing.)	Point B (light doub.)	Point C (low $\tan \beta$ )	Point D (low $\tan \beta$ )	Point E (Dec. limit)	...
$\lambda$	0.54	0.16	0.54	0.63	0.39	...
$\kappa$	0.43	0.29	0.22	0.36	0.58	...
$\tan \beta$	14	20	2	2	18	...
$\mu_{\text{eff}}$ (GeV)	120	1505	219	318	120	...
$M_A$ (GeV)	1700	200	500	600	1900	...
$A_\kappa$ (GeV)	-263	-2000	-263	-147	-495	...
Higgs Spectrum						
$m_{h_1}$ (GeV)	100.5 S	69.9 D	106.6 S	124.5 D	123.1 D	...
$m_{h_2}$ (GeV)	125.2 D	122.8 D	126.3 D	333 S	203 S	...
$m_{A_1}$ (GeV)	285 S	61.6 D	279 S	309 S	512 S	...
$m_{H^\pm}$ (GeV)	1671	110.7	491	589	1874	...
$\chi^2$ (/89 obs.)	75.8	137.7	87.6	85.4	78.6	...

...	Point F (MSSM limit)	Point G (2 CP-even)	Point H (close CP odd)	Point I ( $m_{h_1} < \frac{m_{h_{SM}}}{2}$ )	Point J ( $m_{A_1} < \frac{m_{h_{SM}}}{2}$ )
...	$2 \cdot 10^{-4}$	0.23	0.39	0.23	0.08
...	$2 \cdot 10^{-4}$	0.22	0.36	0.14	0.36
...	20	6	8	16	26
...	1406	120	120	120	1109
...	2000	700	900	1900	200
...	-2000	-147.4	-31.6	-263	-1421
...	123.0 D	122.0 S	123.7 D	48.9 S	69.1 D
...	2012 D	123.4 D	211.7 S	124.3 D	124.0 D
...	2013 D	198 S	123.6 S	244 S	61.7 D
...	2014	$S_{13}^2 \simeq 76\%$	$P_{13}^2 \simeq 99.8\%$	/	$BR(h_1 \rightarrow 2A_1) \sim 0.7$
...	79.3 D	77.0	82.3	82.8	174.1

Table 4: A few ‘best-fit points’ emerging from the ‘global’ scan.

$\sim 125$  GeV in Point G. While ATLAS and CMS may be able to resolve their mass gap of about 1.5 GeV, note that the degeneracy could be at the level of 100 MeV. While points with smaller mass gaps were present in the global scan, none showed a mixing between singlet and doublet components as large as Point G: the latter would allow for the observability of two separate peaks of comparable width in the spectrum.

- Point H involves, in addition to a CP-even doublet, one singlet-like CP-odd state close to  $\sim 125$  GeV. As the corresponding state is singlet at 99.8%, the effect in direct production is completely negligible. Effects in pair production could develop however, due to the  $h_1 - A_1 - A_1$  coupling.
- For the Points I and J, light states are present below  $m_{h_{SM}}/2$ , hence potentially opening unconventional Higgs decays. For Point I, the light state is a CP-even singlet at  $\sim 50$  GeV: even though  $\lambda$  and  $\kappa$  are quite large, the unconventional Higgs decay is suppressed due to an accidental cancellation of the various terms entering the  $h_2 - h_1 - h_1$  coupling: this avoids conflict with the LHC/TeVatron data. The doublet component of the light state is under 1%, explaining its compatibility with the LEP constraints. For Point J, a light doublet-like CP-odd state is present, leading to a large  $h_1 \rightarrow 2A_1$  branching ratio  $\sim 0.7$ : the quality of the fit is correspondingly quite poor, despite the presence of a CP-even doublet at  $\sim 124$  GeV. Note that the case of light CP-odd Higgs states is not really probed in this scan since the low scan density does not allow for many points in the low

$|A_\kappa|$  region (which provides the light CP-odd singlet states).

## 11 Conclusions

This discussion of the NMSSM Higgs scenarii in view of the Higgs-measurement data shows that, even though a conventional SM-like Higgs is expected at  $\sim 125$  GeV, many scenarios that differ very significantly from the SM case remain possible and even give competitive fits to the LHC/TeVatron data. In most cases, these configurations involve light additional degrees of freedom, CP-even and/or CP-odd, singlet or doublet-like, hiding invisibly at lower masses or combining their signals with those of the SM-like state.

The most prominent NMSSM Higgs scenario which turned out to be favoured by the fits carried out in this paper involves a CP-even mostly singlet state with mass below that of the light doublet state (which is identified with the signal observed at LHC) and includes a small mixing of the singlet and doublet components. From the point of view of the model, this setup has the desirable feature of uplifting somewhat the mass of the doublet-like state, arguably rendering a mass of  $\sim 125$  GeV more natural. Small deviations, at the percent level, from the SM rates, e.g. slightly suppressed decays into down-type fermions or slightly enhanced vector channels, can also be generated for the state at  $\sim 125$  GeV via a disturbed proportion in  $H_u$  and  $H_d$  components, which is associated to the appearance of a small singlet component (three-state mixing). Such features are shared with many other configurations however (e.g. perturbation of the couplings via heavier particles contributing at the loop level), and the crucial test of this scenario would lie in the detection of the light CP-even singlet itself. In the most favourable cases, the latter may acquire doublet components of the order of 10% and could thus appear as a ‘miniature’ Higgs boson, with a production cross-section reduced to  $\sim 10\%$  of that of a SM state at the same mass. Its dominant decays would likely be  $b\bar{b}$  and  $\tau^+\tau^-$ , although unconventional rates, e.g. enhanced  $\gamma\gamma$  or even  $c\bar{c}$  channels, could also appear in certain configurations of the doublet composition of the lightest state. As an additional feature, the  $2.3\sigma$  (local) excess noted at LEP in  $e^+e^- \rightarrow Zh \rightarrow b\bar{b}$  could be accommodated with such a singlet carrying a sizable doublet component in the vicinity of  $\sim 100$  GeV. Direct searches, e.g. in the  $\gamma\gamma$  or the  $\tau^+\tau^-$  channel, may thus eventually detect such a particle, provided that those searches are carried out in the low-mass region. On the other hand, reduced doublet components, in the percent range or below, are also compatible with the data and may equally well account for an uplift of the mass of the second lightest CP-even state. Discovery of the light state could then prove difficult and, while effects in Higgs pair production are possible, improved searches would be required to ensure that the singlet does not remain unnoticed.

In contrast, the popular NMSSM scenario where the SM-like Higgs boson decays unconventionally and sizably into lighter Higgs states (CP-even or CP-odd) has been essentially emptied of its phenomenological content, due to the success of the Higgs searches in the standard channels. Yet, light states below  $\sim 63$  GeV are still an open possibility provided the decay of the ‘observed’ Higgs towards them is suppressed. From the point of view of the model, this amounts to a constraint on the Higgs sector. The main consequence for the hypothetical light states is that their coupling to the observed state should remain small, which implies, in particular, that they should be almost purely singlets. This further reduces the prospects for detecting the light Higgs state via channels alternative to the decays from the doublet states, as all couplings to SM particles (hence the cross-section in production channels involving fermions or vector bosons) are correspondingly suppressed.

A more exotic possibility is a scenario with additional quasi-degenerate states at  $\sim 125$  GeV. The NMSSM indeed allows for CP-even singlet states at this mass. While the off-diagonal singlet-doublet mass-entry should then remain small (so that the quasi-degeneracy is not lifted by this off-diagonal term), the mixing of such a singlet with the SM-like state could be as large as 50% (but also as small as 0%). Such a possible scenario motivates experimental efforts to improve the resolution in the mass measurement of the state at  $\sim 125$  GeV, as two separate peaks may eventually become distinguishable. Other possible, but not guaranteed, effects would arise from modified apparent triple-Higgs couplings at 125 GeV. The situation is somewhat different if the additional state is CP-odd. While current limits then favour a mostly singlet state, a sizable doublet component may also be present (hence allow the state to be produced and contribute to the LHC rates). As the CP-odd Higgs does not couple to electroweak gauge

bosons, its decay products, essentially fermionic, would add to those of the SM-like state and displace the apparent proportion among the various channels. Note that this latter case mimicks a scenario with CP-violation in the Higgs sector, where the observed state would have a CP-odd component.

A noteworthy aspect of the NMSSM, as compared to the MSSM, lies in its resilience at low values of  $\tan\beta$ , where specific tree-level contributions associated with a large  $\lambda$  become important. Dependence on the supersymmetric spectrum to generate a Higgs mass close to  $\sim 125$  GeV is of secondary importance in this case, so that the hypothetical presence of light stops and small trilinear couplings can be compatible in the NMSSM with the discovered signal. In addition to the most commonly considered case where the SM-like state is the lightest CP-even Higgs, the previous scenarios, involving e.g. a lighter CP-even singlet or quasi-degenerate states, can be accommodated in this context as well.

Finally, the prospect of a light doublet Higgs sector, with light neutral states below 100 GeV, decoupling from electroweak gauge bosons, cannot be discarded altogether yet. While a significant adjustment of the parameters is necessary to avoid the relevant experimental limits, this scenario can serve as a motivation to cover remaining loopholes in the experimental searches. Further searches for light neutral but also charged Higgs states should soon provide more information about the validity of this scenario.

In summary, while the properties of the detected signal are so far compatible with the Higgs boson of the SM, the analyses of this paper clearly demonstrate that the current results do not necessarily imply a minimalistic phenomenology but, on the contrary, call for a comprehensive investigation and precision tests of the Higgs properties.

## Acknowledgements

The authors acknowledge interesting discussions with U. Ellwanger. They are also grateful to T. Stefaniak and O. Stål for their assistance in the use of HiggsBounds and HiggsSignals, as well as to S. Liebler for his help with SusHi. The authors acknowledge support by the DFG through the SFB 676 “Particles, Strings and the Early Universe”. This research was supported in part by the European Commission through the “HiggsTools” Initial Training Network PITN-GA-2012-316704.

## A Best Fit points in Fig. 2-20

NMSSMTools Parameters	Figure 2 (SM limit)	Figure 3 (Dec. Limit)	Figure 3 (Dec. Limit)	Figure 4 (light sing.)	Figure 4 (2 CP-even)	...
$\lambda$	$1 \cdot 10^{-5}$	0.2	$2 \cdot 10^{-4}$	0.45	0.55	...
$\kappa$	$1 \cdot 10^{-5}$	0.6	$2 \cdot 10^{-4}$	0.35	0.3	...
$\tan \beta$	10.8	23	22	8	8	...
$\mu_{\text{eff}}$ (GeV)	1000	200	200	125	125	...
$M_A$ (GeV)	2000	1000	1000	1000	1000	...
$A_\kappa$ (GeV)	-1000	-1500	-578	-255	-27	...
$M_1$ (GeV)	500	250	250	250	250	...
$M_2$ (GeV)	1000	500	500	500	500	...
$M_3$ (TeV)	3	1.5	1.5	1.5	1.5	...
$m_{\tilde{Q}_{1,2}}$ (TeV)	2	1.5	1.5	1.5	1.5	...
$m_{\tilde{Q}_3}$ (TeV; if $\neq m_{\tilde{Q}_{1,2}}$ )	/	1.1	1.1	1	1	...
$m_{\tilde{L}}$ (GeV)	1000	300	300	200	200	...
$A_t$ (TeV)	-4	-2.3	-2.3	-2	-2	...
$A_{b,\tau}$ (TeV; if $\neq A_t$ )	-1.5	-1.5	-1.5	-1.5	-1.5	...
Higgs Spectrum						
$m_{h_1}$ (GeV)	125.7 D	124.1 D	125.0 D	109.5 S	124.6 D	...
$m_{h_2}$ (GeV)	1732 S	732 S	211 S	124.5 D	124.9 S	...
$m_{A_1}$ (GeV)	1732 S	972 S	589 S	280 S	110 S	...
Other	/	/	/	$S_{13}^2 = 95\%$	$S_{13}^2 = 20\%$	...
$\chi^2$ (/89 obs.)	86.9	80.5	81.4	75.5	80.1	...

Table 5: A few ‘best-fit points’, with NMSSMTools input parameters and some data concerning the Higgs spectrum. The labels (SM limit), (Dec. limit), (light doub.), (light sing.), (CP odd), (large  $\lambda$ ), ( $\lambda$ +sing.), (2 CP-even), (close  $A$ ) refer to the remarkable characteristics of the point, belonging to the class of points respectively in SM-limit, in the decoupling limit, exhibiting a doublet CP-even Higgs much lighter than  $\sim 125$  GeV, exhibiting a singlet CP-even Higgs much lighter than  $\sim 125$  GeV, with a light CP-odd Higgs under  $\sim 125$  GeV, profiting from a large tree level  $\lambda$  effect, involving both a large  $\lambda$  effect and a light CP-even singlet, involving several CP-even Higgs states close to  $\sim 125$  GeV, or a CP-odd Higgs close to  $\sim 125$  GeV. The letters S and D coming together with the masses of the Higgs states indicate whether the state is dominantly singlet or doublet. HB\_4.1.3 + HS\_1.2.0 indicate that the test for a particular point was performed with the versions 4.1.3 and 1.2.0 of HiggsBounds and HiggsSignals instead of versions 4.2.0 and 1.3.1 as for the rest of the points.



...	Figure 4 (CP-odd)	Figure 6 (light sing.)	Figure 8 (light sing.)	Figure 8 (light sing.)	Figure 9 ( $\lambda$ +sing.)	Figure 9 (large $\lambda$ )	...
...	0.55	0.6	0.1	0.1	0.7	0.7	...
...	0.3	0.35	0.05	0.05	0.1	0.1	...
...	8	8	12	12	2	2	...
...	125	125	125	125	361	324	...
...	1000	1000	1655	1367	870	775	...
...	-46	-204	-69	-84	-123	31	...
...	250	250	250	250	75	75	...
...	500	500	500	500	150	150	...
...	1.5	1.5	1.5	1.5	1.5	1.5	...
...	1.5	1.5	1.5	1.5	1.5	1.5	...
...	1	1	1	1	0.5	0.5	...
...	200	200	200	200	110	110	...
...	-2	-1.5	-2	-2	-0.1	-0.1	...
...	-1.5	/	1	1	-1.5	-1.5	...
...							
...	119.8 S	61.8 S	105.3 S	101.6 S	105.3 S	123.2 D	...
...	124.8 D	123.4 D	124.5 D	123.9 D	124.7 D	131.7 S	...
...	124.8 S	-235 S	114.3 S	125.9 S	173 S	79 S	...
...	$P_{13}^2 = 99.4\%$	$S_{13}^2 = 96\%$	$S_{13}^2 = 94\%$	$Br_{h_1 \rightarrow c\bar{c}} \simeq 31\%$	$S_{13}^2 = 94\%$	$S_{13}^2 = 4\%$	...
...	79.4	75.2	79.8	82.4	76.1	76.6	...

...	Figure 9 (2 CP-even)	Figure 12 ( $\lambda$ +sing.)	Figure 12 ( $\lambda$ +sing.)	Figure 13 (CP odd)	Figure 13 (CP odd)	...
...	0.7	0.7	0.7	0.4	0.25	...
...	0.1	0.1	0.1	0.25	0.15	...
...	2	2.25	2.25	8	11	...
...	398	315	343	120	120	...
...	951	826	898	900	1200	...
...	-68	-83	-51	-31	-1	...
...	75	75	75	250	250	...
...	150	150	150	500	500	...
...	1.5	1.5	1.5	1.5	1.5	...
...	1.5	1.5	1.5	1.5	1.5	...
...	0.5	0.5	0.5	1.2	1.2	...
...	110	150	150	300	300	...
...	-0.1	-0.1	-0.1	-2.5	-2.5	...
...	/	/	/	/	/	...
...						
...	123.4 S/D	100.5 S	108.9 S	123.0 D	123.2 D	...
...	123.8 D/S	123.4 D	125.8 D	141 S	144 S	...
...	154 S	145 S	135 S	103.1 S	41.3 ( $P_{13}^2 \simeq 100\%$ )	...
...	$S_{13}^2 = 63\%$	$S_{13}^2 = 81\%$	$S_{13}^2 = 73\%$	$P_{13}^2 = 99.7\%$	$Br_{h_1 \rightarrow 2A_1} \simeq 1 \cdot 10^{-3}\%$	...
...	77.1	77.0	79.2	75.9	78.7	...

...	Figure 13 (CP odd)	Figure 13 (close CP odd)	Figure 17 (2 CP-even)	Figure 18 (2 CP-even)	Figure 19 (light doub.)
...	0.2	0.5	$1 \cdot 10^{-3}$	0.7	0.2
...	0.1	0.4	$1 \cdot 10^{-3}$	0.1	0.6
...	10	11	18	2	9.25
...	120	120	120	403	200
...	1200	1200	1903	963	130
...	4	-31	-350	-75	-1392
...	250	250	250	75	250
...	500	500	500	150	500
...	1.5	1.5	1.5	1.5	1.5
...	1.5	1.5	1.5	1.5	1.5
...	1.2	1.2	1.2	0.5	1.1
...	300	300	300	150	300
...	-2.5	-2.5	-2.5	-0.1	-2.3
...	-1.5	-1.5	-1.5	/	-1.5 ...
...	120.6 S	123.2 D	125.0 S/D	122.9 S/D	75.9 D
...	124.7 D	181 S	125.1 D/S	123.9 D/S	125.1 D
...	6.4 ( $P_{13}^2 \simeq 100\%$ )	124.2 S	355 S	160 S	70.3 D
...	$Br_{h_1 \rightarrow 2A_1} \simeq 98\%$	$P_{13}^2 \simeq 99.8\%$	$S_{13}^2 = 53\%$	$S_{13}^2 = 91\%$	$m_{H^\pm} = 107.3$
...	80.6	76.5	79.8	76.2	HB_4.1.3 + HS_1.2.0: 88.0

## References

- [1] G. Aad *et al.* [ATLAS Collaboration], Phys. Lett. B **716** (2012) 1 [arXiv:1207.7214 [hep-ex]].
- [2] S. Chatrchyan *et al.* [CMS Collaboration], Phys. Lett. B **716** (2012) 30 [arXiv:1207.7235 [hep-ex]].
- [3] H. P. Nilles, “Supersymmetry, Supergravity And Particle Physics,” Phys. Rept. **110** (1984) 1.
- [4] E. Witten, *Nucl. Phys.* **B188** (1981) 513.  
S. Dimopoulos and H. Georgi, *Nucl. Phys.* **B193** (1981) 150.  
E. Witten, *Phys. Lett.* **B105** (1981) 267.  
R. K. Kaul and P. Majumdar, *Nucl. Phys.* **B199** (1982) 36.  
N. Sakai, *Z. Phys.* **C11** (1981) 153.
- [5] S. P. Martin, In \*Kane, G.L. (ed.): Perspectives on supersymmetry II\* 1-153 [hep-ph/9709356].  
D. J. H. Chung, L. L. Everett, G. L. Kane, S. F. King, J. D. Lykken and L. -T. Wang, Phys. Rept. **407** (2005) 1 [hep-ph/0312378].
- [6] U. Ellwanger, C. Hugonie and A. M. Teixeira, Phys. Rept. **496** (2010) 1 [arXiv:0910.1785 [hep-ph]].
- [7] M. Maniatis, Int. J. Mod. Phys. A **25** (2010) 3505 [arXiv:0906.0777 [hep-ph]].
- [8] P. Fayet, *Nucl. Phys.* **B90** (1975) 104.  
P. Fayet, *Phys. Lett* **B69** (1977) 489.  
P. Fayet, S. Ferrara, *Phys. Rept.* **32** (1977) 249.
- [9] J. E. Kim and H. P. Nilles, Phys. Lett. B **138** (1984) 150.
- [10] U. Ellwanger and C. Hugonie, Mod. Phys. Lett. A **22** (2007) 1581 [hep-ph/0612133].
- [11] L. J. Hall, D. Pinner and J. T. Ruderman, JHEP **1204** (2012) 131 [arXiv:1112.2703 [hep-ph]].  
A. Arvanitaki and G. Villadoro, JHEP **1202** (2012) 144 [arXiv:1112.4835 [hep-ph]].  
S. F. King, M. Muhlleitner and R. Nevzorov, Nucl. Phys. B **860** (2012) 207 [arXiv:1201.2671 [hep-ph]].  
Z. Kang, J. Li and T. Li, JHEP **1211** (2012) 024 [arXiv:1201.5305 [hep-ph]].  
J. Cao, Z. Heng, J. M. Yang and J. Zhu, JHEP **1210** (2012) 079 [arXiv:1207.3698 [hep-ph]].  
K. Agashe, Y. Cui and R. Franceschini, JHEP **1302** (2013) 031 [arXiv:1209.2115 [hep-ph]].  
R. Barbieri, D. Buttazzo, K. Kannike, F. Sala and A. Tesi, Phys. Rev. D **87** (2013) 115018 [arXiv:1304.3670 [hep-ph]].  
R. Barbieri, D. Buttazzo, K. Kannike, F. Sala and A. Tesi, Phys. Rev. D **88** (2013) 055011 doi:10.1103/PhysRevD.88.055011 [arXiv:1307.4937 [hep-ph]].
- [12] S. A. Abel, S. Sarkar and P. L. White, Nucl. Phys. B **454** (1995) 663 [hep-ph/9506359].
- [13] S. Heinemeyer, O. Stal and G. Weiglein, Phys. Lett. B **710** (2012) 201 [arXiv:1112.3026 [hep-ph]].  
A. Bottino, N. Fornengo and S. Scopel, Phys. Rev. D **85** (2012) 095013 [arXiv:1112.5666 [hep-ph]].  
M. Drees, Phys. Rev. D **86** (2012) 115018 [arXiv:1210.6507 [hep-ph]].  
K. Hagiwara, J. S. Lee and J. Nakamura, JHEP **1210** (2012) 002 [arXiv:1207.0802 [hep-ph]].  
A. Arbey, M. Battaglia, A. Djouadi and F. Mahmoudi, JHEP **1209** (2012) 107 [arXiv:1207.1348 [hep-ph]].
- [14] P. Bechtle, S. Heinemeyer, O. Stal, T. Stefaniak, G. Weiglein and L. Zeune, Eur. Phys. J. C **73** (2013) 2354 [arXiv:1211.1955 [hep-ph]].
- [15] M. Carena, S. Heinemeyer, O. Stål, C. E. M. Wagner and G. Weiglein, Eur. Phys. J. C **73** (2013) 2552 [arXiv:1302.7033 [hep-ph]].
- [16] The ATLAS collaboration, ATLAS-CONF-2013-090, ATLAS-COM-CONF-2013-107.

- [17] The CMS collaboration, CMS-PAS-HIG-14-020.
- [18] P. Bechtle, O. Brein, S. Heinemeyer, G. Weiglein and K. E. Williams, *Comput. Phys. Commun.* **181** (2010) 138 [arXiv:0811.4169 [hep-ph]].  
P. Bechtle, O. Brein, S. Heinemeyer, G. Weiglein and K. E. Williams, *Comput. Phys. Commun.* **182** (2011) 2605 [arXiv:1102.1898 [hep-ph]].  
P. Bechtle, O. Brein, S. Heinemeyer, O. Stal, T. Stefaniak, G. Weiglein and K. Williams, *PoS CHARGED* **2012** (2012) 024 [arXiv:1301.2345 [hep-ph]].  
P. Bechtle, O. Brein, S. Heinemeyer, O. Stål, T. Stefaniak, G. Weiglein and K. E. Williams, *Eur. Phys. J. C* **74** (2014) 2693 [arXiv:1311.0055 [hep-ph]].  
<http://higgsbounds.hepforge.org/>
- [19] P. Bechtle, S. Heinemeyer, O. Stål, T. Stefaniak and G. Weiglein, *Eur. Phys. J. C* **74** (2014) 2711 [arXiv:1305.1933 [hep-ph]].
- [20] The ATLAS Collaboration, <https://twiki.cern.ch/twiki/bin/view/AtlasPublic/HiggsPublicResults>
- [21] The CMS Collaboration, <https://twiki.cern.ch/twiki/bin/view/CMSPublic/PhysicsResultsHIG>
- [22] T. Aaltonen *et al.* [CDF and D0 Collaborations], *Phys. Rev. Lett.* **109** (2012) 071804 [arXiv:1207.6436 [hep-ex]].  
T. Aaltonen *et al.* [CDF and D0 Collaborations], *Phys. Rev. D* **88** (2013) 5, 052014 [arXiv:1303.6346 [hep-ex]].
- [23] U. Ellwanger, *JHEP* **1203** (2012) 044 [arXiv:1112.3548 [hep-ph]].  
J. -J. Cao, Z. -X. Heng, J. M. Yang, Y. -M. Zhang and J. -Y. Zhu, *JHEP* **1203** (2012) 086 [arXiv:1202.5821 [hep-ph]].  
R. Benbrik, M. Gomez Bock, S. Heinemeyer, O. Stal, G. Weiglein and L. Zeune, *Eur. Phys. J. C* **72** (2012) 2171 [arXiv:1207.1096 [hep-ph]].  
Z. Heng, *Adv. High Energy Phys.* **2012** (2012) 312719 [arXiv:1210.3751 [hep-ph]].  
K. Choi, S. H. Im, K. S. Jeong and M. Yamaguchi, *JHEP* **1302** (2013) 090 [arXiv:1211.0875 [hep-ph]].  
S. F. King, M. Mühlleitner, R. Nevzorov and K. Walz, *Nucl. Phys. B* **870** (2013) 323 [arXiv:1211.5074 [hep-ph]].  
J. W. Fan *et al.*, *Chin. Phys. C* **38** (2014) 073101 [arXiv:1309.6394 [hep-ph]].
- [24] J. F. Gunion, Y. Jiang and S. Kraml, *Phys. Lett. B* **710** (2012) 454 [arXiv:1201.0982 [hep-ph]].  
U. Ellwanger and C. Hugonie, *Adv. High Energy Phys.* **2012** (2012) 625389 [arXiv:1203.5048 [hep-ph]].  
K. Kowalska *et al.* [BayesFITS Group Collaboration], *Phys. Rev. D* **87** (2013) 11, 115010 [arXiv:1211.1693 [hep-ph]].  
C. Beskidt, W. de Boer and D. I. Kazakov, *Phys. Lett. B* **726** (2013) 758 [arXiv:1308.1333 [hep-ph]].  
C. Beskidt, W. de Boer and D. I. Kazakov, arXiv:1402.4650 [hep-ph].  
U. Ellwanger and C. Hugonie, arXiv:1405.6647 [hep-ph].
- [25] L. Randall and M. Reece, *JHEP* **1308** (2013) 088 [arXiv:1206.6540 [hep-ph]].  
B. Kyae and J. -C. Park, *Phys. Rev. D* **87** (2013) 075021 [arXiv:1207.3126 [hep-ph]].
- [26] K. S. Jeong, Y. Shoji and M. Yamaguchi, *JHEP* **1209** (2012) 007 [arXiv:1205.2486 [hep-ph]].  
K. J. Bae, K. Choi, E. J. Chun, S. H. Im, C. B. Park and C. S. Shin, *JHEP* **1211** (2012) 118 [arXiv:1208.2555 [hep-ph]].  
I. Gogoladze, B. He and Q. Shafi, *Phys. Lett. B* **718** (2013) 1008 [arXiv:1209.5984 [hep-ph]].  
J. Cao, D. Li, L. Shang, P. Wu and Y. Zhang, arXiv:1409.8431 [hep-ph].
- [27] S. Moretti, S. Munir and P. Poulose, *Phys. Rev. D* **89** (2014) 1, 015022 [arXiv:1305.0166 [hep-ph]].  
S. Moretti and S. Munir, arXiv:1505.00545 [hep-ph].

- [28] T. Gherghetta, B. von Harling, A. D. Medina and M. A. Schmidt, *JHEP* **02** (2013) 032 [arXiv:1212.5243 [hep-ph]].  
A. Kaminska, G. G. Ross and K. Schmidt-Hoberg, *JHEP* **1311** (2013) 209 [arXiv:1308.4168 [hep-ph]].  
A. Kaminska, G. G. Ross, K. Schmidt-Hoberg and F. Staub, *JHEP* **1406** (2014) 153 [arXiv:1401.1816 [hep-ph]].
- [29] D. A. Vasquez, G. Belanger, C. Boehm, J. Da Silva, P. Richardson and C. Wymant, *Phys. Rev. D* **86** (2012) 035023 [arXiv:1203.3446 [hep-ph]].  
T. Cheng, J. Li, T. Li and Q. -S. Yan, arXiv:1304.3182 [hep-ph].  
T. Cheng and T. Li, *Phys. Rev. D* **88** (2013) 015031 [arXiv:1305.3214 [hep-ph]].
- [30] G. Belanger, U. Ellwanger, J. F. Gunion, Y. Jiang, S. Kraml and J. H. Schwarz, *JHEP* **1301** (2013) 069 [arXiv:1210.1976 [hep-ph]].  
M. Badziak, M. Olechowski and S. Pokorski, *JHEP* **1306** (2013) 043 [arXiv:1304.5437 [hep-ph]].  
M. Badziak, M. Olechowski and S. Pokorski, arXiv:1310.4518 [hep-ph].
- [31] J. F. Gunion, Y. Jiang and S. Kraml, *Phys. Rev. D* **86** (2012) 071702 [arXiv:1207.1545 [hep-ph]].  
S. Munir, L. Roszkowski and S. Trojanowski, *Phys. Rev. D* **88** (2013) 5, 055017 [arXiv:1305.0591 [hep-ph]].
- [32] Z. Kang, J. Li, T. Li, D. Liu and J. Shu, *Phys. Rev. D* **88** (2013) 1, 015006 [arXiv:1301.0453 [hep-ph]].  
J. Cao, Z. Heng, L. Shang, P. Wan and J. M. Yang, *JHEP* **1304** (2013) 134 [arXiv:1301.6437 [hep-ph]].  
D. T. Nhung, M. Muhlleitner, J. Streicher and K. Walz, *JHEP* **1311**, 181 (2013) [arXiv:1306.3926 [hep-ph]].  
U. Ellwanger, *JHEP* **1308** (2013) 077 [arXiv:1306.5541 [hep-ph]].  
C. Han, X. Ji, L. Wu, P. Wu and J. M. Yang, *JHEP* **1404** (2014) 003 [arXiv:1307.3790 [hep-ph]].  
L. Wu, J. M. Yang, C. P. Yuan and M. Zhang, *Phys. Lett. B* **747** (2015) 378 [arXiv:1504.06932 [hep-ph]].
- [33] M. M. Almarashi and S. Moretti, arXiv:1205.1683 [hep-ph].  
J. Rathsmann and T. Rossler, *Adv. High Energy Phys.* **2012** (2012) 853706 [arXiv:1206.1470 [hep-ph]].  
D. G. Cerdeno, P. Ghosh and C. B. Park, *JHEP* **1306** (2013) 031 [arXiv:1301.1325 [hep-ph]].  
J. Cao, F. Ding, C. Han, J. M. Yang and J. Zhu, *JHEP* **1311** (2013) 018 [arXiv:1309.4939 [hep-ph]].
- [34] N. E. Bomark, S. Moretti, S. Munir and L. Roszkowski, arXiv:1409.8393 [hep-ph].  
N. E. Bomark, S. Moretti and L. Roszkowski, arXiv:1503.04228 [hep-ph].
- [35] N. D. Christensen, T. Han, Z. Liu and S. Su, *JHEP* **1308** (2013) 019 [arXiv:1303.2113 [hep-ph]].
- [36] S. F. King, M. Muhlleitner, R. Nevzorov and K. Walz, arXiv:1408.1120 [hep-ph].
- [37] D. Buttazzo, F. Sala and A. Tesi, arXiv:1505.05488 [hep-ph].  
M. Guchait and J. Kumar, arXiv:1509.02452 [hep-ph].
- [38] U. Ellwanger, J. F. Gunion and C. Hugonie, *JHEP* **0502** (2005) 066 [hep-ph/0406215].  
U. Ellwanger and C. Hugonie, *Comput. Phys. Commun.* **175** (2006) 290 [hep-ph/0508022].  
U. Ellwanger, J. F. Gunion, C. Hugonie, *JHEP* **0502** (2005) 066, arXiv:hep-ph/0406215  
U. Ellwanger, C. Hugonie, *Comput. Phys. Commun.* **175** (2006) 290, arXiv:hep-ph/0508022  
<http://www.th.u-psud.fr/NMHDECAY/nmssmtools.html>
- [39] F. Domingo, U. Ellwanger, E. Fullana, C. Hugonie and M. -A. Sanchis-Lozano, *JHEP* **0901** (2009) 061 [arXiv:0810.4736 [hep-ph]].  
F. Domingo, U. Ellwanger and M. -A. Sanchis-Lozano, *Phys. Rev. Lett.* **103** (2009) 111802

- [arXiv:0907.0348 [hep-ph]].  
F. Domingo, JHEP **1104** (2011) 016 [arXiv:1010.4701 [hep-ph]].
- [40] F. Domingo and U. Ellwanger, JHEP **0712** (2007) 090 [arXiv:0710.3714 [hep-ph]].
- [41] F. Domingo and U. Ellwanger, JHEP **0807** (2008) 079 [arXiv:0806.0733 [hep-ph]].
- [42] G. Belanger, F. Boudjema, C. Hugonie, A. Pukhov and A. Semenov, JCAP **0509** (2005) 001 [hep-ph/0505142].  
G. Belanger, F. Boudjema, A. Pukhov and A. Semenov, Comput. Phys. Commun. **185** (2014) 960 [arXiv:1305.0237 [hep-ph]].
- [43] G. Belanger, B. Dumont, U. Ellwanger, J. F. Gunion and S. Kraml, Phys. Rev. D **88** (2013) 075008 [arXiv:1306.2941 [hep-ph]].
- [44] R. Barate *et al.* [LEP Working Group for Higgs boson searches and ALEPH and DELPHI and L3 and OPAL Collaborations], Phys. Lett. B **565** (2003) 61 [hep-ex/0306033].
- [45] R. Aaij *et al.* [LHCb Collaboration], JHEP **1305** (2013) 132 [arXiv:1304.2591 [hep-ex]].
- [46] G. Aad *et al.* [ATLAS Collaboration], arXiv:1407.6583 [hep-ex].
- [47] U. Ellwanger, Phys. Lett. B **698** (2011) 293 [arXiv:1012.1201 [hep-ph]].
- [48] R. V. Harlander, S. Liebler and H. Mantler, Comput. Phys. Commun. **184** (2013) 1605 [arXiv:1212.3249 [hep-ph]].  
S. Liebler, Eur. Phys. J. C **75** (2015) 5, 210 [arXiv:1502.07972 [hep-ph]].
- [49] B. A. Dobrescu and K. T. Matchev, JHEP **0009** (2000) 031 [hep-ph/0008192].  
O. Stal and G. Weiglein, JHEP **1201** (2012) 071 [arXiv:1108.0595 [hep-ph]].
- [50] G. Abbiendi *et al.* [OPAL Collaboration], Eur. Phys. J. C **27** (2003) 311 [hep-ex/0206022].
- [51] G. Belanger, B. Dumont, U. Ellwanger, J. F. Gunion and S. Kraml, Phys. Lett. B **723** (2013) 340 [arXiv:1302.5694 [hep-ph]].
- [52] E. Fuchs, S. Thewes and G. Weiglein, Eur. Phys. J. C **75** (2015) 254 [arXiv:1411.4652 [hep-ph]].
- [53] F. Domingo and T. Lenz, JHEP **1107** (2011) 101 [arXiv:1101.4758 [hep-ph]].